DISS. ETH NO. 26765

IDENTIFICATION OF SCD1 AS A HEART FAILURE-PROMOTING GENE BY WHOLE GENOME MICROARRAY GENE EXPRESSION PROFILING AND TRANSGENIC TECHNIQUES

A thesis submitted to attain the degree of

DOCTOR OF SCIENCES of ETH ZURICH

(Dr. sc. ETH Zurich)

presented by

YAHYA FAHAD M. JAMOUS

Master degree of sciences in pharmacy (pharmaceutics)

King Saud University, Riyadh, Saudi Arabia

born on 21.03.1980

citizen of Saudi Arabia

accepted on the recommendation of

Prof. Dr. Ursula Quitterer

Prof. Dr. Hanns Ulrich Zeilhofer

2020

Table of Contents

1. SUMMARY

With aging of the global society, cardiovascular diseases and heart failure are becoming leading causes of cardiovascular morbidity and mortality worldwide. The high morbidity and mortality of heart failure is partially attributed to insufficient treatment options and a lacking knowledge of pathomechanisms. The aim of this thesis was to identify pathomechanisms underlying the pathogenesis of heart failure in experimental models. The study used gene expression data of mouse models, which recapitulate major cardiovascular risk factors, chronic pressure overload and atherosclerosis. Chronic pressure overload was imposed by abdominal, aortic constriction (AAC), and as a model of atherosclerosis the study used apolipoprotein E-deficient (Apoe-/-) mice with hypercholesterolemia. Cardiac whole genome microarray gene expression data were analyzed of three different heart failure models of Apoe-/- mice, i.e. (I) aged, 18-month-old Apoe-/- mice, (II) young, 6-month-old Apoe-/- mice with AAC-induced chronic pressure overload, and (III) 8-month-old Apoe-/- mice with heart failure symptoms triggered by rosiglitazone, which is a heart failure-enhancing agonist of the adipogenic transcription factor, *Pparg*. The control groups were (I) age-matched, 18-month-old non-transgenic B6 mice, (II) 6-month-old Apoe-/- mice without AAC, and (III) 8-month-old Apoe-/- mice without rosiglitazone treatment. Gene ontology (GO) analyses of differentially expressed genes between failing hearts and respective control groups revealed the predominant up-regulation of genes from the cardiac lipid metabolic process in the three different heart failure models. The up-regulation of cardiac lipid genes was not only a characteristic feature of failing Apoe-/- hearts with hypercholesterolemia but was also triggered by AAC-induced chronic pressure overload of non-transgenic B6 mice.

In search for potential heart failure-promoting genes, whole genome microarray gene expression data analysis identified *Scd1*, the stearoyl-coenzyme A desaturase 1, as one of the lipid metabolism genes with the highest, more than 10-fold up-regulation, in failing hearts. To investigate the role of cardiac *SCD1* up-regulation in vivo, transgenic mice with myocardium-specific expression of *SCD1* under control of the alpha-MHC promoter were generated. *SCD1*-transgenic mice were identified by genotyping PCR of ear-punch biopsies and used for further breeding. Two different transgenic Tg-*SCD1* mouse lines were generated. Immunoblot analysis demonstrated the increased cardiac SCD1 protein level of *SCD1*-transgenic (Tg-*SCD1*) mice with 1.9±0.6-fold and

4.3±0.8-fold increased SCD1 protein levels compared to those of non-transgenic B6 controls. Phenotyping showed that 6-months-old Tg-*SCD1* mice had developed cardiac hypertrophy with a significantly increased heart-to-body weight ratio. Concomitantly, echocardiography revealed a significantly decreased left ventricular cardiac ejection fraction of Tg-*SCD1* mice (with high SCD1 protein level) of 35.2 ± 6.1 % compared to 52.7 ± 5.2 % of non-transgenic B6 controls (±s.d., n=6, p=0.0002). Histology analysis of hematoxylin-eosin-stained, paraffin-embedded cardiac sections further documented the cardiac hypertrophy of Tg-*SCD1* hearts, and immunohistology confirmed the increased SCD1 protein contents of the hypertrophied Tg-*SCD1* hearts. Whole genome gene expression profiling was performed to detect differentially expressed genes between Tg-*SCD1* and non-transgenic B6 control mice. Data analysis showed that Tg-*SCD1* hearts had significantly increased expression levels of heart failure-related genes, i.e. adiponectin (*Adipoq*), fatty acid synthase (*Fasn*) and resistin (*Retn*).

In view of the heart failure phenotype induced by an increased cardiac *SCD1* level, the next part of my thesis investigated pathomechanisms triggered by *SCD1*. A well-established pro-hypertrophic and failure-enhancing protein is the angiotensin II AT1 receptor, Agtr1. Radioligand binding studies with cardiac membranes and the radioligand, Sar^1, $[^{125}I]$ Tyr^4, Ile^8-angiotensin II, detected a significantly increased number of AT1 receptor binding sites of Tg-*SCD1* hearts compared to those of non-transgenic hearts, i.e. the number of AT1-specific binding sites was 1.6±0.2-fold higher of Tg-*SCD1* hearts compared that of non-transgenic B6 mice. Autoradiography with anti-AT1 receptor antibodies confirmed the increased AT1 receptor protein level of Tg-*SCD1* hearts and showed the predominant left ventricular localization of the up-regulated AT1 receptor on cryo-sections of Tg-*SCD1* hearts with signs of heart failure.

Next, the study investigated whether an increased *SCD1* level was sufficient to mediate up-regulation of the AT1 receptor protein in isolated cells. To this end, HEK cells were transfected with an expression plasmid encoding the AT1 receptor without and with co-transfection of *SCD1*. Radioligand binding studies showed that *SCD1* also increased the protein level of the AT1 receptor in HEK cells, i.e. the number of AT1 receptor binding sites was 2.2±0.4-fold higher of cells with AT1-receptor and *SCD1*-cotransfection compared to that of AT1-receptor-transfected cells. The direct effect of *SCD1* on the AT1 receptor was further analyzed by fluorescence spectroscopy, which quantified the cellular AT1-Cerulean protein without and with co-transfection of *SCD1*. The expression of *SCD1* significantly increased the cellular

protein levels of the AT1-Cerulean protein, which was determined by fluorescence spectroscopy compared to the cellular fluorescence of HEK cells transfected with AT1-Cerulean only.

Taken together, my thesis showed the predominant up-regulation of the cardiac lipid metabolic process in different heart failure models by whole genome microarray gene expression data analysis. Among different lipid metabolism genes, the impact of *SCD1* up-regulation on heart function was investigated by generation of *SCD1*-transgenic mice. Moderately increased *SCD1* levels (4.3-fold above the non-transgenic control) were sufficient to promote symptoms of heart failure such as cardiac hypertrophy and cardiac dysfunction. In addition, *SCD1* triggered up-regulation of heart failure-related genes. And finally, *SCD1* directly increased the protein level of the pro-hypertrophic and heart failure-enhancing angiotensin II AT1 receptor.

2. ZUSAMMENFASSUNG

Mit zunehmender Alterung der globalen Gesellschaft werden kardiovaskuläre Erkrankungen und Herzinsuffizienz zu Hauptursachen der kardiovaskulären Morbidität und Mortalität weltweit. Die hohe Morbidität und Mortalität von Herzinsuffizienz wird teilweise auf ungenügende Behandlungsmethoden und fehlende Kenntnis der zugrundeliegenden Pathomechanismen zurückgeführt. Das Ziel dieser Doktorarbeit war die Identifizierung von Pathomechanismen, die der Pathogenese von Herzinsuffizienz in experimentellen Modellen zugrunde liegen. Die Studie verwendete Genexpressionsdaten von Mausmodellen, die wichtige kardiovaskuläre Risikofaktoren wie chronische Druckbelastung und Atherosklerose rekapitulieren. Chronische Druckbelastung wurde durch abdominale Aortenkonstriktion (AAC) ausgelöst, und als Modell der Atherosklerose benutzte die Studie Apolipoprotein E-defiziente (Apoe-/-) Mäuse mit Hypercholesterolämie. Es wurden kardiale Mikroarray-Genexpressionsdaten des Gesamtgenoms von drei verschiedenen Herzinsuffizienz-Modellen der Apoe-/- Mäuse analysiert: (i) gealterte, 18 Monate alte Apoe-/- Màuse, (ii) junge, 6 Monate alte Apoe-/- Mäuse mit AAC-induzierter chronischer Druckbelastung, und (iii) 8 Monate alte Apoe-/- Mäuse mit Symptomen von Herzinsuffizienz, die durch Rosiglitazon ausgelöst wurden. Rosiglitazon ist ein Agonist des adipogenen Transkriptionsfaktors, PPARG, der die Entwicklung von Herzinsuffizienz-Symptomen beschleunigt. Die Kontrollgruppen waren (i) 18 Monate alte, nicht-transgene B6 Mäuse, (ii) 6 Monate alte Apoe-/- Mäuse ohne AAC, und (iii) 8 Monate alte Apoe-/- Mäuse ohne Rosiglitazon-Behandlung. Die Analyse der Genontologie (GO) von Genen mit differentieller Expression zwischen den insuffizienten Herzen und den zugehörigen Kontrollen zeigte die prädominierende Hochregulation von Genen des kardialen lipidmetabolischen Prozesses in den drei verschiedenen Herzinsuffizienz-Modellen. Die Hochregulation der kardialen lipidmetabolischen Gene war nicht nur ein charakteristisches Merkmal von insuffizienten Apoe-defizienten Herzen mit Hypercholesterolämie, sondern wurde auch durch AAC-induzierte chronische Druckbelastung in nicht transgenen B6 Mäusen ausgelöst.

Auf der Suche nach potentiellen Herzinsuffizienz-fördernden Genen identifizierte die Analyse der Gesamtgenom-Mikroarray-Genexpressionsdaten Scd1, die Stearoyl-Coenzym A Desaturase 1, als eines der Gene des Lipidmetabolismus mit der höchsten, mehr als 10-fachen Hochregulation in den Herzen mit Herzinsuffizienz. Um die Rolle der Hochregulation der kardialen SCD1 in

vivo zu untersuchen, wurden transgene Mäuse mit Myokardium-spezifischer Expression von SCD1 unter Kontrolle des alpha-MHC-Promoters generiert. SCD1-transgene Mäuse wurden durch Genotypisierung mittels PCR-Analyse von Biopsie-Gewebe aus dem Ohrläppchen identifiziert und für die weitere Zucht eingesetzt. Es wurden zwei verschiedene SCD1-transgene Mauslinien generiert. Eine Immunoblot-Analyse zeigte den erhöhten kardialen Gehalt an SCD1-Protein von SCD1-transgenen (Tg-SCD1) Mäusen mit 1.9±0.6-fach und 4.3±0.8-fach erhöhten SCD1-Proteingehalt im Vergleich zu nicht-transgenen B6 Kontrollen. Die Phänotypisierung zeigte, dass 6 Monate alte, SCD1-transgene Mäuse eine kardiale Hypertrophie mit einem signifikant erhöhten Verhältnis von Herzgewicht zu Körpergewicht entwickelt hatten. Gleichzeitig zeigte die Echokardiographie eine signifikant verminderte linksventrikuläre kardiale Ejektionsfraktion der SCD1-transgenen Mäuse mit hohem SCD1 Proteingehalt von 35.2 ± 6.1 % im Vergleich zu 52.7 ± 5.2 % bei nicht-transgenen B6 Kontrollen (±s.d., n=6, p=0.0002). Darüber hinaus dokumentierte die histologische Analyse von Paraffinschnitten, die mit Hämatoxylin-Eosin gefärbt waren, die kardiale Hypertrophie von SCD1-transgenen Herzen, und der immunhistologische Nachweis von SCD1 bestätigte die erhöhten SCD1-Proteinmenge der hypertrophen, SCD1-transgenen Herzen. Um unterschiedlich exprimierte Gene zwischen SCD1-transgenen und nicht-transgenen B6 Kontrollmäusen zu identifizieren, wurde eine Genexpressionsstudie des gesamten Genoms durchgeführt. Die Datenanalyse zeigte, dass SCD1-transgene Herzen eine signifikant erhöhte Expression von Genen zeigten, die mit Herzinsuffizienz assoziiert sind, wie z. B. Adiponectin (Adipoq), Fettsäure-Synthase (Fasn) und Resistin (Retn).

Angesichts des Phänotyps der Herzinsuffizienz, der sich infolge eines erhöhten kardialen SCD1-Spiegels entwickelte, untersuchte der nächste Teil der Doktorarbeit Pathomechanismen, die durch SCD1 ausgelöst werden. Der Angiotensin II AT1 Rezeptor, Agtr1, ist ein gut etabliertes, Hypertrophie-stimulierendes und Herzinsuffizienz-verstärkendes Protein. Durch Bindungsstudien mit dem Radioliganden Sar1, [125I] Tyr4, Ile8-Angiotensin II wurde an kardialen Membranen eine signifikant erhöhte Anzahl an AT1-Rezeptor-Bindungsstellen bei SCD1-transgenen Herzen im Vergleich zu nicht transgenen Herzen detektiert, d.h. die Anzahl an AT1-spezifischen Bindungsstellen war bei SCD1-transgenen Herzen 1.6±0.2-fach höher als bei nicht transgenen Herzen, die aus B6 Mäusen isoliert worden waren. Die autoradiographische Analyse mit AT1 Rezeptor-spezifischen Antikörpern bestätigte die erhöhte AT1 Rezeptorproteinmenge von SCD1-

transgenen Herzen und zeigte die überwiegend linksventrikuläre Lokalisierung des hochregulierten AT1 Rezeptors auf Gefrierschnitten von SCD1-transgenen Herzen mit Symptomen von Herzinsuffizienz.

Im nächsten Schritt wurde untersucht, ob ein erhöhter SCD1-Spiegel ausreicht, eine Hochregulation des AT1 Rezeptorproteins in isolierten Zellen zu bewirken. Um diese Frage zu untersuchen, wurden HEK Zellen mit einem Expressionsplasmid transfiziert, das für den AT1 Rezeptor kodiert. Zusätzlich wurden die Zellen entweder mit einem SCD1-kodierenden Expressionsplasmid oder einem Kontrollplasmid transfiziert. Radioligandenbindungsstudien zeigten, dass eine Zunahme von SCD1 auch die Menge des AT1 Rezeptorproteins in HEK Zellen erhöhte. Die Anzahl an AT1 Rezeptor-Bindungsstellen nach SCD1 Kotransfektion war 2.2±0.4-fach höher als bei Zellen, die den AT1 Rezeptor ohne zusätzliche SCD1-Expression exprimierten. Der direkte Effekt von SCD1 auf den AT1 Rezeptor wurde außerdem mit Fluoreszenz-Spektroskopie analysiert, die das zelluläre AT1-Cerulean-Protein mit oder ohne SCD1 Kotransfektion quantifizierte. Die Expression von SCD1 erhöhte signifikant den zellulären Proteinspiegel des AT1-Cerulean-Proteins, das mittels Fluoreszenzspektroskopie im Vergleich zur zellulären Fluoreszenz von HEK Zellen bestimmt wurde, die nur mit AT1-Cerulean transfiziert worden waren.

Zusammenfassend zeigt diese Doktorarbeit durch eine Analyse von Mikroarraygenexpressions-Daten des gesamten Genoms die prädominierende Hochregulation des kardialen lipidmetabolischen Prozesses in verschiedenen Modellen der Herzinsuffizienz. Unter den verschiedenen Genen des Fettstoffwechsels wurde SCD1 ausgewählt und der Einfluss der Hochregulation von SCD1 auf die Herzfunktion durch Generierung von SCD1-transgenen Mäusen untersucht. Ein moderat erhöhter SCD1-Spiegel (4.3-fach höher als die nicht transgene Kontrolle) war ausreichend, um Symptome der Herzinsuffizienz, wie z. B. kardiale Hypertrophie und kardiale Dysfunktion, auszulösen. Zusätzlich bewirkte SCD1 die Hochregulation von Herzinsuffizienz-assoziierten Genen. Und schließlich erhöhte SCD1 direkt den Proteinspiegel des Hypertrophie-stimulierenden und Herzinsuffizienz-verstärkenden Angiotensin II AT1 Rezeptors.

3. ABBREVIATIONS

a.u.	Arbitrary unit
AAC	Abdominal aortic constriction
Acc	Acetyl-CoA carboxylase (murine gene symbol)
ACE	Angiotensin converting enzyme
ACEI	Angiotensin converting enzyme inhibitors
Adipoq	Adiponectin (murine gene symbol)
Ampk	AMP-activated protein kinase
ApoE	Apolipoprotein E
APS	Ammonium persulfate
AT1R	Aangiotensin II type I receptor
B6	C57BL/6 mouse
BBS	BES-buffered saline
BES	N, N-bis[2-hydroxyethyl]-2-aminoethanesulfonic acid
BMI	Body mass index
BSA	Bovine serum albumin
CAD	Coronary artery disease
cAMP	3',5'-cyclic adenosine monophosphate
cDNA	Complementary DNA
CHF	Congestive heart failure
Cpt1	Carnitine palmitoyltransferase 1 (murine gene symbol)
cRNA	Complementary RNA
CRP	C-reactive protein
CVD	Cardiovascular disease
DGAT2	Diacylglycerol acyltransferase 2
dH2O	Distilled water
DMEM	Dulbecco's Modified Eagle's Medium
DNA	Deoxyribonucleic acid
E. coli	Escherichia coli
EDTA	Ethylenediaminetetraacetic acid
eNOS	Endothelial nitric oxide synthase

ET-1	Endothelin-1
Fasn	Fatty acid synthase (murine gene symbol)
FBS	Fetal bovine serum
FCS	Fetal calf serum
Gapdh	Glyceraldehyde 3-phosphate dehydrogenase
GCOS	GeneChip® operating software
GLP1	Glucagon-like peptide-1
Gnb	Guanine nucleotide-binding protein subunit beta
GO	Gene ontology
hCG	Human chorionic gonadotropin
HEK293	Human embryonic kidney 293 cells
HEPES	4-(2-hydroxyethyl)-1-piperazineethanesulfonic acid
HF	Heart failure
HFpEF	Heart failure with preserved ejection fraction
HFrEF	Heart failure with reduced ejection fraction
IgG	Immunoglobulin G
IVT	In vitro transcription
KDa	Kilodalton
LPS	Lipopolysaccharide
LVEF	Left ventricular ejection fraction
LXR	Liver X receptor
MHC	Myosin heavy chain
mRNA	Messenger ribonucleic acid
MUFAs	Monounsaturated fatty acids
NF-1	Nuclear factor 1
NO	Nitric oxide
PBS	Phosphate-buffered saline
PBST	PBS-Tween
PCR	Polymerase chain reaction
PDE-5A	Phosphodiesterase-5A
Pparg	Peroxisome proliferator-activated receptor gamma (murine gene symbol)

PUFAs	Polyunsaturated fatty acids
Retn	Resistin (murine gene symbol)
RNA	Ribonucleic acid
RNAse	Ribonuclease
rRNA	Ribosomal ribonucleic acid
RT	Room temperature
Scd1	Stearoyl-CoA desaturase (murine gene symbol)
SCD1	Stearoyl-CoA desaturase (human gene symbol)
SCD1	Stearoyl-CoA desaturase (protein symbol)
SD	Standard deviation
SDS-PAGE	Sodium dodecyl sulfate–polyacrylamide gel electrophoresis
SFAs	Saturated fatty acids
SOB	Super optimal broth
SOC	Super optimal broth with catabolite repression
SP1	Specificity protein 1
SPT	Serine palmitoyltransferase
SREBP	Sterol regulatory element-binding proteins
TAG	Triacylglycerol
Taq	Thermus aquaticus
TBE	Tris, boric acid, EDTA
TE	Tris, EDTA
TEMED	Tetramethylethylenediamine
Tg	Transgenic
Tris	Tris(hydroxymethyl) amino methane
tRNA	Transfer ribonucleic acid
TSB	Transformation and storage buffer

Gene and protein symbols are according to the HUGO Gene Nomenclature Committee (HGNC).

4. INTRODUCTION

Cardiac dysfunction, commonly known as heart failure (HF) is characterised by the inability of the heart to pump sufficiently to maintain blood and oxygen supply to other body organs including kidneys, liver and brain. The weakness of the heart muscle is commonly associated with numerous possible serious conditions and risk factors such as myocardial infarction, uncontrolled high blood pressure, obesity, diabetes, heart infections and inherited heart disorders [1]. HF is a pandemic disease and major cause of mortality, which affects approximately 26 million people worldwide [2]. About 1-3 % of health care expenditure is attributed to HF treatment costs in North America, Western Europe and Latin America [2]. The average prevalence of HF is 1-2% globally (Figure 1) [2].

North America
Canada	1.5%
USA	1.9%

Europe ~1–2%
France	2.2%
UK	1.3%

Asia
China	1.3%
Japan	~1%
Malaysia	6.7%
Singapore	4.5%

Latin America
No population-based estimates

Africa
No population-based estimates

Middle East
Oman	0.5%

Australasia
Australiaᵃ	1.3%
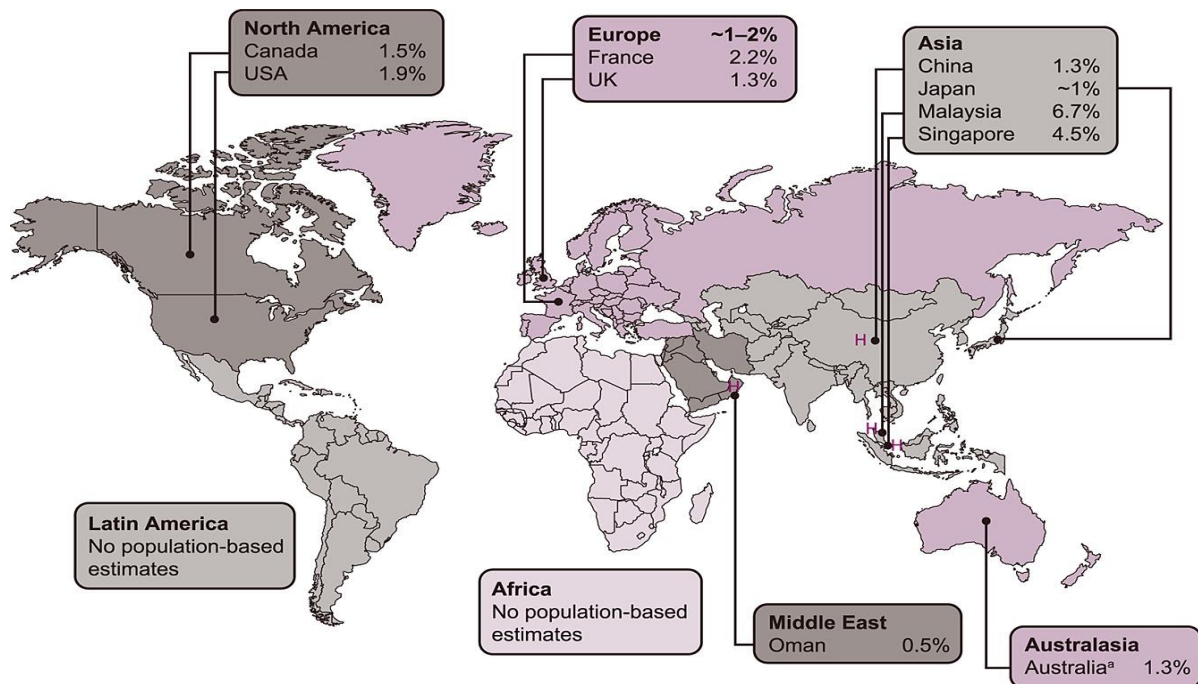
Figure 1: Percentage of people living with HF in North America, Europe, Asia, Australia and Middle East.
The high prevalence of HF is predicted to increase further, causing extreme pressure on healthcare systems and related costs in the future [3].
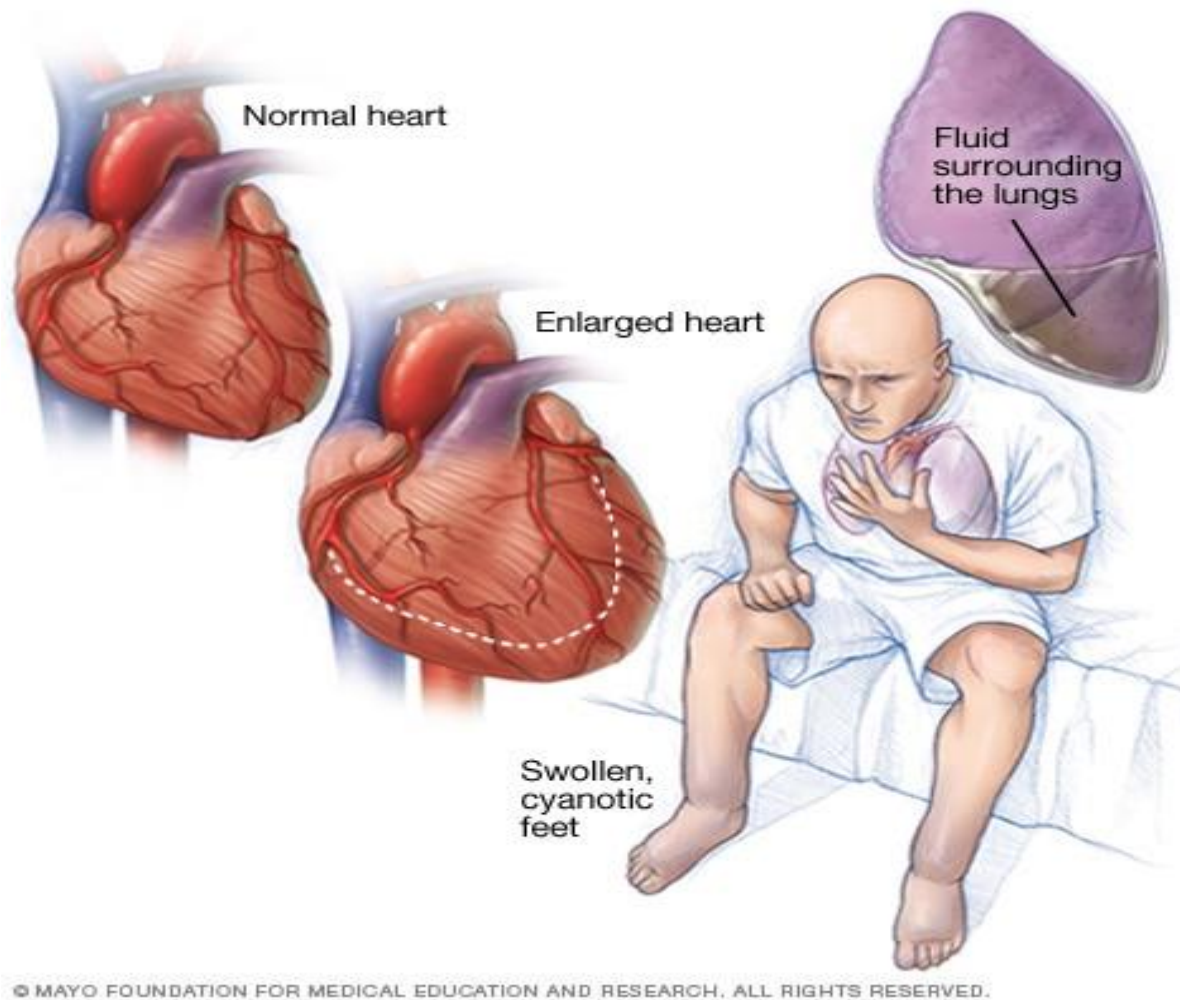
Figure 2: Common signs and symptoms of HF. (source: Mayo Foundation for Medical Education and Research).

The most common signs and symptoms of HF include reduced vitality, fatigue, breathing difficulties, pulmonary edema, swollen cyanotic feet, abdominal swelling, cardiac hypertrophy, irregular heartbeat and reduced left ventricular ejection fraction (LVEF) [4]. A LVEF of below 45 percent is considered as a potential marker of heart problems. Cardiac hypertrophy can also help to assess the severity of HF and guide the physician to select appropriate treatments (Figure 2) [5, 6].

4.1. Risk factors of cardiovascular disease and heart failure

4.1.1. Hypertension

Hypertension or high blood pressure is a long-term elevation of pressure in arteries. Based on a report from the Framingham Heart Study (FHS) and the National Heart, Lung and Blood Institute (NHLBI) in the US, people who had high blood pressure with CVD, had a lower rate of longevity [7]. In the US, published studies between 1975-1992 and between 1988-2006 revealed that the mortality rate of hypertensive patients with CVD is substantially higher than those without hypertension[8]. In addition, the causal association between chronic hypertension and the pathogenesis of HF is well documented by many studies [9]. Moreover, younger hypertensive individuals were associated with an increased risk of all-cause death including CVD and congestive heart failure (CHF) [10]. This indicates that early intervention could be helpful to minimize the risk of CVD mortality and HF caused by elevated blood pressure.

4.1.2. Diabetes mellitus

Diabetes mellitus is a metabolic disorder characterised by long-term elevation of blood glucose, which is caused by impairment of insulin secretion and/or insulin action. The decline in the level of insulin or the incidence of insulin resistance at the level of the insulin receptor and down-stream signalling cascades in tissues such as adipose tissue, skeletal muscles, and liver, might be a key for metabolic abnormalities. The intensity of symptoms depends on the type and duration of diabetes. Some people who become diabetics are unlikely to have symptoms, especially those people that are in the early years of type 2 diabetes. However, symptoms of diabetes in individuals with significant hyperglycaemia and children with complete insulin deficiency generally include weight loss, polyuria, polydipsia, polyphagia, blurred vision. Untreated diabetes can be life-threatening leading to coma and stupor, which is caused by ketoacidosis or rarely by nonketotic hyperosmolar syndrome [11, 12]. There is an association between diabetes mellitus and CVD. CVD is the integral factor for mortality and morbidity in diabetic patients [13]. The risk for CVD mortality and morbidity in adult populations with diabetes mellitus is ranged from 1 to 3 In male, and 2 to 5 in female compared to people without diabetes [14]. The intervention of diabetes in patients with CVD has a tendency to decrease the risk of mortality. Some risk factors such as obesity, hypertension and dyslipidaemia, are usually accompanied by diabetes mellitus, which make the treatment to be more challenging.

Additionally, several studies have indicated that many factors such as oxidative stress, elevated blood coagulability, impaired endothelial function and autonomic neuropathy are usually associated with diabetes mellitus and may increase the incidence of CVD [14].

Diabetes mellitus is also a major risk factor accelerating the pathogenesis of HF. Recent studies document that patients with diabetes type 2 have a >2-fold increased risk of developing HF. In addition, the prognosis of patients with HF and diabetes is worse than that of HF patients without diabetes [15].

4.1.3. Dyslipidemia

Arteriosclerosis is one of the most common risk factors of CVD, which results from high level of LDL-cholesterol. Arteriosclerosis is the leading cause of coronary artery disease (CAD), ischemic stroke, and peripheral vascular occlusive disease. Dyslipidaemia is a metabolic abnormality causing a chronic elevation in the level of cholesterol and triglycerides. There are recently three categories of dyslipidaemia. These categories are hypercholesterolemia, hypertriglyceridemia, and hyperlipidaemia which includes both hypercholesterolemia and hypertriglyceridemia [16]. An increased level of lipids can elevate the response of the blood vessel wall leading to impaired endothelial function, accumulation of lipids, proliferation of smooth muscle cells, leading to death of tissues and plaque formation [17]. Dyslipidemia and other cardiac risk factors can occur during childhood even though the symptoms of CVD caused by dyslipidaemia and other risk factors are usually observed during adulthood [18]. Because CAD and CVD caused by hypercholesterolemia and ensuing atherosclerosis predispose to the development of hypertension and myocardial infarction, CAD is also a major risk factor for the development of HF.

4.1.4. Tobacco smoking

Cigarette smoking is one of the most preventable cause of death in the entire world. According to one study performed in North America, the number of deaths attributed to smoking represents approximately 25% of the overall adult mortality while the number of deaths of smokers with CVD accounts for nearly 42.1% of overall adult deaths [19]. Smoking of cigarette causes endothelial dysfunction through reduced nitric oxide (NO) biosynthesis, hypercoagulability, elevated oxidative stress and stimulated inflammatory response [20-23].

Given the above, smoking is a key factor for CVD mortality[24]. Furthermore, the elevated oxidative stress and inflammation attributable to smoking has a direct influence on the myocardium with impaired both systolic and diastolic function. Moreover, smoking can worsen the other risk factors of HF such as hypertension, diabetes and atherosclerosis [25-27].

4.1.5. Obesity

Overweight and obesity are an abnormal accumulation of fat in the body which could be risky to the health. Overweight assessment is based on body mass index (BMI), which can be calculated by weight of the person in kilograms divided by the square of height in meters. The BMI of obese individuals is generally equal or more than 30 kg/m^2 whereas overweight people mainly have a BMI of 25-29.9 kg/m^2 [28]. People who are overweight, especially with central deposition of adipose tissues, are associated with an increased incidence of CVD mortality and morbidity [29]. Obesity may play a role in causing elevated blood pressure, dyslipidemia, diabetes, insulin resistance, and increased fibrinogen and C-reactive protein levels, all of which can enhance the development of CVD and HF [30]. Notably, it has been revealed that obesity is likely to increase the risk of hypertension [31], and chronic elevation of blood pressure is not only the leading cause of stroke, MI, and renal dysfunction but also HF [9, 32].

4.1.6. Physical inactivity

Physical inactivity is another important risk factor for CVD [33]. The regular physical activity is important to decrease the risk for the progression of metabolic syndrome. Physical activity is useful to enhance insulin sensitivity and decrease the incidence of dyslipidemia, elevated blood pressure, weight gain, all of which are leading causes of developing the metabolic syndrome [34-36]. Weight loss due to physical activity tends to normalize the diastolic blood pressure (DBP) and the level of triglycerides and fasting glucose [37]. It is recommended to keep physically active for a minimum of 150 minutes per week in order to significantly reduce the development of diabetes mellitus and then minimize the risk of CVD, and hypertension, all of which are also risk factors of HF [38]. Regular exercise by youths is less likely to increase body fat and protect against weight gain. Youths who are physically active can have an ideal level of fasting triglycerides and high density lipoprotein in addition to a normal systolic blood

pressure (SBP) [39]. Children and youths who have more physical activity and less sedentary activity usually have less metabolic risk factors [40]. The inverse association between physical activity and the risk of CVD is higher in elderly people. Research has shown that a moderate intensity of physical activity is more beneficial for elderly in terms of the risk of CVD compared to people of the same age and being fully inactive [41]. Even in patients with symptomatic chronic HF, physical inactivity has been shown to be associated with higher cardiac mortality and number of deaths by all causes [42]. Vice versa, modest activity (up to 89 min per week) resulted in a decreased cardiac and all-cause mortality of patients with chronic HF [42].

4.1.7. Nutrition

Dietary pattern has become essential and widely recognized in recent years [43]. Several studies have indicated that there is a correlation between nutrition and CVD, depending on the kind of foods in the meals. However, CVD risk factors induced by foods can be avoided through replacement diet. For example, replacement of saturated fat with unsaturated fat or grains is substantially helpful to decrease the risk of CVD. While replacing saturated fat with carbohydrate is not valuable [44]. Food-based dietary guidelines focus on dietary pattern and recommended foods. Dietary guidelines generally recommend healthy foods such as vegetables, fruits, grains, low fat foods, sources of lean protein, nuts and vegetable oils, and fish. Some guidelines have listed the foods that should be consumed in limited amount such as carbohydrates, saturated fat, dietary cholesterol and sodium [45]. While the above-listed nutritional recommendations are valid for risk reduction of CVD, nutritional recommendations for HF patients focus on sodium and fluid intake. Effective nutritional interventions, which improve the outcome of patients with HF, mainly recommend limited sodium and fluid intake together with nutritional counseling, although a very low sodium diet (< 2g/d) increases the risk of hospital admission and death from HF [46].

4.2. Cardiac remodeling

4.2.1. The impact of cardiac remodeling on heart failure

Cardiac remodeling, also known as left ventricular remodeling, usually occurs due to cardiac muscle injuries as a result of multiple pathological conditions or genetic factors, which may consequently change the size, shape and function of the heart ventricle. The pathological conditions that cause cardiac remodeling mainly include myocardial infarction, heart muscle problems, elevated blood pressure and heart valve diseases. In cardiac remodeling, the heart becomes abnormally enlarged with the development of myocardial fibrosis and enhanced cardiomyocyte death [47, 48]. For example, HF triggered by myocardial infarction can cause acute death of cardiomyocytes and an abrupt rise in myocardial loading conditions in both the infracted border zone and normal myocardium. The alteration in cardiac loading conditions eventually results in cardiac hypertrophy and dilation with the appearance of a more globular instead of a cone-shaped heart. Long-term injuries and alteration in cardiac shape can have detrimental effects on heart function and its contractility causing more complications on the patient situation (Figure 3) [49].

4.2.2. Diagnosis of cardiac remodeling and heart failure

Patients with cardiac remodeling can clinically be examined by an echocardiography that can be requested by physicians or cardiologists. Echocardiography is a non-invasive and safe examination tool which can be frequently used to detect the ventricular remodeling in individuals who have HF symptoms and evaluate the progression of HF treatments. The role of this measurement is to determine the percentage of LVEF which can be significantly reduced in patients with cardiac remodeling. In addition, echocardiography has a tremendous advantage of being able to easily and precisely provide information regarding abnormal cardiac shape, size and functions [50].
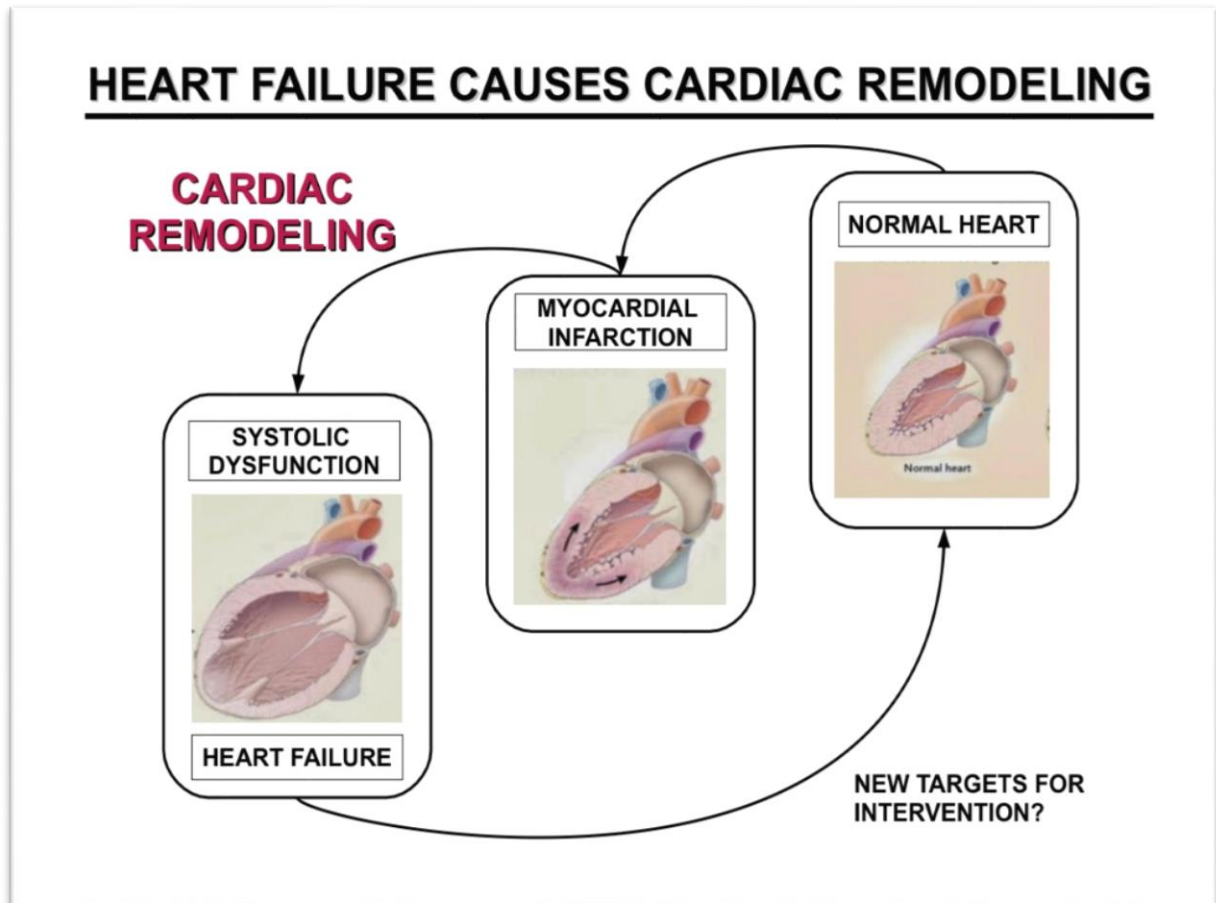
Figure 3: Cardiac remodeling after the incident of myocardial infarction.
After hours or days, the infarcted area starts to expand leading to cardiomyocyte death and thinning of the myocardium. After days or months, the affected heart becomes more globular causing ventricular dilatation and reduced systolic function. (Images adapted from:[51]).

4.2.3. Evidence-based therapeutic approaches for heart failure and cardiac remodeling by targeting the neurohormonal activation

The aim of current medications is to minimize the progression of myocardial remodeling. Therefore, medications that have the ability to delay or prevent the cardiac remodeling process are considered to be optimal therapies for cardiac dysfunction. Optimal therapy means that the intervention is efficacious in reducing HF mortality and all-cause mortality according to the best available evidence. Evidence-based pharmacological therapies for HF generally target the pathologic neurohormonal activation of the sympathetic nervous system and the renin-angiotensin-aldosterone system. Neurohormonal activation is triggered by the insufficient cardiac output of the failing heart. Neurohormonal blockade agents including beta blockers (β-blockers) such as carvedilol, angiotensin converting enzymes inhibitors (ACEI), and

aldosterone receptor blockers are mostly used to retard the adverse remodeling process [52, 53]. Many factors can have considerable impact on the success of treatment. These factors generally involve the severity of heart damage, induction of HF-promoting genes and frequent myocardial infarction.

4.2.3.1. Role of β-blockers in cardiac remodeling treatment

β-blockers are class of drugs that are widely used to treat cardiac arrhythmias, and hypertension, and reduce the risk of recurrent myocardial infarction [54, 55]. β-blockers block the receptor sites for adrenaline and noradrenaline on beta adrenergic receptors of the sympathetic nervous system, which regulate the acute stress response. Hence beta-blockers decrease the cardiac automaticity and conduction velocity and inhibit the heart failure-related neurohormonal activation of the sympathetic nervous system. In addition, beta1-adrenoceptor antagonists decrease renin release and can reduce blood pressure [56]. According to evidence-based criteria, the selective beta1-adrenoceptor antagonists, bisoprolol and metoprolol, and the non-selective adrenoceptor antagonist, carvedilol, improved survival in patients with heart failure with reduced ejection fraction (HFrEF) [57-59]. Based on best available evidence, bisoprolol, metoprolol and carvedilol are recommended as first-line treatment according to current HF guidelines together with an ACE inhibitor [60]. Antiadrenergic treatment has been clinically trialed in a considerable number of patients [57-59, 61, 62]. It was discussed that carvedilol has greater anti-adrenergic activity compared to other β-blocking agents as it is a non-selective blocker of beta-1 (β1), beta-2 (β2), and alpha-1 (α1)- adrenergic receptors, and it also has antioxidant activities, which collectively substantiate the inhibition of cardiac adrenergic drive and work [63, 64]. Whether these differences of carvedilol translate into a measurable clinical outcome is not clear because the beta1-selective antagonists (bisprolol and metoprolol), and the non-selective antagonist, carvedilol, all decreased the mortality of patients with HFrEF [60]. Treatment with a beta-blocker improves systolic function of HF patients. In addition, carvedilol was shown to delay the enlargement of the ventricle chamber in patients who suffer from mild to moderate chronic HF. Similar beneficial treatment effects were also observed with the highly beta1-selective adrenoceptor antagonist, bisoprolol [59]. The beneficial effect of chronic HF treatment is independent of the severity and cause of HF [60]. To avoid potential side effects of severely ill patients with NYHA class III-IV, close

observation at the beginning of therapy and during dose titration is recommended [60, 65, 66]. Despite this caveat, patients with severe HF apparently profit more from beta-blocker therapy in the long-term compared to less symptomatic patients [65, 66].

4.2.3.2. Aldosterone blockade for the treatment of HFrEF and cardiac remodeling

Aldosterone is a mineralocorticoid hormone which is regulated by the renin-angiotensin-aldosterone system and strongly activates pathways related to cardiac remodeling [67, 68]. Several studies have revealed that aldosterone is likely to have harmful effects on the cardiovascular system including myocardial fibrosis, cardiac hypertrophy and apoptosis, impaired endothelial function, oxidative stress, renal fluid and sodium retention and sudden death [69-73]. In addition, the aldosterone receptor blocking agents such as spironolactone and eplerenone can delay the progression of morphological and functional alterations of the heart in a number of models with an impaired cardiac function [74-78]. In clinical trials, mineralocorticoid receptor antagonists decreased the number of deaths and hospitalization in patients with impaired systolic function after myocardial infarction and in patients with reduced LVEF [79-82]. Consequently, according to best available evidence, current treatment guidelines recommend addition of an aldosterone receptor antagonist for treatment of patients with HFrEF to standard treatment with beta-blocker and ACE inhibitor [60].

4.2.3.3. Role of ACEI agents in treatment of cardiac remodeling

ACEIs are mainly used to treat elevated blood pressure but these drugs also have great potential to minimize cardiac dilation and hypertrophy [83, 84]. The mechanism of ACEI is the inhibition of the angiotensin converting enzyme (ACE) that is responsible for the production of angiotensin II (AngII) by the cleavage of the angiotensin I (AngI). AngII is a peptide that has the ability to bind with the angiotensin II receptor type I (AT1) to cause vasoconstriction and cardiac remodelling [85]. In patients with HFrEF post-infarction, treatment with several different ACE inhibitors had a documented survival benefit in a large number of trials [86]. In view of the reduced mortality, ACE inhibitors are recommended as first-line treatment for patients with HFrEF [60]. Several research studies have indicated that both ACEI and AT1 blockers have nearly the same efficacy in the protection against ventricular dilatation and reducing the

mortality in patients with HFrEF [87, 88]. Consequently, an AT1 receptor antagonist is recommended for patients, who cannot tolerate an ACE inhibitor [60].

4.2.3.4. Angiotensin receptor and neprilysin inhibitor (ARNI) for treatment of HFrEF and myocardial remodeling

The most recent advancement of HFrEF treatment is the introduction of Entresto®, which is the combination of the neprilysin inhibitor, sacubitril, with the AT1 receptor antagonist, valsartan. This combination is named ARNI, which is the abbreviation for angiotensin receptor and neprilysin inhibitor. By inhibition of neprilysin, sacubitril prevents the degradation of natriuretic peptide(s), which promote vasodilation, a decrease in the overactive sympathetic nervous system activity, and a reduction in aldosterone levels, cardiac hypertrophy, fibrosis and overall myocardial remodeling. In addition to break-down of natriuretic peptides, neprilysin also degrades bradykinin and angiotensin II. To avoid accumulation of pathological angiotensin II upon neprilysin inhibition, the neprilysin inhibitor, sacubitril, needs to be combined with an AT1 receptor antagonist. In combination with the AT1 receptor antagonist, the neprilysin inhibitor, sacubitril, resulted in a clear survival benefit compared to standard HF treatment involving the ACE inhibitor enalapril of patients with HFrEF in the PARADIGM study [89]. In view of the improved overall survival, Entresto received a class I recommendation, for treatment of HFrEF by international HF treatment guidelines [60]. Taken together, current treatment options of HF, which prolong the life of patients with HF, target the neurohormonal activation and cardiac remodeling.

4.3. Therapeutic approaches without documented improvement of heart failure prognosis

4.3.1. Antihyperlipidemic agents

HMG-CoA (3-hydroxy-3-methylglutaryl coenzyme A) inhibitors are well established in reducing cholesterol and provide powerful protection to patients having various types of ischemic heart disease [90]. Anti-remodeling effects of these "statins" could occur in addition to those realized through conventional therapy (aldosterone blockers, ACE inhibitors and β-blockers) [91]. Nevertheless, the CORONA trial (Controlled Rosuvastatin Multinational Trial in Heart Failure), mentioned that rosuvastatin was able to decrease cardiovascular morbidity but did

not reduce the primary endpoint or the number of deaths by all causes in older patients having systolic heart failure [92]. In the GISSI-HF trial (Gruppo Italiano per lo Studio della Sopravvivenza nell'Insufficienza Cardiaca - Heart Failure), a 10 mg daily dose of rosuvastatin also was not able to change the clinical outcomes of patients with any type of chronic HF [93].

4.3.2. Vasopressin blocker

In addition to the two principal neurohormonal cascades, the sympathetic and renin-angiotensin-aldosterone axes, cascades initiated by endothelin and vasopressin are activated during the heart-failure pathogenesis [94]. Activation of the vasopressin V1A receptor, which enhances the intracellular Ca^{2+} concentration, can induce remodeling of myocytes and cardiac hypertrophy. Furthermore, activation of V2 receptors can elevate the expression and membrane incorporation of aquaporin-2 water channels into the cells of the renal collecting duct, causing absorption of fluids. Agents that antagonize the vasopressin receptors (for example conivaptan, lixivaptan, mozavaptan and tolvaptan), can block V1A or V2 receptors, or both receptors. In the EVEREST (Efficacy of Vasopressin Antagonism in Heart Failure Outcome Study with Tolvaptan) clinical study, administration of oral tolvaptan with standard treatment for patients, who were admitted to the hospital because of HF, showed improvement in the signs and symptoms of some patients without causing serious adverse effects [95]. Nevertheless, tolvaptan, which was administered as an acute therapy for hospitalised HF patients, had no impact on the hospitalization or death [96].

4.3.3. Endothelin-1 (ET-1) receptor blocker

Endothelins, including endothelin-1 (ET-1), increase the growth and myofibrillogenesis of cardiomyocytes and enhance cardiac contractility. Thereby, endothelins promote cardiac hypertrophy and cardiac enlargement [97]. ET-1 has the ability to bind with the endothelin ET_A receptor and evokes a broad spectrum of responses, including stimulation of ion channels that improve cardiomyocyte contractility and enhance the growth of heart cells, and activate protein kinases. It also can increase the expression of nuclear transcription factors [97]. Unfortunately, many trials, which have examined various types of endothelin antagonists, had a negative outcome. These trials include: RITZ-4 (Randomised Intravenous TeZosentan), EARTH (Efficacy and safety of iRbesarTan and olmesartan in patients with Hypertension), and ENCOR (Enrasentan Cooperative Randomised) [98-100].

4.3.4. Anti-inflammatory agents

Pro-inflammatory cytokines promote cardiac enlargement, necrosis and extracellular matrix remodeling, all of which have a role in HF progression [101]. Furthermore, elevation of pro-inflammatory cytokine levels in HF is linked to a poor clinical prognosis [102]. Nevertheless, clinical studies indicated that approved TNFα inhibitors, infliximab and etanercept, had a negative or neutral influence on morbidity and mortality of HF or other causes [103].

4.3.5. Glucagon-like peptide-1 (GLP1)

Metabolic disorders are important factors of HF pathogenesis. Lipotoxicity and insulin resistance are certainly accepted as indicators of diabetic cardiomyopathy and dilated cardiomyopathy [104, 105]. Pharmacological stimulators of the glucagon-like peptide (GLP1) receptor by GLP1 receptor agonists are approved for the treatment of insulin resistance and type 2 diabetes [106]. GLP1 is a physiological incretin, which enhances the release of insulin postprandially, after intake of a meal or glucose [106, 107]. In addition to that function, GLP1 also exerts beneficial effects in the cardiovascular system. For instance, GLP1 activates myocardial glucose uptake in dilated cardiomyopathy by P38 mitogen-activated protein kinases (MAPKs) [108]. Improved left ventricular systolic function and survival appeared in HF rat models chronically treated by GLP1 [109]. In agreement with the beneficial profile of GLP1 in animal models, the LEADER trial showed a reduced number of cardiovascular events including HF, a decreased cardiovascular mortality and all-cause mortality of high-risk patients with type 2 diabetes, who were treated with the GLP1 receptor agonist, liraglutide [110, 111].

4.3.6. Agents with vasodilator properties

A defect in cGMP-dependent pathways can cause cardiac remodeling and myocardial dysfunction. Specific phosphodiesterases control the duration, amplitude, and compartmentalisation of cyclic nucleotide signalling. Some drugs such as sildenafil, which is an inhibitor of phosphodiesterase-5A (PDE-5A), improved left ventricular diastolic function and right ventricular systolic function in small-scale studies in heart failure with preserved ejection fraction (HFpEF) [112]. However, another study indicated that the administration of a PDE-5A inhibitor (sildenafil) to patients with HFpEF for a period of 24 weeks was unable to result in a substantial improvement regarding the exercise capacity or clinical conditions [113].

Nitric oxide (NO) generation by the enzyme called endothelial nitric oxide synthase (eNOS) has the capacity to restrict cardiac hypertrophy, apoptosis and fibrosis, leading to a reduced adverse remodeling of the heart [114]. Consequently, an experimental approach of targeting and increasing eNOS activity has been investigated. Preclinical trials of AVE9488, which is an oral agent that has the ability to target eNOS, interfered with pathologic left ventricular remodeling including reduced cardiac hypertrophy, dilation and fibrosis, and increased contractility; however, this had no impact on the mass of the left ventricle [115].

4.3.7. Cardiac myosin activators

Another, experimental group of therapeutic agents used for treatment of cardiac remodeling are cardiac myosin activators, which include omecamtiv mecarbil known as CK-1827452[116]. This compound binds the myosin catalytic domain, and enhances the transition of myosin into the force-generating actin-myosin complex. As a result, more myosin heads bind to actin filaments, which creates more force per beat. Consequently, omecamtiv mecarbil increases the force of contraction without altering the contraction rate [116]. This mechanism prolongs the systolic ejection time (SET), leading to an increased systolic function, without enhancing the demand of myocardial oxygen. This result in a substantial increase in cardiovascular function. A phase II clinical study showed that omecamtiv mecarbil has no major side effects in patients with stable HF, and can enhance the stroke volume and reduce end-systolic and end-diastolic volumes [117]. Another, phase II clinical study with stable, symptomatic chronic HF patients confirmed these data and showed an improved cardiac function and a decreased ventricular diameter [118].

4.4. The need of new approaches to fully reverse cardiac remodeling

The global HF mortality and morbidity rates are still extremely high due to the inability of current medications to completely reverse the cardiac remodeling process and revert the heart into a normal heart condition. As a result, the focus of current research is to find new approaches to fully reverse the cardiac remodeling process by identifying more mechanisms contributing to signs and symptoms of HF [119, 120].

4.5. Experimental heart failure research

4.5.1. Experimental models of heart failure

Great efforts have been exerted by scientists to analyse pathomechanisms underlying the progression of HF. Animal models, which are clinically relevant to HF can be used for the experimental analysis. HF in experimental models can be induced by major cardiovascular disease (CVD) risk factors such as chronic pressure overload and atherosclerosis. Chronic pressure overload in mice is often imposed by weeks to months of transverse aortic constriction (TAC) or abdominal aortic constriction (AAC) of non-transgenic B6 mice and atherosclerosis-prone apolipoprotein E-deficient (ApoE-/-) mice [121, 122]. ApoE-/- mice usually show a high accumulation of cholesterol in blood due to the weakness of lipoprotein clearance [123]. Another model applies aged ApoE-/- mice that have long-term atherosclerosis, which triggers pressure overload by aortic coarctation due to excessive aortic plaque accumulation at an age of >18 months [124].

In addition, certain agents can be administered to mice with hypercholesterolemia to increase the incidence of hyperlipidaemia and HF. One example of these agents is rosiglitazone, which is an agonist of the peroxisome proliferator-activated receptor gamma (*Pparg*), an adipogenic transcription factor, and enhances the incidence of HF in experimental models and patients [125-127].

Finally, gene mutation-induced HF models mimic the phenotype of a gene-induced cardiomyopathy of patients with inherited cardiomyopathies [128].

4.5.2. The whole genome microarray gene expression analysis of heart failure models

Whole genome microarray gene expression profiling is usually performed to analyse the most up-regulated cellular processes at the onset of cardiac disease in experimental models of HF, in which HF is either induced by exposure to various cardiac risk factors or by a heart failure-promoting gene [125, 129].

After gene expression profiling, strongly up-regulated genes are identified. For instance, by whole genome microarray gene expression profiling, it has been shown that there are a

number of cardiac lipid metabolic process genes, which are highly upregulated in chronic pressure overload-triggered HF in mice [125]. However, to date it is not clear for many up-regulated genes of the lipid metabolic process, which genes are detrimental, and which genes could potentially be protective against the progression of HF.

One of those genes up-regulated during chronic pressure overload-mediated HF is the gene encoding the Stearoyl-CoA desaturase (*Scd1*) enzyme that could eventually exert a beneficial function. By transforming detrimental saturated fatty acids (SFAs) into cardioprotective unsaturated lipids. The up-regulated *SCD1/Scd1* gene could potentially counteract the detrimental accumulation of saturated lipids occurring during the course of HF pathogenesis [130]. Hence, a more detailed analysis of gene expression data from various HF models is needed, and the in vivo role of an up-regulated cardiac gene such as *Scd1* must be performed to clarify the role of *Scd1* during HF pathogenesis in animal models and humans.

4.5.3. Generation and phenotyping of transgenic mice, which reproduce the in vivo function of potential HF-related genes

After gene expression profiling, the function of highly regulated genes needs to be analysed in vivo, e.g. by generation of a transgenic mouse model, which mimics the disease-related gene regulation and/or modification [128, 130, 131]. Transgenic mice with transgenic expression of a specific gene can be generated and applied to investigate the impact of certain genes on the cardiac phenotype of experimental HF models. In frame of this study, transgenic *SCD1* (Tg-*SCD1*) mice were generated and their phenotype was analysed. To generate transgenic mice for HF research, the gene of interest can be inserted into a certain plasmid under the control of a cardiac tissue-restricted expression promotor such as the alpha-myosin heavy chain (α -MHC) promoter [132]. Transgenic founder mice are usually identified by genotyping PCR, and the presence of the transgenic protein as a result of transgenic expression can be confirmed by immunoblot detection [133].

In order to analyse the phenotype of transgenic mice, an echocardiography measurement is a useful diagnostic tool to determine the LVEF and identify cardiac dysfunction and symptoms of HF [124, 134]. The LVEF value of transgenic models with cardiac dysfunction could be significantly reduced. Additionally, the comparison of heart-to-body weight ratio between the

transgenic and non-transgenic models is also essential to identify whether the transgenic mice have cardiac hypertrophy [130]. Moreover, cardiac histological image analysis using hematoxylin-eosin staining has a valuable role in the determination of any cardiac morphological changes [133]. Furthermore, immunohistological analysis is a method that can detect the existence and position of specific proteins in tissue specimen sections using antibodies that have high affinity for a certain protein. Peroxidase is an enzyme that is conjugated to a secondary antibody and, after a substrate reaction, helps to visualize the bound primary antibodies by immunohistology analysis under the microscope. Peroxidase is an enzyme, which catalyses a chemical reaction to produce a coloured precipitate at the location of the target protein [135]. In addition, a whole genome microarray study has the ability to detect the most up-regulated HF-related genes and HF marker genes in the isolated hearts of transgenic mice [133].

4.6. Stearoyl-CoA desaturase 1 (SCD1) enzyme

Investigation of the cardiac function of *SCD1* (Stearoyl-CoA desaturase 1) is a major focus of this thesis because the murine *Scd1* was found to be up-regulated at the onset of experimental HF triggered by chronic pressure overload [124]. In frame of this research focus, the following chapter provides an overview of the current knowledge about physiological and pathological functions of *SCD1/Scd1*.

Stearoyl-CoA desaturase 1 (SCD1) is a delta-9 desaturase enzyme that has a molecular mass of 37 kilodalton (kDa). The enzyme is located in the endoplasmic reticulum. It has a role in formation of monounsaturated fatty acids (MUFAs) from diet or from endogenous saturated fatty acids (SFAs) [136, 137]. For instance, SCD1 leads to the production of monounsaturated palmitoleate and oleate from the SFAs, palmitate and stearate, respectively (Figure 4) [137].
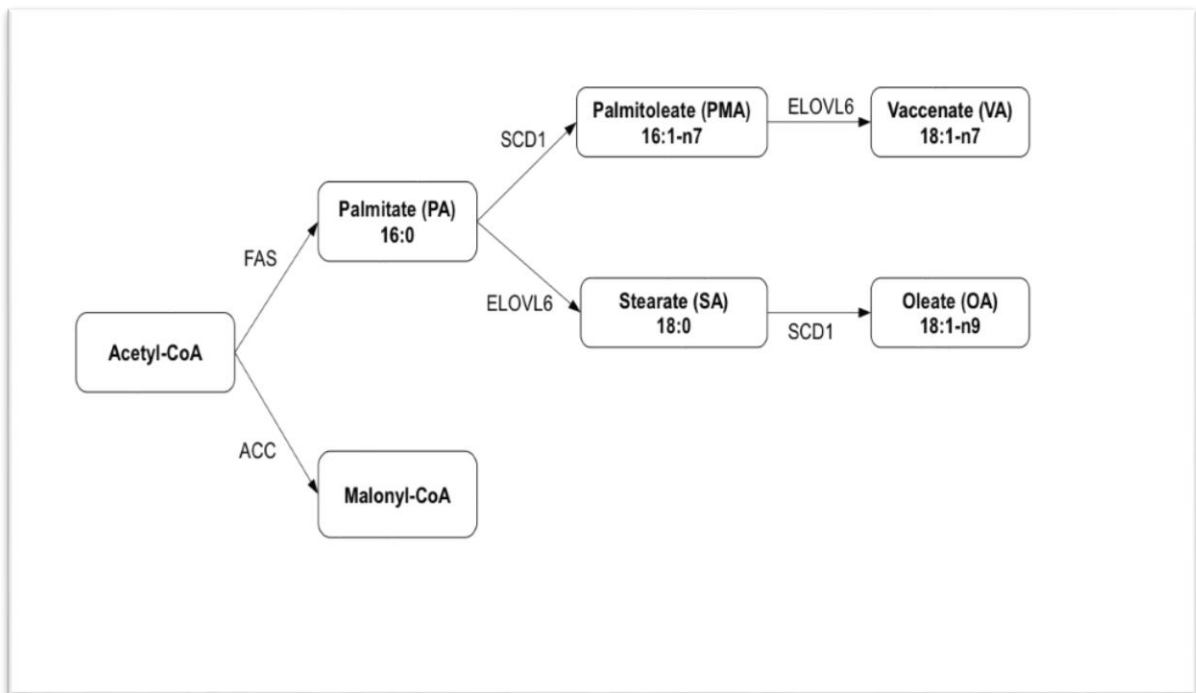
Figure 4: The endogenous synthesis of MUFAs by SCD1.
ACC, acetyl-CoA carboxylase; FAS, fatty acid synthase; ELOVL6, elongase 6; SCD1, stearoyl-CoA desaturase 1 [137].

Monounsaturated palmitoleate and oleate are the most common MUFAs in humans and considered the key components of membrane lipid structure involving phospholipids, cholesterol esters and triacylglycerols (TAGs). The primary structure of SCD1 indicates that both the amino and carboxylic termini are facing the cytosol. In addition, histidine residues are involved in the enzymatic function of SCD1. Histidines possibly facilitate binding of SCD1 to the catalytic metal ions such as iron [137].

The SCD1 enzyme requires the reduced form of nicotinamide adenine dinucleotide (NADH), flavoprotein cytochrome b_5 reductase, electron acceptor cytochrome b_5 and oxygen molecules to insert a cis single double bond at the delta-9 location of 12–19 SFAs to produce MUFAs (Figure 5) [137, 138].
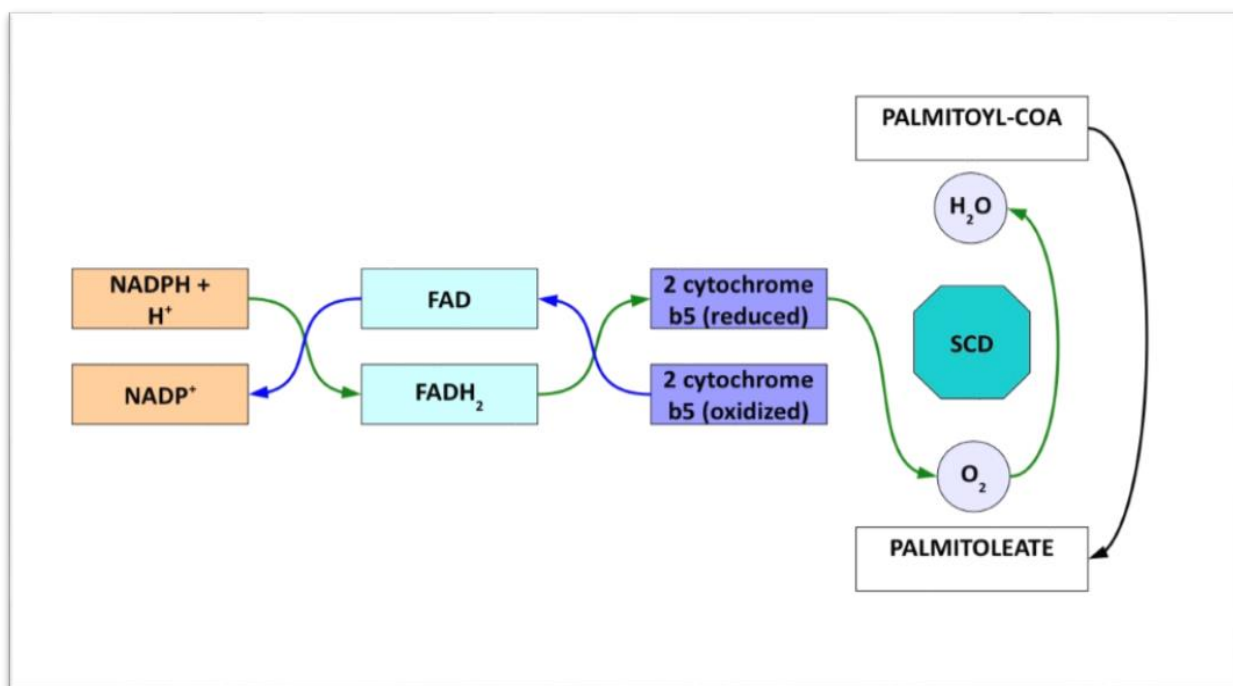
Figure 5: A series of redox reactions is required for the desaturation of FA by SCD1.
The SCD1-catalyzed reactions involve oxygen molecules, NAD(P)-cytochrome b5 reductase, and the electron acceptor cytochrome b5 to transfer an electron from NADPH to the terminal electron acceptor oxygen molecule and liberate water [137].

4.6.1. *SCD* isoforms

4.6.1.1. Human SCD isoforms

In humans, the only *SCD* isoforms are *SCD1* and *SCD5* [139]. The human *SCD1* is located on chromosome number 10 and it is very similar to all murine *SCD* isoforms with about 85 percent homology [140, 141]. Both human and murine *SCD1* are highly expressed in the liver and adipose tissue but they also have been identified in different other tissues such as a skeletal muscle, heart, brain, lung and pancreas [139]. Unlike *SCD1*, the human *SCD5* isoform, which is located on chromosome number 4, is a primate-specific *SCD* isoform, which is not present in mice [139, 142]. Thus, *SCD1* is the only human isoform that is extremely similar to murine isoforms.

4.6.1.2. Murine SCD isoforms

Murine *Scd* isoforms are useful for research due to the similarity with human isoforms. Mice have four different isoforms expressed in their bodies including *Scd1*, *Scd2*, *Scd3* and *Scd4* and

are found on chromosome number 19. The average length of murine *Scd* genes is 350 to 360 amino acids and they have approximately more than 80% amino acids sequence similarity to each other. The differences between isoforms occurs in the sequence of 5' flanking gene which accounts for different tissue expression [138]. Both murine *Scd1* and *Scd2* have ubiquitous expression, contain about 358 amino acids and are extremely identical in their amino acid sequence with homology of about 87%. However, *Scd2* is highly expressed in specific organs such as the brain although it can also be found in most body tissues except the liver [143]. It has been shown that carbohydrate-rich foods are likely to upregulate the expression of *Scd1* as well as *Scd2* in lungs, heart, kidney and spleen [137].

Scd3 is another murine isoform that has a length of 359 of amino acids and shows a great extent of identity with *Scd1*. Unlike other isoforms, *Scd3* is particularly expressed in a mouse skin [144]. The *Scd3* isoform can also be detected in glands such as Harderian and preputial gland [145]. *Scd4* has approximately 79% identity with the other murine *Scd* isoforms and contains 352 amino acids but its expression was mainly identified in the heart. The *Scd4* gene can be substantially induced by excessive carbohydrate intake and liver X receptor α (LXRα) agonists but unlike *Scd1*, it cannot be repressed by foods enriched with polyunsaturated fatty acids (PUFAs) [146]. Taken together, *SCD1/Scd1* is expressed in humans and mice.

4.6.2. Modulation of *SCD1* gene expression

PUFAs, carbohydrates, and hormones, in particular insulin and leptin, are factors that regulate *SCD1* gene expression in both humans and other species. These parameters aid the binding of transcription factors to the *SCD1* promotor to modulate its expression [147]. Main transcription factors that affect the expression of the *SCD1* gene include sterol regulatory element binding protein 1c (SREBP-1c), liver X receptor (LXR), and proliferator-activated receptor alpha (PPAR-alpha) [147, 148].

4.6.2.1. Modulation of *SCD1* gene expression in the liver and adipose tissue by fatty acids

Based on many studies, fatty foods may potentially affect the *SCD1* gene expression in many tissues, in both humans and mice. High-fat feeding significantly rose the expression of *Scd1* in the liver of obese C57BL/6 mice [149]. It has been shown that some SFAs such as stearate,

induced the expression of the Scd1 protein in the liver of mice whereas *Scd1*-deficient mice have no induction of hepatic *Scd1* gene after dietary SFA feeding [150]. This effect could be due to the fact that SFAs tend to activate the *Scd1* transcription by the induction of transcription factors such as SREBP-1c and PPARs [147, 151]. On the other hand, the expression of *Scd1* can be repressed by PUFAs, both in liver and adipose tissue. Eicosanoids which are derivatives produced by PUFAs could have the ability to repress the expression of genes responsible for lipogenic gene induction including the Scd1 protein in adipose tissue [152]. For example, arachidonate and linoleate decreased the *Scd1* content in 3T3-L1 adipocytes, which is a cell line derived from mouse tissue [153]. Studies showed that the repression of *Scd1* by PUFAs is more significant in the liver than in adipose tissue. This can be triggered via the mechanism of inhibition of SREBP-1c activation by PUFAs [154, 155].

4.6.2.2. Effects of carbohydrates on *SCD1* gene expression in the liver and adipose tissue

Carbohydrates are considered as one of the most potent *SCD1* expression modulators. Studies have shown that high carbohydrate foods significantly induced the expression of *Scd1* in the mouse liver [137, 156, 157]. Many transcriptional regulators including SREBP-1c, carbohydrate response-element binding protein (ChREBP), and nuclear factor 1 (NF-1) have a role in the induction of hepatic *Scd1* expression by carbohydrates [137, 147, 157, 158]. Insulin via phosphoinositide 3-kinase (PI3K), protein kinase B (AKT), and mammalian target of rapamycin (mTOR)-dependent signaling pathways can also upregulate the expression of the hepatic *Scd1* gene through insulin-response elements (IREs) of the *Scd1* promoter [147, 159]. According to several studies, sucrose, glucose and fructose are carbohydrates that potentially induce the expression of hepatic *Scd1* [160-162]. However, the impact of high carbohydrate-rich diets on the expression of *Scd1* in adipose tissue has not been fully understood. Some studies analyzing the 3T3-L1 cell line indicate that carbohydrates can activate the Scd1 protein in adipose tissue via the induction of the activity of SREBP-1c, NF-1 and CCAAT/Enhancer-Binding-Protein, CEBP [147, 162, 163].

4.6.2.3. Modulation of *SCD1* gene expression in the liver and adipose tissue by hormones

Hormones such as leptin, estrogen and thyroid hormones are clearly involved in the regulation of *SCD1* expression as well as its activity. Leptin hormone tends to work as an inhibitory regulator by reducing the *Scd1* expression in the adipose tissue and liver in obese (ob/ob) mice [164]. An experiment that was performed on a human liver carcinoma cell line (HepG2) showed that leptin has the ability to target the leptin response element of the *SCD1* promotor through signaling pathways. These pathways include both extracellular signal-regulated kinases (ERK1/2) and Janus kinase 2 (JAK2), which can target the downstream transcription factor specificity protein 1 (SP1) on the *SCD1* promoter [165]. In addition, leptin may prevent the induction of *SCD1* activity since it causes a defect in the capability of insulin to activate the gene expression of *SCD1*, and impair the initial regulatory steps of the insulin signaling pathway (e.g. autophosphorylation of the insulin receptor, and the tyrosine phosphorylation of insulin receptor substrates). Furthermore, leptin can also negatively affect the stability of the SCD1 protein [147]. Taken together, leptin has a substantial inhibitory effect on *SCD1* expression through different mechanisms.

It has been evidenced that estrogen hormone has also a role in blunting the *SCD1* expression in human adipose tissue and mice consuming a high fat diet [166, 167]. This effect is most probably due to a reduction of SREBP-1c expression [167]. Estrogen administration also has an inhibitory effect on hepatic *SCD1* expression [167]. Vice versa, estrogen-deficient mice showed higher *Scd1* contents in the liver compared to control mice [168]. This is because estrogen is able to target genes responsible for the induction of signal transducer and activator of transcription 3 (*Stat3*) in the liver causing a reduction in the expression of genes responsible for hepatic lipogenesis including the *Scd1* gene [168, 169].

The thyroid hormone is another example of a hormone that tends to reduce *SCD1* expression. It has been shown that the active form of the thyroid hormone, the so-called triiodothyronine (T3), substantially decreased the expression of *SCD1/Scd1* in the murine liver as well as in HepG2 cells [170].

Studies also revealed that retinoic acid inhibited the expression of *Scd1* in 3T3-L1 preadipocytes followed by a sudden increase in the expression of *Scd1* during differentiation [171]. More

experiments were performed on livers and demonstrated the regulation of *SCD1* transcription by the retinoic acid receptor through a mechanism involving heterodimerization with the retinoid X receptor [172].

4.6.2.4. Modulation of *SCD1* gene expression in the heart by carbohydrates, fatty acids and hormones

Gene expression of *Scd1* is also regulated in the heart. In one study, a real-time polymerase chain reaction (RT-PCR) was used to examine the upregulation of *Scd1* gene expression after the incubation of neonatal rat cardiac myocytes with glucose, insulin and fatty acids. A high dose of glucose or insulin induced the *Scd1* messenger RNA (mRNA) expression in cardiac myocytes. In addition, SFAs including palmitate and stearate increased the expression of cardiomyocyte *Scd1* mRNA [155]. However, MUFAs such as oleate and linoleic acid, had no effect on *Scd1* gene expression. Taken together, a high plasma level of glucose, insulin and free fatty acids have an obvious role in the induction of cardiac *Scd1* expression in obese rats [155]. Consequently, these factors could also account for an enhanced Scd1 gene expression during HF pathogenesis.

4.6.3. Role of *SCD1* in causing diseases

The products resulting from *SCD1* catalysis reaction are mainly MUFAs. MUFAs are considered as substrates for the synthesis of lipids involving phospholipids and triglycerides. Additionally, MUFAs can be used as regulators in terms of cell signaling and cellular differentiation. Therefore, any variation in SCD1 activity in humans and animals is predicted to make substantial effects on several physiological processes such as cellular differentiation, and insulin sensitivity. In addition, variations in SCD1 activity can contribute or cause diseases including metabolic syndrome and obesity. It has been shown that the loss of SCD1 function helps to prevent overweight even after intake of high fat meals [140]. The highly upregulated *SCD1* is also associated with the elevation of triglyceride levels which can increase the incidence of hyperlipidemia [173]. It has been shown that the hepatic *Scd1* and other lipogenic genes are overexpressed in mice, which consumed high carbohydrate food. The up-regulation of *Scd1* was accompanied by a substantial increase in the production of MUFAs and hepatic

triglycerides. The induction of *Scd1* by carbohydrates can be attributed to the activation of *SREBP-1c* mediated by the action of insulin [174].

It has also been demonstrated that *Scd1* deficiency caused an upregulation of genes responsible for lipid oxidation and down regulation of genes responsible for lipid synthesis, which subsequently caused a reduction in triglyceride synthesis and storage [175].

Scd1 reduction can also improve insulin signaling. This could be due to the inhibition of protein-tyrosine phosphatase 1B. Therefore, the targeting of the *SCD1* gene could be a key for the treatment of insulin resistance and diabetes [176].

The elevation of *SCD1* might have the ability to promote the progression of cancer, such as breast cancer. This is more likely because cancer cells require an increased synthesis of FA to proliferate. The massive amount of FA synthesis is mainly obtained by overexpression of genes encoding FA biosynthetic enzymes. The increased MUFAs due to the enhanced FA desaturation by *SCD1* could be a key factor for progression of malignant cells [177].

4.6.3.1. Role of *SCD1* in obesity

Obesity is a substantial health concern that can cause increased blood pressure, insulin resistance, diabetes, CAD and HF. *SCD1* is considered as an important body-weight regulator. *SCD1* is the rate-limiting enzyme in the synthesis of MUFAs, of which the most common fatty acids and MUFAs are found in triglycerides, cholesterol esters, wax esters and phospholipids. Mice with *Scd1* deficiency have an enhanced energy expenditure and insulin sensitivity, and a decreased body adiposity. Besides, *Scd1* knockout mice show an up-regulated expression of genes responsible for lipid oxidation and a down-regulated expression of genes encoding enzymes responsible for lipid synthesis. Taken together, reduction of *SCD1/Scd1* expression could be beneficial to treat obesity and overweight [178].

4.6.3.2. Role of *SCD1* in heart diseases

Heart diseases such as CAD, hypertension and cardiomyopathy are the main consequences of obesity and leptin resistance, which promote FA overload in cardiac muscles and cardiac lipid accumulation [179]. Based on several studies, the accumulation of excessive fatty acids and

the subsequent lipotoxic metabolites such as ceramides have a role in HF, cardiomyopathy and cardiomyocyte apoptosis [180, 181]. Scd1 can regulate the metabolism of ceramide. The deficiency of *Scd1* may lead to a reduction of the activity of serine palmitoyltransferase (SPT) and the level of its mRNA. SPT is the enzyme responsible for de novo synthesis of ceramide. The reduction of SPT activity as well as the level of long-chain fatty acyl-CoA such as palmitoyl-CoA can substantially reduce the content of ceramide in oxidative muscles of *Scd1* knockout mice [182]. The *Scd1* knockout mice are not susceptible to weight gain and hypometabolism. Mice with *Scd1* gene mutation were substantially leaner and had more energy expenditure than the control mice. In addition, the *Scd1* mutation led to a better liver condition and lower levels of triglycerides and very low density lipoprotein (VLDL) [183].

Another study demonstrated that mice lacking the *Scd1* gene show an inhibited uptake and oxidation of FA but an increased transport and oxidation of glucose in the heart. This switch from FA to glucose utilization is enhanced by the induction of insulin signaling, reduced FA contents and a reduced expression of cardiac FA oxidation genes [184]. Taken together, *Scd1* deficiency could be beneficial to avoid HF risk factors.

4.6.3.3. Role of *SCD1* in lipid synthesis

An obvious feature of mice with *Scd1* deficiency is the absence of obesity during a high carbohydrate regimen. Most research studies indicate that *Scd1*-deficient mice are protected from diet-induced overweight due to a reduction in hepatic lipogenic gene expression [175]. Additionally, the lack of *Scd1* could lead to lower levels of lipids in most body parts because the *Scd1* gene is ubiquitously expressed in the body [150]. Furthermore, the reduction of *Scd1* gene expression in mice noticeably affected the expression of hepatic genes that are responsible for the synthesis of fatty acids. These genes include fatty acid synthase (*Fasn*), acetyl-CoA carboxylase (*Acc*), SREBP-1c and fatty acid elongase 6 (*Elovl6*) [157, 175].

Moreover, inhibition of *Scd1* affects most tissues such as liver and adipose tissue, and *Scd1*-deficient mice have a lower production of different kinds of lipids including TAGs, cholesterol esters, phospholipids, wax esters, and alkyl-diacylglycerols [185, 186]. For example, monounsaturated palmitoleate and oleate are the main MUFAs of adipose tissue and hepatic TAGs, cholesterol esters and phospholipids (Figure 6) [157, 187]. Man et al. (2006), mentioned another hypothesis of

lipid biosynthesis by the action of *Scd1* [188]. Their experiments with HeLa cells showed that SCD1 can co-localize with diacylglycerol acyltransferase 2 (DGAT2) on the endoplasmic reticulum [188]. There are two isoforms of DGAT. The liver isoform is DGAT1 while the adipose tissue isoform is DGAT2. These isoforms can have a role in the synthesis of most endogenous triglycerides [189, 190]. Unlike DGAT1, which is downstream of DGAT2 and works mainly on exogenous FA, DGAT2 is likely to be associated with diacylglycerol production by the process of esterification of endogenously synthesized FA [189, 191].
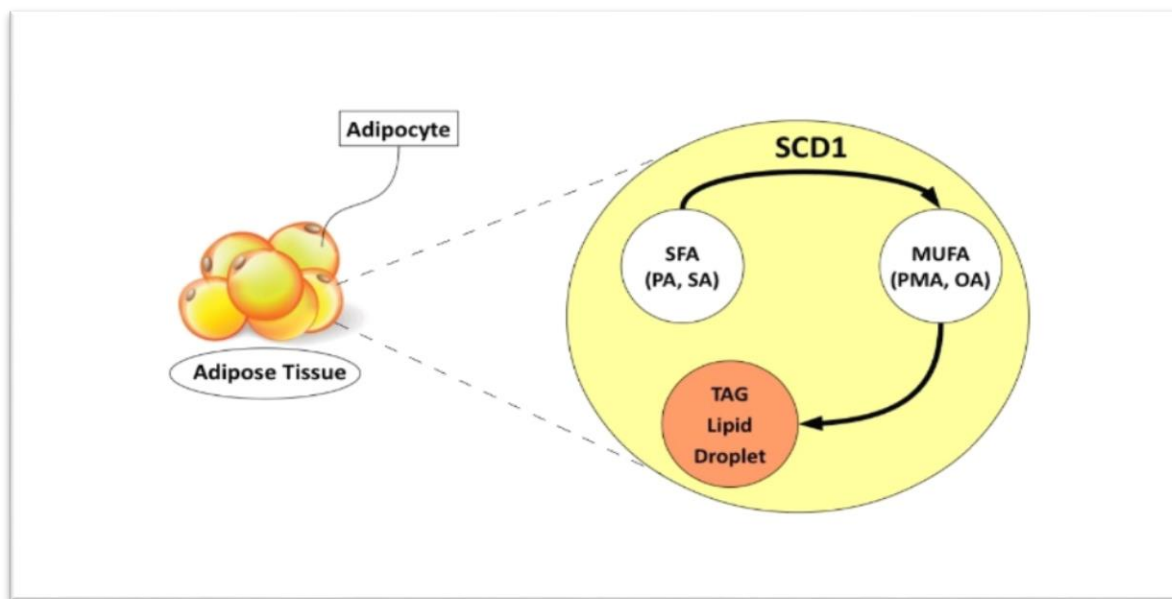
Figure 6: The MUFAs provided by SCD1 are the main fatty acids utilized for TAGs synthesis in lipogenic tissues including the adipose tissue and liver.
MUFAs, monounsaturated fatty acids; SCD1, stearoyl-CoA desaturase 1; TAGs, triacylglycerol; PA, palmitate; SA, stearate; PMA, palmitoleate; OA, oleate [157, 187].

Man et al. (2006), demonstrated that the desaturation of both ingested and endogenous palmitate and stearate, by SCD1 is likely to be channeled through DGAT2 for the production of TAGs. This process can be inhibited by the reduction of SCD1 activity. Additionally, it has been indicated that reduction of SCD1 tends to reduce TAGs synthesis due to the lack of SCD1, which can reduce the level of SFA and inhibit FA synthesis as well as MUFAs causing TAG formation [136, 160, 192].

4.6.3.4. Role of SCD1 in fatty acid oxidation

It seems that *Scd1*-deficient mice have protections against overweight not only because of reduction of FA and lipid synthesis, but also due to the elevation of FA oxidation and energy expenditure [188]. There are many hepatic genes responsible for FA oxidation including carnitine palmitoyltransferase 1 (*Cpt1*), very long chain acyl-CoA dehydrogenase (*Vlcad*) and acyl-CoA oxidase (*Acox*). The expression of these genes are increased in *Scd1* knockout mice compared to the control ones [175]. In addition, the activity of AMP-activated protein kinase (Ampk) was elevated in *Scd1* knockout mice compared to controls. AMP-activated protein kinase has a crucial role in FA oxidation. The phosphorylation of Ampk can stop the activity of Acc through the action of phosphorylation leading to reduced malonyl-CoA contents. Then, the transport of FA into mitochondria for the purpose of FA oxidation can be enhanced by Cpt1 because the reduction of malonyl-CoA can reduce Cpt1 inhibition [193]. Moreover, the contents of SFAs are usually increased in mice that lack the *Scd1* gene. SFAs can contribute to a reduction of malonyl CoA level leading to enhanced FA oxidation [175].

4.6.3.5. Role of *SCD1* in adipocyte differentiation

Adipocyte differentiation, which is known as adipogenesis, is a complicated pathway that comprises the induction of genes responsible for lipid biosynthesis. The mechanism of adipocyte differentiation has been elucidated in recent years. In vitro experiments, which were performed on cell lines such as 3T3-L1 and F-442A preadipocytes, are useful to study the pathway of adipocyte differentiation. These cells express certain genes such as activated CCAAT/enhancer-binding protein alpha (C/EBP-α) and *PPARG* to aid the induction of lipogenic genes. Many possible factors such as hormones, certain foods and genetic constitution can affect adipose tissue expression by affecting the expression of transcription factors. C/EBP and PPAR groups are the main examples of transcription factors and regulators of adipogenesis. Studying these transcription factors and their regulatory effects on adipose tissue development, provides insights into adipocyte differentiation as well as prevention of obesity and related pathologies [194].

It has been shown that the expression levels of *Scd1* and *Scd2* were increased 20-fold and 1.8-fold, respectively, during 3T3- cell culture. The upregulation of both *Scd1* and *Scd2* appeared through the differentiation of 3T3-L1 preadipocytes to adipocytes together with increased

contents of adipocyte determination and differentiation factor 1 (*Add1*) as well as *Srebp-1c*. Taken together, induction of both *Scd1* and *Scd2* transcription in 3T3-L1 preadipocytes is associated with increased levels of nuclear *Srebp-1c* and *Add1* [163]. It has also been observed that the *Scd1* mRNA level and activity substantially rose via 3T3-L1 differentiation. The significant induction of *Scd1* has led to a production of massive amounts of endogenous MUFAs that are involved in the formation of phospholipids and triglyceride cellular membrane components. These led to increased amounts of lipids inside developing adipocytes. Kim and Ntambi (1999), have demonstrated that the mRNA of *Scd1* and *Scd2* were significantly induced in parallel with the induction of MUFAs (palmitoleate and oleate) during the differentiation of 3T3-L1 preadipocytes to adipocytes [195]. Altogether, a substantial rise in *Scd1* expression and activity is the leading cause of excessive lipid production in growing adipocytes.

4.6.3.6. Role of SCD1 in cell membrane fluidity

SCD1 activity has the potential to affect the fluidity of cell membranes. MUFAS which are produced by the help of SCD1 are considered as the main components of phospholipids of membranes. Consequently, any change in SCD1 activity can influence the ratio between SFAs and MUFAs and ultimately change the membrane fluidity as well as cell signaling pathways affecting many parameters including insulin sensitivity. For example, *Scd1*-deficient mice showed increased levels of SFAs compared to MUFAs in phospholipids and have a decreased fluidity of the cell membrane. The decreased membrane fluidity could promote insulin signalling impairment.

4.6.3.7. Role of SCD1 in Alzheimer's disease

Alzheimer's disease is the main cause of dementia in adults and associated with memory loss, deficits in language processing, and visuospatial impairment [196]. Age is the main risk factor for Alzheimer's disease. Up to date, there is an incomplete understanding of the association between aging and pathological Alzheimer's disease factors including excessive accumulation of Aβ peptides and hyperphosphorylated tau protein in brains. However, it is well documented that the progression of Alzheimer's disease is affected by various age-related conditions that are associated with metabolic disorders such as atherosclerosis and diabetes [197-199]. Particularly, there is an association between changes in the metabolism of lipids and Alzheimer's disease. As an

example, some inherited isoforms of the lipid -carrier protein, such as apolipoprotein E (ApoE), are known to enhance the incidence of Alzheimer's disease [200]. In addition, multiple studies of frozen brain samples have documented the presence of excessive amounts of many lipids in patients with Alzheimer's disease. The lipid abnormalities include alteration in ceramides, n-3 PUFAs and PUFAs-derived signalling lipids. Recent studies indicated that the level of MUFAs are substantially elevated in brain tissue of patients with Alzheimer's disease. This elevation was apparently accompanied by cognitive impairment and increased transcription of brain tissue *SCD1*, which is responsible for the production of MUFAs [201-205].

4.6.3.8. Role of SCD1 in cancer

A lower SFA/MUFA synthesis ratio has been observed in patients who suffer from pancreatic, liver, colon, rectum, breast and prostate cancer. A change in the ratio of SFA to MUFA has been indicated to be a sign of breast and prostate cancer [206-210]. An elevated level of MUFAs was identified in transformed cells and cancerous tissues [211-215]. This evidence is consistent with findings that the expression of *SCD1* was substantially increased in many human malignant cells [216-219]. In addition, the elevated *SCD1* expression was associated with poor prognosis and tumour aggressiveness in patients with malignancies of liver, thyroid, prostate, pancreas, kidney, skin, and breast [213, 220-223]. Therefore, targeting of *SCD1* expression could be considered as a key factor to treat cancer.

4.6.3.9. Role of *SCD1* in inflammation

The results of recent studies regarding the impact of *SCD1* on inflammation are relatively paradoxical. Many studies indicate that the lack of *SCD1* is likely contributing to increased inflammation while other studies opposed this concept. It has been shown, that a pro-inflammatory condition, which was induced by the elevation of pro-inflammatory cytokines such as IL-6, IL-1β and IL-12p70, has appeared in mice with dyslipidemia lacking *SCD1* and low-density lipoprotein (LDL) receptor (Ldlr-/-) in comparison with same kind of mice but having *SCD1* [224].

4.6.3.9.1. Role of *SCD1* in cellular inflammation

SCD1 is an enzyme that is responsible for regulating the homeostasis of SFAs and MUFAs, which are essential fatty acids in humans and animals. The role of fatty acids in the regulation of cellular inflammation has been recognized in many studies. Previous research studies mentioned that intake of (n-6) PUFAs including arachidonic acid [20:4(n6)] can lead to an elevation of cellular inflammation. The inflammatory effect generally occurs when arachidonic acid is converted into eicosanoids by the help of cyclooxygenase enzymes [225]. However, long-chain (n-3) PUFAs including eicosapentaenoic acid and docosahexaenoic acid that can be incorporated into phospholipids of cell membranes have the ability to decrease the conversion of arachidonic acid to eicosanoids and, subsequently, reduce inflammation [226]. Several research studies noted that free fatty acids, in particular SFAs, have a pro-inflammatory effect on different kinds of cells including macrophages, liver and muscle cells [227-229]. SFAs can work as ligands for immune receptors of the cell surface and directly elevate inflammation. Members of the Toll-like receptor (TLR) family are examples of immune cell receptors that bind ligands including SFA [227, 230]. Consequently, by the conversion of SFAs into various kinds of MUFAs, *SCD1* is expected to have multiple and diverse effects on inflammatory processes.

4.6.3.9.2. Role of *SCD1* in the regulation of inflammation in liver cells

The liver plays an important role in regulating many metabolic processes. That makes researchers interested in investigating the impact of hepatic *Scd1* deficiency on the regulation of metabolism. A reduction in hepatic *Scd1* expression has a substantial metabolic impact on liver steatosis. Various studies concluded that *Scd1* up-regulation is beneficial to maintain the function of the liver after exposure to various stressful situations [231, 232]. Rizki et al. (2006) have noted that mice fed a methionine- and choline-deficient diet (MCD) had a significantly reduced *Scd1* expression in their livers. A methionine- and choline-deficient diet induces hepatic steatosis in experimental models [231, 232]. Suffering of the liver, liver cell apoptosis and the enhancement of the stress response in liver cells have been clearly seen in mice lacking *Scd1* that were consuming MCD, although these mice had reduced liver steatosis [231, 232]. This is probably caused by insufficient breakdown of toxic SFAs into beneficial MUFAs leading to reduced storage of MUFAs in the liver. This report is consistent with another study which showed that *Scd1* knockout mice, which consumed a very low-fat diet, had an extreme

hepatocellular stress response and liver damage together with a reduced expression of genes involved in lipid detoxification [233].

4.6.3.9.3. Role of *SCD1* in Beta cell (β-cell) impairment

Some pathological conditions appear after *SCD1* inhibition due to the generation of inflammatory and cellular stress responses induced by SFA-associated inflammation. Various studies have revealed that *SCD1* suppression contributes to increased cellular stress and pancreatic β-cell impairment [234-236]. β-cells are commonly very responsive to SFA- mediated lipotoxicity [236, 237]. The induction of *SCD1* expression in β-cells makes these cells able to be protected from SFA-induced toxicity and apoptosis. In contrast, *SCD1* inhibition is more likely to develop harmful consequences of SFAs on β-cells [238]. *SCD1* catalyses the conversion of lipotoxic SFAs to MUFAs, and possibly this pathway is a key factor for maintaining the function of β-cells [235, 239]. Despite the in vitro observations that a reduction of *SCD1* appeared to have negative effects on β-cells, *Scd1*-/- models have revealed that a decreased *Scd1* level might also have useful effects on β-cells such as an improvement of insulin sensitivity [140, 240, 241]. The results of both in vitro and in vivo experiments relating to the association of *SCD1* activity and diabetes seemed inconsistent. Experiments that used obese (ob/ob) mice have also identified effects of *Scd1* on β-cell function. Obese (ob/ob) mice with *Scd1* knockdown are resistant to weight gain but these mice are more susceptible to SFA induced lipotoxicity and impairment of insulin secretion causing severe diabetes [242, 243]. On the other hand, *Scd1* inhibition during diet-induced weight gain of ob/ob mice revealed that the expression of the leptin gene is essential to develop insulin sensitivity during *Scd1* deficiency. The mechanism of this action is not yet fully understood [242].

4.6.3.9.4. Role of *SCD1* in adipose tissue and adipocyte inflammation

Even though a decrease of *SCD1* levels is seemingly harmful for the function of β-cells due to cellular stress responses, these responses did not appear in other kinds of cells. A study revealed that *Scd1* shortage provided a significant protection against white adipose tissue inflammation in mice with high-fat intake-induced weight gain [244]. The study used isolated primary adipocytes and showed that the inhibition of *Scd1* in adipose cells induced a reduction in the inflammatory response to lipopolysaccharide (LPS). Not only this, but *Scd1*

inhibition also evoked a limited paracrine activation of inflammation in macrophages as well as endothelial cells [244]. The diminished paracrine impact on inflammation was apparently caused by *Scd1* inhibition which in turn resulted in a reduction in the level of oleate (a major MUFA product). The relative contents of SFAs were strongly increased in adipocytes with *Scd1* deficiency in comparison with control adipocytes. A different study indicated that the addition of oleate to macrophage cells also triggered inflammation [230]. Another study reported that the expression of *Scd1* was elevated in parallel with increased white adipose tissue and liver inflammation in mice with genetic predisposition to insulin resistance and tissue inhibitor of metalloproteinase 3 deficiency [245].

4.6.3.9.5. Role of *SCD1* in macrophage inflammation and atherosclerosis

Macrophage inflammation is considered a contributing factor to an increased risk of developing atherosclerosis, a fatal CVD. *SCD1* seems to be involved in regulating pathomechanisms of atherosclerosis through the regulation of inflammatory responses of macrophages. One research study performed on elderly Swedish people indicates that the increase in serum C-reactive protein (CRP) level, which is an acute – phase protein that is responsible for inflammation and CAD, was apparently associated with an increased *SCD1* activity [246]. Another study showed that the induction of *SCD1* activity provided high CRP levels in a large group of adult Swedish men, who have been monitored for about twenty years [247].

4.6.3.9.6. Protective role of *SCD1* in endothelial cell inflammation

Endothelial cell inflammation can also be regulated by *SCD1*. Endothelial cells are considered as an essential type of cells responsible for the metabolic syndrome [248, 249]. Endothelial cells are major constituents of blood vessels such as cardiac arteries. Any defect in the homeostasis of endothelial cells as a result of lipotoxicity under the condition of metabolic disorders can induce systemic inflammation and contribute to harmful effects associated with metabolic diseases such as CVD [250-252]. The *SCD1* enzyme has received great attention because of its contribution in maintaining the function of endothelial cells [253]. The study analyzed the expression of *SCD1* in human arterial endothelial cells, found that human arterial endothelial cells did not show an enhanced expression of *SCD1* when exposed to SFA compared to other cell types. As a result, these cells are more sensitive to lipotoxicity, cell

apoptosis and induction of inflammatory cytokines [253]. Based on the same study, after the activation of LXR signalling pathway using LXR activator (TO-901317) for the purpose to substantially increase *SCD1* expression, human arterial endothelial cells appeared to be resistant to SFA (palmitate)-induced lipotoxicity, due to elevated desaturation of SFA and facilitated esterification and lipid storage.

4.6.3.9.7. Role of *SCD1* in the regulation of myocyte function

Several studies suggested that any change in *SCD1* expression has effects on the modulation of myocyte function. However, the functions of SCD1 in the myocytes are diverse. On one hand, reports indicated that the loss of *SCD1* in myocytes might have positive effects including downregulation of protein tyrosine phosphatase 1B, reduction in ceramide formation by decreased expression of serine palmitatoyl transferase, and increased breakdown of fatty acids and β-oxidation [176, 182, 254]. On the other hand, other reports indicated that *SCD1* is potentially able to maintain the function of muscles. *SCD1* expression was significantly increased in human skeletal muscles after aerobic activity which had led to a significant prevention of FA-mediated insulin resistance [255]. This impact was related to the breakdown of FA and their metabolites forming neutralized lipids such as triglycerides, and a subsequently decreased muscular pro-inflammatory response. In addition, upregulation of *SCD1* expression in cultivated rat L6 myocytes has been shown to increase the esterification of triacylglycerol and decreased the accumulation of ceramide and diacylglycerol, and eventually provided a protection to myocytes against FA-mediated cellular toxicity [256]. According to several studies that used primary human myotubes, overexpression of *SCD1* was negatively associated with inflammation and positively related to insulin sensitivity [257].

4.6.3.9.8. Role of *SCD1* in sebaceous gland hypoplasia and skin inflammation

As mentioned previously, *SCD1* expression is ubiquitous in most tissues, including the sebaceous gland that is present in the skin of mammals [258]. Sebum can be produced by the sebaceous gland and it has high levels of lipids, including cholesterol, cholesteryl ester, wax esters and triglycerides. In fact, these kinds of lipids are important for the functionality of the skin as they provide skin lubrication plus the protection against skin dryness [185]. Endogenous MUFAs formed as a consequence of *SCD1* induction can play an important role

for the development and maintenance of skin integrity. Some experiments indicate that global *Scd1* knockout and skin-specific *Scd1* knockout (Scd1 SKO) mice noticeably had a severe pathological skin phenotype including hair loss, sebaceous gland hypoplasia, skin inflammation and enhanced skin barrier permeability [185, 259, 260]. The occurrence of skin abnormalities can be attributed to a reduction of *Scd1* expression. The reduction of *Scd1* was accompanied by a significant change in the lipid profile of the skin causing insufficient levels of cholesteryl ester, wax esters and triglycerides in skin, although the levels of free cholesterol ester were dramatically increased [185].

4.6.3.9.9. Role of *SCD1* in intestinal colitis

Beside of liver stress and aortic atherosclerosis, *SCD1* has been identified to play a role in a kind of inflammation, which is called intestinal colitis. The metabolic profiling study indicated that the expression of *Scd1* in the liver was decreased in mouse models with acute colitis induced by dextran sulfate sodium [261]. This research also revealed that the induction of severe colitis by dextran sulfate sodium was aggravated in *Scd1* knockout mice whereas the diet supplementation of oleate relieved the phenotype. The importance of *Scd1* expression in modulating dextran sulfate sodium-induced intestinal colitis could be seen in frame of the relationship between metabolic disease, inflammation and cellular detoxification. However, results of this study were complex because *Scd1*-deficient mice consumed more water and the provision of dextran sulfate sodium was made by water. After adjustment of dextran sulfate sodium consumption according to the amount of water consumed, *Scd1* null mice showed no more severe intestinal colitis than wild-type mice [262]. Therefore, the contribution of *Scd1* to acute colitis requires more studies.

Taken together, SCD1 is a multifaceted enzyme with many physiological and pathophysiological functions, whose role in the pathogenesis of prevailing metabolic and cardiovascular diseases is only at the dawn of being elucidated.

4.7. Aim of thesis

The main goal of this thesis is to analyze and identify pathomechanisms contributing to signs and symptoms of HF and cardiac remodeling. To identify genes regulated during the pathogenesis of HF and cardiac remodeling, a gene ontology (GO) analysis of cardiac whole genome microarray gene expression data from different HF models is performed to identify most upregulated genes at the onset of HF. The study applies data from chronic pressure overload-induced HF models of Apoe-/- and non-transgenic B6 mice, HF triggered by atherosclerosis- induced aortic coarctation of aged, 18-month-old Apoe-/- mice and HF trigged by fluid retention and cardiac lipotoxicity of Apoe-/- mice treated with the *Pparg* agonist, rosiglitazone. The chosen experimental models are clinically relevant to human HF as they reproduce major HF risk factors such as chronic pressure overload and long-term hypercholesterolemia.

The second aim of this thesis is to investigate the impact of an increased cardiac *SCD1* content on the cardiac phenotype of transgenic mice with myocardium specific expression of *SCD1* by determination of the LVEF, and the heart-to-body weight ratio in combination with histological analysis to characterize the cardiac phenotype.

The third aim is to characterize the cardiac phenotype of *SCD1*-transgenic mice using genome microarray gene expression analysis determination of heart failure-related genes.

The fourth aim is to search for pathomechanisms underlying *SCD1*- induced cardiac dysfunction focusing on the impact of *SCD1* on the protein levels of the heart failure- enhancing angiotensin II AT1 receptor via in vivo and in vitro experiments.

5. MATERIALS AND METHODS

5.1. Materials

Substance	Company	Lot No
b-mercaptoethanol	Sigma-Aldrich	63689
2-[4-(2-hydroxyethyl)-1-piperazin]ethanesulfonic acid (HEPES)	Biosolve	0008042359BS
2-Propanol	Merck	1.09634.1000
3,3'-diaminobenzidine tetrahydrochloride (DAB)	Sigma Aldrich	D3939
30% Acrylamide/Bis solution	Bio-Rad Laboratories AG	1610158
4x LDS sample buffer	Invitrogen	B0008
Acetic Acid, glacial	Merck	1.00063.1000
Acetone	Merck	1.00014.2500
Agarose MP	Cleaver Scientific	9012-36-6
Ammonium persulfate (APS)	Bio-Rad Laboratories AG	1610700
Boric acid	Merck	1.00165.1000
Bovine Serum Albumin (BSA)	Sigma-Aldrich	A8022
Coomassie brilliant blue	Merck	1.12553.0025
D (+)-glucose monohydrate	Merck	1.04074.0500
Desoxyribonucleotide Desoxyribonucleotide mixture (dNTPs)	New England BioLabs	N0447S
Dimethyl sulfoxide (DMSO)	Sigma-Aldrich	D2438
ECL Western Blotting detection reagent	Amersham Prime	RPN2232
EndoFree Plasmid Maxi Kit	QIAGEN	12362
Eosin Y solution 0,5% aqueous	Sigma-Aldrich	HT110216
Ethanol	VWR Chemicals	20821.296
Ethidium bromide	Merck	1.11608.0030
Ethylenediaminetetraacetic acid (EDTA) solution (0.5M)	Sigma-Aldrich	O3690
Fetal bovine serum (FBS)	Thermo Fisher Scientific AG hyclone	RZG35920
Formalin solution, neutral buffered, 10%	Sigma-Aldrich	SLBT5369
GeneRuler 1kb DNA ladder 0.5 µg/µL	Thermo Fischer Scientific AG	SM0311
Herculase II fusion DNA polymerase	Agilent Technologies AG	600675
Herculase II Reaction buffer 5x	Agilent Technologies AG	600675
Hind III	England BioLabs	R0104S
Human chorionic gonadotropin (hCG)	Sigma-Aldrich	C0434
Hyaluronidase from bovine testes	Sigma-Aldrich	H3884
Hydrogen peroxide (30%)	Merck	1.07209.0250

M16 medium	Sigma-Aldrich	M7292
M2 medium	Sigma-Aldrich	M7167
Magnesium sulfate heptahydrate (MgSO4x7H2O)	Merck	1.05886.0500
Mayer's hemalum solution	Merck	1.09249.0500
Methanol	Merck	1.06009.5000
Mineral oil	Sigma-Aldrich	M5310
MOPS SDS running buffer	Invitrogen	B000102
PageRuler Plus Prestained Protein Ladder	Thermo Fisher Scientific AG	26619
PBS (Dulbecco's phosphate buffered saline)	Sigma-Aldrich	D8537
Penicillin–Streptomycin Solution Hybri-Max	Sigma-Aldrich	P7539
Penicillin-Streptomycin	Sigma-Aldrich	P0781
Phosphate buffered saline (PBS)	Sigma-Aldrich	D8537
Poly-Mount Xylene	Polyscience	24176
Polyethylene glycol (PEG) 3000	Merck	8.17019.1000
Potassium chloride	Sigma-Aldrich	1.04936.1000
Pregnant mare serum gonatropin (PMSG)	Sigma-Aldrich	G4877
Protease inhibitor cocktail	Sigma-Aldrich	P8340
Proteinase K	Roche	03115879001
PureLink HiPure Plasmid Purification Miniprep Kit	Invitrogen	K2100-02
PureLink HiPure Plasmid Purification Midiprep Kit	Invitrogen	K210015
PureLink HiPure Plasmid Purification Maxiprep Kit	Invitrogen	K210016
PVDF membrane (Immobilon-P, 0.45 μm)	Merck	IPVH00010
QIAquick Gel Extraction Kit	QIAGEN	28704
RNAlater	QIAGEN	76104
Rneasy Midi kit	QIAGEN	75142
Roti®-Quant	Roth GmbH + Co. KG	KG K015.02
Sal I	New England BioLabs	R0138T
Sodium chloride (NaCl)	Sigma-Aldrich	71380
Sodium desoxycholate	Sigma-Aldrich	D6750
Sodium Dodecyl Sulfate (SDS)	Bio-Rad Laboratories AG	1610302
Sodium fluoride (NaF)	Merck	1.064490250
Sodium hydroxide (NaOH)	Merck	1.06469.1000
T4 DNA Ligase (6 U/μL)	New England BioLabs	M0202
Taq polymerase	Sigma-Aldrich D1806	D1806 TC-100
TE buffer (10 mM TRIS pH 8, 0.1 mM EDTA)	Invitrogen	12090015
TEMED (N,N,N',N'-tetramethylethylenediamine)	Carl Roth GmbH + Co. KG	2367.3
Tetenal Superfix MRP	Tetenal	104462
Tetenal, Roentoroll HC	Tetenal	104450
Tris(hydroxymethyl)aminomethane (Tris)	Biosolve	0020092391BS
Triton X-100	Merck	1.08603.1000

Trizma® hydrochloride solution (1M)	Sigma-Aldrich	T2194
Tryptan blue	Sigma-Aldrich	T6146
Tween 20	Merck	8.22184.0500
Urea Merck	Merck	1.08487.1000
X-ray films (Super R, Fuji Medical x-ray film)	Fuji Medical	
XL1 Blue E. coli bacteria	Stratagene	200249

5.2. Molecular biology methods

Polymerase chain reaction (PCR) for deoxyribonucleic acid (DNA) amplification and single colony screening

Herculase II fusion DNA polymerase (Agilent) was used for amplifying complementary DNA (cDNA) fragments, whereas Taq DNA polymerase (NEB) was utilised for single colony screening of bacterial colonies. The PCR was conducted in the provided buffers (supplemented with 2.0 mM magnesium (Mg^{2+})), with 1 μL of Herculase II or 1.25 Units of Taq polymerase per 50 μL reaction. Deoxyribonucleotide triphosphate (dNTPs) were employed at a concentration of 200 μM while 0.1-1 ng DNA acted as the template. The standard concentration of each oligonucleotide primer was 0.4 μM. The process of amplifying the DNA was conducted on a Thermocycler 3000 (Biometra) with a standard program as detailed below (Table: 1).

Step	Temperature	Time	Cycles
1	95°C	2 min	1X
2	95°C	20 s	
3	55-60°C	20 s	25-30X
4	72°C	60 s/1000bp	
5	72°C	10 min	1X

Table 1: Standard PCR program.
In Step 1, the double stranded DNA (dsDNA) was firstly melted, then 25-30 amplification cycles were performed. Each amplification cycle consisted of Step 2 (dsDNA melting), followed by Step 3 (annealing), and then Step 4 (primer extension). The standard PCR program was completed by a final elongation step of 10 minutes at 72 °C (Step 5).

Preparation of agarose gel electrophoresis

Separation of PCR products was performed via agarose gel electrophoresis. DNA resolution is influenced by the concentration of the agarose and the constitution of the buffer. Separation of smaller fragments was achieved using 2% (w/v) agarose, whereas for larger fragments, 0.8-1.5% (w/v) agarose gels were employed. To visualise the DNA, ethidium bromide (stock solution: 10 mg/ml) at an ultimate concentration of 0.5 µg/ml was utilised. Preparation of the gel was conducted using either standard Tris base, acetic acid and EDTA (TAE) buffer (40 mM Tris, 20 mM glacial acetic acid, 2 mM ethylenediaminetetraacetic acid (EDTA)) or Tris-borate-EDTA (TBE) buffer (89 mM Tris, 89 mM boric acid, 2 mM EDTA) for small-sized fragments. To identify the size of the fragments, a DNA ladder (Generuler 1 kb; Thermofisher) was operated concurrently to the samples.

Extraction of gene fragments from agarose gels

The process of cleaning the PCR products and removing primers, enzymes, dyes and salts, involved the separation of PCR samples via agarose gel electrophoresis. Excision of the DNA from the gel was performed under ultraviolet light (UV)-light (365 nm) followed by extraction utilising a QIAquick Gel Extraction Kit according to the protocol of the manufacturer (Qiagen). Purification of a maximum of 10 µg DNA for each column was achieved in line with the protocol supplied by the manufacturer, followed by elution using 30 µl Tris-EDTA buffer (TE) buffer.

Digestion of DNA by restriction enzymes

For digestion of DNA by restriction enzymes, appropriate enzymes were selected. Enzymes were acquired from New England BioLabs (NEB). Supplied buffer was utilised and the reaction parameters were selected in accordance with the guidelines provided by the manufacturer.

Ligation of DNA fragments

Ligation of the digested PCR fragments and vector backbone was performed in a reaction volume of 10 µL overnight using T4 DNA Ligase in the provided T4 DNA Ligase Reaction Buffer (NEB) at a temperature of 16°C. The amount of vector backbone (usually 200 ng) to insert was set at molar ratio of 1:4.

Heat shock transformation of XL1 blue *Escherichia coli* (*E.coli*)

Transformation of bacteria was performed using heat shock transformation. To this end, thawing of 100 µl of competent *Escherichia coli (E. coli)* XL1 blue bacteria (Stratagene) was performed on ice, followed by the addition of 10 µl of ligation mixture or 1 µl of DNA stock solution. After an incubation on ice for 20 min, the bacteria-DNA complex was heat-pulsed in a water bath at 42°C for a period of 45 seconds, followed by incubation on ice for 2 minutes. Super optimal broth with catabolite (SOC) medium (900 µl) that had been warmed to 37° was introduced to the mixture, which was then incubated in the shaker (200 rpm) at 37°C for 30 min. A sample of the DNA-bacteria mixture (10-100 µl) was streaked onto warmed (37 °C) lysogeny broth (LB) agar plates which contained the suitable antibiotic for selecting the transformed bacteria. After overnight incubation at 37°C, single colonies were picked, inoculated in 2 ml lysogeny broth (LB) medium and bacteria were grown for 3-4 h at 37°C in a rotating incubator at a speed of 200 rpm. Thereafter, bacteria from the 1 ml culture medium were pelleted in a centrifuge at 16'000 x g for 1 min, then lysed using 100 µl of sterile water and subsequently employed for PCR screening of individual colonies.

Super optimal broth with catabolite repression (SOC) medium and Super Optimal Broth (SOB) medium preparation

50 ml of SOC medium was prepared by mixing 48 ml of SOB medium, 0.5 ml of 1 M $MgCl_2$, 0.5 ml of 1 M magnesium sulfate ($MgSO_4$), and 1 ml of 20 % (w/v) D(+)-glucose monohydrate.

To prepare 200 ml of SOB medium, 4 g of bacto-tryptone (Becton Dickinson), 1 g of bacto-yeast extract (Becton Dickinson), and 0.1 g sodium chloride (NaCl) were added to water and then mixed and sterilized.

Lysogeny broth (LB) medium and agar preparation

The preparation of LB medium was performed by dissolving 1 % (w/v) bacto-tryptone, 0.5% bacto-yeast extract, and 1 % (w/v) NaCl in water.

LB agar plates contained LB agar, which was prepared of 1.5 % (w/v) bacto-agar (Becton Dickinson) in LB medium.

Preparation of competent bacteria

E. coli XL1 blue bacteria were streaked onto LB plates without antibiotics and then allowed to grow overnight at a temperature of 37 Celsius (°C). A single colony was picked, inoculated in 5 ml of LB medium and cultivated overnight in a rotating incubator (200 rpm) at 37 °C. The next day, 1 ml of the resulting bacterial suspension was incubated with 119 ml of LB medium, and allowed to grow to mid-log phase (optical density (OD) 600 nm: 0.4-0.6). Bacteria were then isolated by pelleting in the centrifuge at a temperature of 4°C at 3000 x g for 10 minutes. The resulting pellet was re-suspended in 12 ml of transformation and storage buffer (TSB) buffer on ice, followed by aliquoting, flash freezing in liquid nitrogen and then storage at -80°C.

Transformation and storage buffer (TSB) medium preparation

For preparation of 100 ml of TSB medium, 10 g of polyethylene glycol (PEG) 3000 were dissolved in 40 ml of LB medium and the pH was adjusted to be 6.1. Then, 5 ml of dimethyl sulfoxide (DMSO), 2 ml of 1 M $MgSO_4$, and 2 ml of 1 M magnesium chloride ($MgCl_2$) were added. Finally, LB medium was added to make a final volume of 100 ml.

Isolation of plasmid DNA

A PureLink HiPure Plasmid Purification Kit (Invitrogen™ by ThermoFisher Scientific) was utilised to isolate plasmid DNA from the bacterial culture. A Plasmid Midiprep Kit was used to isolate low-copy plasmids from 100 ml of bacterial culture, while 25 ml of the culture were utilised to prepare the high-copy plasmid DNA. When using the Plasmid Maxiprep Kit, the volume of bacterial culture utilised was increased 8-fold. The process of preparing the materials was conducted in accordance with the manufacturer's guidelines (Invitrogen™ by ThermoFisher Scientific).

Quantification of DNA

Quantification of the dsDNA was performed via optical density (OD). Dilution of the DNA was conducted with 10 mM Tris-HCl, pH 7.5 and a Biophotometer (Eppendorf) was used to measure the absorbance at 260 nm. The purity of the sample was ascertained utilising the

260/280 ratio. A 260/280 ratio of 1.8-2.0 was utilised as an indicator of DNA with sufficiently high purity.

DNA sequencing and oligonucleotide primer synthesis

Sanger sequencing of DNA was conducted by Microsynth AG (Switzerland) in order to control for DNA sequence identity. Synthesis of the oligonucleotide primers was also performed by Microsynth AG (Switzerland).

Real-time quantitative reverse transcription PCR (real-time qRT-PCR)

For real-time qRT-PCR, total ribonucleic acid (RNA) was isolated from adherent human embryonic kidney 293 cells (HEK293) cells. After culture of cells for 36-42 h after transfection, adherent cells were rapidly washed with sterile, ice-cold phosphate-buffered saline (PBS), detached by scraping, collected by centrifugation at 4 °C in an Eppendorf centrifuge (12 000 rpm, 4 °C), and immediately lysed by the lysis buffer provided with the kit (RNeasy Mini Kit, Qiagen). Subsequent steps of total RNA isolation were performed according to the protocol of the manufacturer (Qiagen). Isolated RNA was quantified by the absorbance peak of 260 nm, and RNA quality was controlled by the absorbance ratio of A260/A280, which was ~2.0. RNA integrity and the absence of RNA degradation were confirmed by the presence of bright bands of the 18S and 28S ribosomal ribonucleic acid (rRNA) by denaturing formaldehyde-containing agarose gel electrophoresis. mRNA was reverse transcribed into cDNA and subjected to quantitative real-time PCR with LightCycler 480 SYBR Green I Master on a LightCycler 480 instrument (Roche Diagnostics) according to the protocol of the manufacturer (Roche Molecular Systems). Quantitative assessment of relative gene expression levels of *SCD1*, and angiotensin II receptor type 1 (*AGTR1*) or *AGTR1-Cerulean* was performed and normalized to the expression level of the endogenous control gene, beta actin (*ACTB)*, which did not change in relative expression.

The following primers were used for real-time qRT-PCR.
AGTR1 forward: 5`- CCG CCT TCG ACG CAC AAT GC - 3`
AGTR1 reverse: 5`- GGT CAG GCC CAG CCC TAT CG - 3`
SCD1 forward: 5` - TTC GTT GCC ACT TTC TTG CG - 3`
SCD1 reverse: 5` - AAG TTG ATG TGC CAG CGG TA - 3`

ACTB forward: 5`- AGG ATT CCT ATG TGG GCG AC - 3`

ACTB reverse: 5` - ATA GCA CAG CCT GGA TAG CAA - 3`

Analysis of RNA by denaturing, formaldehyde-containing agarose gel electrophoresis

For analysis of RNA integrity, denaturing, formaldehyde-containing agarose gel electrophoresis was performed.

For RNA denaturation, the RNA sample was heated for 15 minutes at 65 °C in denaturing buffer composed of:

COMPOSITION	VOLUME
TOTAL RNA (UP TO 30 µg):	4.5 µl
FORMALDEHYDE RUNNING BUFFER (10 X)	1.0 µl
FORMALDEHYDE	3.5 µl
FORMAMIDE	10.0 µl
ETHIDIUMBROMIDE (1 mg/ml)	1.0 µl

Table 2: Composition of denaturing buffer.
The composition of the formaldehyde running buffer (10-fold concentrated) was as follows:0.2 M 3-(N-morpholino)propanesulfonic acid (MOPS), pH 7.0, 50 mM sodium acetate, 10 mM EDTA, pH 8.0. Before loading, 2 µL of loading buffer (50 % (v/v) glycerol, 1 mM EDTA, pH 8.0, 0.25 % bromophenol blue, 0.25 % xylene cyanol FF) was added to the RNA sample. The RNA electrophoresis was performed on formaldehyde-containing agarose gels (1 g - 1.5 g agarose/100 ml, 10 ml/100 ml 10-fold concentrated formaldehyde running buffer, 5.1 ml/100 ml of 37 % HCHO) and electrophoresed in 1-fold concentrated running buffer.

5.3. Protein detection by immunoblot

Ultrapure deionized water (PURELAB Ultra, Lab water purification system; ELGA, United Kingdom) was utilised for all protein techniques.

5.3.1. Separation of proteins using sodium dodecyl sulfate–polyacrylamide gel electrophoresis (SDS-PAGE)

Samples of protein were dissolved in a suitable amount of 5x- sodium dodecyl sulfate (SDS) sample loading buffer, either including or not including urea. Protein samples were incubated at 50 °C for 30 minutes, and separated by SDS-PAGE. The gel was cast as a separating gel (7.5%-10% acrylamide and 0.2-0.27% bisacrylamide (w/v), 375 mM Tris-HCl (pH 8.8), 0.1% SDS) and then layered with a stacking gel (3.75% acrylamide and 0.16% bis-acrylamide (w/v), 125 mM Tris-HCl (pH 6.8), 0.1% SDS). Initiation of the polymerisation of the polyacrylamide was done with ammonium persulfate (APS), and acceleration of the reaction was facilitated by tetramethylethylenediamine (TEMED). In total, 0.0325% (w/v) of APS and 0.5 µl/ml of TEMED were utilised in the separation gel, while 0.1% (w/v) of APS and 1 µl/ml of TEMED were employed in the stacking gel. The process of resolving the proteins was conducted at 80 V in SDS running buffer (192 mM glycine, 25 mM Tris-HCl and 0.2% SDS) for 2-3 h. A pre-stained protein molecular weight marker (PageRuler Plus Prestained Protein Ladder, ThermoFisher Scientific) was loaded concurrently for the purpose of monitoring the separation of proteins in the electrophoresis process as well as to evaluate the efficiency of blotting. After protein separation, the stacking gel was cut off, and then the separation gel was either utilised for Western blotting or proteins were visualized directly in the gel by staining with Coomassie brilliant blue dye. The Coomassie brilliant blue staining procedure was performed by incubation of the gel with gentle agitation for >1 h in fixing solution (Staining solution without Coomassie) followed by incubation for > 1h in the Coomassie staining solution. Thereafter the staining solution was removed and the gel destained by incubation for 4-24 h in the destaining solution with gentle agitation and at least two changes of the solvents.

Coomassie staining solution

acetic acid	10%
methanol	50%
Coomassie brilliant blue R250	0.05%
dH2O	40 %

Destaining solution

acetic acid	10%
methanol	50%
dH2O	40 %

Table 3: Composition of Coomassie brilliant blue staining- and destaining solutions for Coomassie brilliant blue staining of proteins in SDS-PAGE gels.

5.3.2. Transfer of proteins onto polyvinylidene difluoride (PVDF) membranes using semi-dry blotting

Separation of the proteins by SDS-PAGE was followed by transferring them onto a PVDF membrane. Hence, a PVDF membrane (Immobilon-P, 0.45 µm) was initiated in methanol for a period of 7 minutes, then equilibrated in transfer buffer for further 30 minutes. Additionally, incubation of the acrylamide gel and two filter papers (Extra thick blot paper, Bio-Rad) was performed in transfer buffer for 45 minutes. During this time, the transfer buffer containing the gel was replaced twice. The process of blotting the proteins onto the membranes involved semi-dry blotting at 20 volt (V) and 0.04 ampere (A) for 40 minutes (Trans Blot SD semi-dry Transfer Cell, Bio-Rad). After electrophoretic protein transfer to the PVDF membrane, rinsing of the membrane in deionized water was performed five times for the purpose of removing any remaining methanol or gel debris, and then the membrane was stored in PBS (phosphate buffered saline) at a temperature of 4°C until further use.

The transfer buffer consisted of 192 mM glycine, 25 mM Tris, 0.2% (w/v) SDS and 20% (v/v) methanol. The PBS consists of 137 mM NaCl, 2.7 mM KCl, 6.5 mM Na_2HPO_4 and 1.5 mM KH_2PO_4.

5.3.3. Detection of proteins by immunoblot

Subsequent to transferring the proteins to the PVDF membrane, the blotting membrane was immersed in blocking buffer (PBS containing 0.5 % volume per volume (v/v) Tween 20 and 5 % weight by volume (w/v) bovine serum albumin (BSA)), followed by incubation for 1 h, during which the membrane was agitated. Thereafter, the primary antibody solution was added in blocking buffer for 1 h (dilution 1:2000) under gentle agitation. Subsequently, washing of the blot with PBST (phosphate buffered saline supplemented with Tween 20, 0.5 % (v/v)) was repeated four times, followed by incubation with the peroxidase (POD)-conjugated secondary antibody dilution (1: 40 000 of peroxidase-conjugated AffiniPure F(ab)$_2$ fragment goat anti-rabbit IgG, Fc fragment-specific with minimal cross-reaction to human serum proteins (Jackson ImmunoResearch Laboratories) or by enzyme-coupled protein A (Merck Millipore) dilution for a period of 30 minutes. Following the removal of the POD-conjugate dilution, six washing steps of the membrane were performed using PBST for 5 minutes each, and then additional washing processes were applied using PBS for the purpose of removing any remaining detergents. The bound POD-conjugate was visualised via chemiluminescence using a substrate for enhanced chemiluminescence (ECL^{TM}) Western Blotting detection reagent (ECL Prime Western Blotting Detection Reagent, or ECL Select, Amersham^{TM}, GE Healthcare Life Sciences). Visualisation of emitted light was performed by exposing X-ray films to the membrane. Afterwards, development (Tetenal, Roentoroll HC) and fixing (Tetenal Superfix MRP) of the films was conducted.

5.4. Antibodies used for the study

The following antibodies were used for the study: rabbit polyclonal anti-SCD1 antibodies (ab38869, Abcam) were raised against a synthetic peptide conjugated to keyhole limpet hemocyanin (KLH) derived within residues 50-150 of human SCD1; affinity-purified rabbit polyclonal anti-FASN antibodies were raised against an antigen encompassing amino acids 2305-2504 of human FASN [124]; rabbit monoclonal adiponectin antibody (C45B10) was

raised against human adiponectin (No, 2789; Cell Signaling); affinity-purified rabbit polyclonal anti-AT1 receptor antibodies were raised against an antigen encompassing amino acids 306-359 of human AGTR [263]. Secondary, peroxidase-conjugated AffiniPure F(ab)$_2$ fragment goat anti-rabbit IgG, (Fc fragment specific with minimal cross-reaction to human serum proteins) were obtained from Jackson ImmunoResearch Laboratories.

5.5. Cell culture and cell transfection methods

Cell thawing

For all experiments, fresh cultures of HEK293 cells (ATCC®) and HEK293 cells with stable expression of the AT1 receptor, *AGTR1* (HEK293-AT1) were used between passage numbers 5-12. Frozen aliquots of HEK293 and HEK293-AT1 cells (3 x 106 cells) stored in liquid nitrogen were thawed by incubation in sterile water at 37 °C. Thereafter, cells were gradually introduced to 10 ml complete medium. The cell suspensions were placed in a centrifuge, which was operated at 300 rpm at room temperature (RT) for 5 minutes. Subsequently, the pelleted cells were re-suspended in 10 ml of complete medium, plated on culture dishes of 60 cm^2 (TPP Techno Plastic Products AG, Switzerland), and incubated in a humidified atmosphere at 37 °C under 5% carbon dioxide (CO_2).

Culture of HEK293 cells in complete medium

HEK293 and HEK293-AT1cells were cultured in complete Dulbecco's Modified Eagle's Medium (DMEM) medium (D6429, Sigma-Aldrich), which was supplemented with 10 % (v/v) fetal bovine serum (FBS) (Hyclone, ThermoFisher Scientific) and 100 U/ml penicillin/100 µg/ml streptomycin (Sigma-Aldrich).

Culturing of adherent HEK293 cells was performed in the complete medium in an incubator at 37 °C in a humidified atmosphere with 5% CO_2. The medium used to culture the cells was replaced on the third day. Prior to cell-splitting, adherent cells were washed with PBS (Dulbecco's phosphate buffered saline, Sigma-Aldrich), followed by trypsinization with 0.05% Trypsin-EDTA (Sigma-Aldrich) for 2-3 minutes. Cells were detached and suspended by gentle pipetting, and the trypsin in the cell suspension was inactivated by the addition of three volumes of medium containing 10% FBS.

Determination of the cell number

To determine the number of cells, the cell suspension was combined with an equivalent amount of 0.4% (w/v) Trypan Blue (Sigma-Aldrich) in PBS. Cell counting was performed with a Neubauer hemocytometer (LO-Laboroptik GmbH, Germany) in accordance with the manufacturer's guidelines. Subsequent to the application of 10 µl of the 1:1 diluted cell suspension, the number of surviving cells within four squares was determined. Concentration of cells (cells/ml) was computed based on the following formula:

$$Cells/ml = number\ of\ cells \times 10\,000/number\ of\ squares \times dilution\ factor \times 100$$

Transfection of HEK cells by calcium phosphate co-precipitation method

For transient transfection utilising the calcium phosphate co-precipitation transfection technique, adherent HEK293 cells were cultured to 80-90% confluency on 100 mm diameter cell culture plates. Prior to transfection, the cells were divided 1:3 and then placed in a humidified incubator for 3-4 h at 37 °C under a 5 % CO_2 atmosphere.

After the incubation period, the plasmid-DNA / calcium phosphate transfection mixture was prepared as detailed in Table 4. The plasmid-DNA/ calcium chloride mixture was introduced in drops to 500 µl of 2 x BES-buffered saline (BBS) while vortexing to induce plasmid DNA-calcium phosphate co-precipitation. Co-precipitation was allowed to proceed during an incubation for 20 minutes at room temperature. Thereafter, the co-precipitation mixture was added dropwise to the cells. After an incubation for 12-16 h in the humidified incubator at 37 °C with 5 % CO_2, cell washing with PBS was conducted, and a new complete medium was supplied. Cells were used for experiments 36-42 hours after the transfection.

1	plasmid DNA	20 µg
2	water	to a volume of 450 µl
3	2.5 M $CaCl_2$ x 2 H_2O	50 µl

Table 4: Reaction mixture for the calcium phosphate transfection.

BES-buffered saline (BBS) (2 x) preparation

Preparation of 2 x BBS was performed by dissolving 280 mM NaCl, 1.5 mM Na_2HPO_4, and 50 mM N,N-bis[2-hydroxyethyl]-2-aminoethanesulfonic acid (BES) (Sigma-Aldrich) in water, followed by adjusting the pH to 6.95 at room temperature. The dilution of plasmid DNA (*AGTR1*-Cerulean in pcDNA3.1; *SCD1* in pcDNA3.1; and plasmid pcDNA3.1, which was used to adjust the total amount of plasmid DNA to 20 µg) was performed in water in a reaction volume of 450 µl followed by the addition of 50 µl of 2.5 M calcium chloride ($CaCl_2$).

Measurement of cellular fluorescence

The cellular fluorescence of *AGTR1*-Cerulean-expressing HEK293 cells without and with co-expression of *SCD1* was measured with a fluorescence spectrophotometer approximately 36-42 h after the transfection. Background fluorescence was determined with HEK293 cells without *AGTR1*-Cerulean expression. Cells were maintained in DMEM (supplemented with 0.2% fetal calf serum (FCS)) for 3 h prior to the experiment. After washing of the adherent cells by 10 ml of PBS, cells were detached by short trypsinization (1-2 minutes) with 2 ml of trypsin-EDTA (0.025 % trypsin, 0.01 % EDTA in PBS) and pipetting up and down with a Pasteur pipette, immediately transferred to a centrifugation tube containing 10 ml of medium and collected by centrifugation at 300 rpm for 5 minutes at RT. After a second washing step with incubation buffer, cells were suspended in 2 ml of incubation buffer (140 mM NaCl, 5.4 mM KCl, 1 mM $MgCl_2$, 1.8 mM $CaCl_2$, 20 mM 4-(2-hydroxyethyl)-1-piperazineethanesulfonic acid (HEPES), pH 7.4), and the cell number was adjusted to $0.8 - 1.0 \times 10^6$ cells/ml. The cell suspension (2 ml) was placed into the fluorescence cuvette, and cell emission spectra (450 nm - 600 nm) of *AGTR1*-Cerulean-expressing cells were recorded under constant stirring with a magnetic stirrer by excitation at 430 nm (excitation and emission slit width: 10 nm; scan velocity: 100 nm / min). Background fluorescence of HEK293 cells without *AGTR1*-Cerulean expression was subtracted. Measurements were conducted with a Perkin Elmer LS55 fluorescence spectrometer, and data recording was performed with the FLWinLab software.

Animal models and mouse phenotyping methods

All animal experiments were conducted in accordance with the guidelines of the National Institutes of Health, and approval was obtained from the local Committee on Animal Care and

Use (Kantonales Veterinäramt, Zürich). Male mice, which were housed in groups of 4-5, were used for all studies. Mice were housed under specified pathogen-free conditions, in a regime alternating between 12 h of light and 12 h of darkness with unrestricted availability of nutrition and water.

5.6. Generation of Tg-*SCD1* mice

Transgenic mice were created in line with a standard protocol [131]. In order to generate transgenic mice successfully, it is essential that the time schedule is precise and the following five fundamental stages are involved:

1. The process of designing, cloning and linearizing the transgenic construct was conducted. To express *SCD1* under control of the alpha-MHC promoter, the cDNA encoding *SCD1* was inserted into the *Sal I* and *Hind III* sites of the alpha-MHC plasmid [132]. For pronuclear injection of DNA, linearization of the transgenic vector and removal of plasmid sequences was performed by *Not I* digestion. A scheme of the alpha-MHC-promoter-SCD1 transgene used for generation of Tg-*SCD1* mice is shown in Figure 11A. Oligonucleotides used for cloning of the alpha-MHC-promoter-SCD1 plasmid are shown in Appendix 13.1, and DNA sequencing data of the alpha-MHC-promoter-SCD1 plasmid are shown in Appendix 13.2.
2. Harvesting of donor zygotes was conducted subsequent to hormone treatment and mating in accordance with the schedule detailed in (Table: 5).
3. The transgenic construct was microinjected into the pro-nucleus.
4. After overnight incubation, the microinjected two-cell stage embryos were implanted into recipient foster mice with pseudo-pregnancies (Day 5). Vasectomies were performed on male CD1 mice to initiate pseudo-pregnancies in female foster mice on day 4.
5. Approximately 19 days following the implantation of embryos, the birth of the pups occurred. Lastly, the processes of genotyping and identifying founder mice were performed.

	Day1	Day 2	Day 3	Day 4	Day 5
Donor F (B6)	10 U PMSG at 14:00		10 U hCG at 13:00	Collection of zygotes at 11:00, followed by pro-nuclear injection of DNA	
Donor M			mating with Donor F at 20:00		
Foster F CD1		Housing of CD1 F with vasectomized CD1 M Separated by a barrier		mating at 20:00	Implantation of two-cell stage DNA-injected embryos into pseudopregnant CD1 foster mice
Vasectomized CD1 M					

Table 5: Timeline for the application of hormones and mating necessary for generating donor zygotes (F: female mouse, M: male mouse).

Preparation of DNA for pronuclear injection

In order to successfully generate transgenic mice, linearization of DNA was performed along with removal of the plasmid backbone. To prepare the endotoxin-free plasmid DNA, an EndoFree Plasmid Maxi Kit was employed in accordance with the manufacturer's guidelines (Qiagen). Linearization of the transgenic DNA and removal of the plasmid backbone was achieved via *Not I* digestion, while purification of DNA was performed by agarose gel electrophoresis. Quantification of the linearized DNA was via agarose gel electrophoresis by referencing a commercial DNA ladder, followed by dilution to a concentration of 2 ng/µl in injection buffer (8 mM Tris-HCl pH 7.4 (diluted from a 1 M Trizma® hydrochloride solution, Sigma-Aldrich), 0.15 mM EDTA (diluted from a 0.5 M EDTA solution, SigmaAldrich).

Mouse vasectomy procedure

Prior to the vasectomy procedure, male CD1 mice were weighed and anesthetized by intraperitoneal injection of ketamine/xylazine (100/10 mg/kg body weight). For vasectomy, the mouse was positioned on its back, with the abdomen facing upwards, and ethanol (70%) was used to sterilise the lower segment of the abdomen. After pushing down both testes into the scrotal sacs, an incision of 1 cm length was made through the skin along the midline of the scrotal sac followed by a 5-mm incision in the testes membrane, close to the left side of the midline wall. The vas deferens was located and pulled out while the testis was held in place. Thereafter, the vas deferens was cauterized with the hot tips of a pair of forceps. The same process was applied to the opposite side of the reproductive tract. After the procedure, the skin was sewed together. Thereafter, the mouse was placed in a clean cage, kept warm by placing the cage on a warming pad until recovery from the anaesthesia. The postsurgical observation of the mouse followed the local guidelines. After 10-14 days, vasectomized male CD1 mice were used for mating.

Collection of zygotes and removal of cumulus cells with hyaluronidase

For the process of creating zygotes for pronuclear injection, hormone treatment was administered to female B6 mice (≥10). On the first day, 10 IU of pregnant mare serum gonatropin were injected (i.p.) into the female mice. On the third day, ovulation was initiated by injecting 10 IU of human chorionic gonadotropin. Subsequent to injecting hCG, mating of the male and female mice was facilitated overnight.

On the fourth day, isolation of the fertilised oocytes was performed. To summarise, after the super-ovulated mice were sacrificed via cervical dislocation, the abdominal cavity was opened. A small hole was made in the mesometrium membrane, in close proximity to the oviduct. The oviduct with the ovary and fat pad were pulled with forceps so that a cut could be made in the uterus close to the oviduct. This was followed by the transfer of the oviduct and ovary to a small Petri dish that contained M2 medium supplemented with antibiotics (Penicillin-Streptomycin Solution Hybri-Max™, final concentration 50 IU penicillin and 50 µg/ml streptomycin). The same procedure was performed with the opposite side of the uterine horn.

Separation of the oviduct from the ovary was performed under a stereo-microscope, and the oviduct was then moved to a dish that contained M2 medium with hyaluronidase (final concentration: 0.3 mg/ml in M2 medium containing antibiotics). The segment of the oviduct that had the greatest swelling was opened, thus allowing zygotes to be carefully pushed out, if this did not happen automatically. After further incubation with hyaluronidase for several minutes until the cumulus cells fell off, the zygotes were rapidly picked up by a mouth-controlled pipetting instrument and transferred to a Petri dish with microdrops of 50 μl of fresh M2 medium covered with mineral oil. Removal of the hyaluronidase solution with cumulus cells and debris was performed by rinsing through several drops of fresh M2 medium. Then, the zygotes were transferred to a microdrop culture dish of fresh M16 medium covered with mineral oil and kept at a temperature of 37°C inside an incubator with a 5% CO_2 atmosphere until needed.

DNA pronuclear injection

The process of preparing the microinjection platform involved placing two 50 μl microdrops of M2 medium onto the lid of a sterilised 6-well-plate (Costar, Corning Life Sciences). Approximately 20-25 of the zygotes were moved to the M2 medium and then the microinjection platform was gently positioned on the microscope stage.

M2 medium was added to the holding capillary (VacuTip; 5175108.000; Eppendorf), which was filled up to two thirds utilising a microloader (5242956.003; Eppendorf). The holding capillary

was subsequently put into the connector piece of a pneumatic microinjector (CellTram Air, Eppendorf). The DNA solution was inserted into the injection capillary, which was positioned on the micromanipulator and then attached to the microinjector (FemtoJet; 5247000.013; Eppendorf).

The holding capillary was utilised for stabilising and holding the zygote. Penetration of the pro-nucleus was performed using the injection capillary (BioMedical Instruments, Zöllnitz, Germany) thus allowing injection of the DNA. The microinjected zygotes were kept overnight in M16 medium at a temperature of 37°C in a humidified 5% CO_2-containing atmosphere prior to being implanted.

Oviduct transfer of mouse embryos into pseudo-pregnant foster mice

In order to acquire pseudo-pregnant foster mice, mating was performed one day prior to the implantation between a female CD1 foster mouse and a male CD1 mouse that had undergone a vasectomy. On the next morning (5th day), CD1 mice with vaginal plugs were distinguished and subsequently utilised to implant the embryos.

First, the recipient mouse was weighed and anesthetized by i.p. injection of ketamine/xylazine. Following the application of the anaesthetic, the side of the pseudo-pregnant mouse that was selected for the implantation process was shaved and sterilized with 70 % ethanol. Then, a small, 1 cm incision was made in the skin, the fat pad was located, and a small incision just over the ovary was made. Subsequently, the ovarian fat pad was picked up with blunt forceps and the attached ovary, oviduct and uterus were pulled out. A vessel clip was used to fix the oviduct and ovary, thus exposing the infundibulum. Twenty zygotes that had reached the two-cell stage were loaded into a reimplantation capillary (BioMedical Instruments), and insertion of this capillary into the infundibulum was performed under a stereo-microscope. By blowing on the transfer pipette, the zygotes were steadily transferred into the oviduct. Both the ovary and fat pad were returned to their original positions in the abdomen, the body wall was sewed up and the skin was closed using wound clips. As applicable, the same procedure was repeated with the second oviduct. After the procedure, the mouse was placed into a clean cage and kept warm by placing the cage onto a warming pad. Recovery of the mouse from anaesthesia and during the post-implantation period was closely monitored according to the local guidelines.

5.7. Genotyping

Genomic DNA extraction from mouse ear-punch biopsies

Extraction of genomic DNA from ear-punch biopsies of 3-4-week-old mice was performed via hot digestion. In summary, incubation of the ear-punch biopsies was conducted overnight at a temperature of 57°C on a shaking platform (1000 rpm) in 210 µl of lysis buffer supplemented with the addition of 10 µl of a 20 mg/ml proteinase K solution. The reaction was terminated and the proteinase K was rendered inactive via a process in which the sample was boiled for 30 minutes at 99°C. The supernatant was utilised as the template for the genotyping PCR.

Lysis buffer for DNA extraction from ear-punch biopsies

10% sodium lauroyl sarcosinate	2.5 ml
5 M NaCl	1 ml
Chelex – 100	2.5 g
dH2O	ad 50 ml

Table 6: Constitution of the lysis buffer for genomic DNA extraction from mouse ear-punch biopsies.

Identification of Tg-*SCD1* mice by genotyping with PCR

The identification of *SCD1*-positive transgenic mice, which had stable integration of the *SCD1*-transgene into the genomic mouse DNA, was performed by genotyping PCR. Genotyping was performed with genomic DNA from ear punch biopsies. The PCR reaction utilized Taq Polymerase in the provided buffer with the addition of 2.5 mM $MgCl_2$ and 200 µM dNTPs. Specific primers for the alpha-MHC-promoter vector backbone (Primer: HGH-reverse) and the *SCD1* transgene (Primer: SCD1-forward) were utilised at 0.625 µM. DNA was amplified in a reaction volume of 50 µl with 0.5 - 1 µl of genomic mouse DNA lysate according to the PCR program, as shown in Table 7.

Step	Temperature	Time	Cycles
1	95°C	2 min	1X
2	95°C	45 s	
3	60°C	60 s	40X
4	72°C	60 s	
5	72°C	10 min	1X

Table 7: Genotyping PCR program.
The dsDNA was initially melted (Step 1), then the DNA was amplified in 40 cycles. Each amplification cycle consisted of a melting step of dsDNA (Step 2), an annealing step (Step 3) and a primer extension step (Step 4). A last step of extension completed the PCR process (Step 5). After the PCR reaction, the amplified PCR products were analysed by agarose gel electrophoresis and *SCD1*-positive mice were identified by the presence of the *SCD1*-specific amplification product. *SCD1*-positive founder mice were used for further breeding and generation of Tg-*SCD1* mouse lines. Tg-*SCD1* mice were deposited to the Janvier Labs mouse repository (Mouse strain No. 181.078 ETH Zurich).

Sequences of the oligonucleotide primers used for genotyping PCR of Tg-*SCD1* mice

SCD1 - forward: 5`- GGT TTC ACT TGG AGC TGT GGG TGA GG - 3`

HGH - reverse: 5`- ATT AGG ACA AGG CTG GTG GGC ACT GGA GTG - 3`

5.8. Phenotyping of Tg-*SCD1* mice

Phenotyping of transgenic mice involved the detection of the transgenic SCD1 protein by immunoblotting. The levels of cardiac SCD1 protein of Tg-*SCD1* mice were determined by quantitative immunoblotting and compared to those of non-transgenic B6 mice. The western blot method of protein detection in transgenic mouse hearts and non-transgenic B6 control hearts was also used for the detection of Fasn (fatty acid synthase) and Adipoq (adiponectin) proteins. Other methods of phenotyping include the determination of cardiac function by echocardiography, the heart-to-body weight measurement, the histology analysis, whole

genome microarray gene expression profiling and the determination of the heart failure-promoting AT1 receptor by radioligand binding studies and autoradiography.

5.8.1. Identification of the transgenic protein by immunoblotting Isolation of mouse hearts

For immunoblot detection of the SCD1 protein, histology analysis, radioligand binding studies and autoradiography, hearts were isolated from eight-month-old, male Tg-*SCD1* mice and age-matched, non-transgenic, male B6 mice as controls. For the isolation of mouse hearts, mice were weighed, anesthetized with ketamine/xylazine (100/10 mg/kg), and perfused transcardially. Thereafter, mouse hearts were isolated, and immediately frozen in liquid nitrogen, used for membrane preparation to perform radioligand binding studies, or processed for preparation of paraffin sections and cryosections for autoradiography determination of the AT1 receptor.

Extraction of proteins from mouse hearts

For protein extraction, the frozen mouse hearts were grinded under liquid nitrogen, utilising a pestle and mortar, and the homogenised powder was lysed in 500-750 µl of extraction buffer on ice by gentle agitation. The removal of cell debris was achieved with a centrifugation step at 16 000 x g at 4°C for 10 minutes. The supernatant was moved to a clean 2 ml microcentrifuge tube and precipitation of the proteins was conducted through the addition of 1 ml of acetone. Subsequent to incubating the precipitated proteins at 4°C, they were pelleted, the supernatant was disposed and the resulting pellet was dissolved in a suitable volume of 4x Laemmli SDS-sample buffer that contained urea (final concentration 8 M).

PROTEIN EXTRACTION BUFFER COMPOSITION

TRIS PH7.4	10 mM
SODIUM DESOXYCHOLATE	1%
SDS	0.1 %
EDTA	5 mM
BETA-GLYCEROPHOSPHATE DISODIUM	1 mM
SODIUM FLUORIDE (NAF)	20 mM
SODIUM ORTHOVANADATE	1 mM
SODIUM MOLYBDATE	1 mM
PHENYLMETHYLSULFONYL FLUORIDE (PMSF)	1 mM
PROTEASE INHIBITOR COCKTAIL	1:100

Table 8: Composition of the protein extraction buffer.

LAEMMLI SDS-SAMPLE BUFFER (4X) COMPOSITION	VOLUME
TRIS (1.0 M, PH 6.8)	10 ml
SDS	4.0 g
GLYCEROL	20 ml
BETA-MERCAPTOETHANOL	10 ml
BROMOPHENOL BLUE	0.1 g
DH2O	to 50 ml

Table 9: Laemmli sample buffer composition.

5.8.2. Radioligand binding studies and radioimmunohistochemistry

For radioligand binding studies, sarcolemmal membranes were prepared from mouse hearts isolated from eight-month-old, male Tg-*SCD1* mice with high and low cardiac levels of *SCD1*, and from age-matched, non-transgenic B6 controls. For membrane preparation, mouse heart tissue from 3 animals was combined and homogenised on ice with an Ultraturrax at 15 000 rpm in a 10-fold volume of homogenization buffer (10 mM Tris, 1 mM EDTA pH 7.4, with 300 mM sucrose, and supplemented with proteinase inhibitor cocktail). The homogenate was centrifuged at 1000 x g for 10 minutes at 4 °C. The supernatant was collected and centrifuged for 30 minutes at 4 °C (40 000 x g). After resuspending the resulting pellet in 0.6 M KCl and 30 mM histidine, pH 7.0, and another centrifugation step (20 minutes, 40 000 x g, 4 °C), the final pellet was resuspended in binding buffer (50 mM Tris, pH 7.4, 10 mM magnesium chloride (MgCl$_2$), 0.2 % BSA) supplemented with protease inhibitor cocktail) and stored at -80 °C for further use. Radioligand binding studies were performed with Sar^1, [^{125}I], Tyr^4, Ile^8-angiotensin II (specific activity 2200 Ci/mmol, Perkin Elmer) in a total volume of 100 µL with 100 µg of membrane protein in binding buffer for 60 minutes at 18 °C. The reaction was stopped by addition of 4 ml of ice-cold binding buffer and rapid filtration over glass fiber filters (Whatman GF/C). After three washing steps with binding buffer, filter-bound radioactivity was determined by scintillation counting in a beta-counter. The total number of binding sites (Bmax) was determined by saturation binding curves with increasing concentrations of radioligand (0.1 nM – 10 nM). Non-specific binding was determined in the presence of a 1000-fold molar excess of losartan. All binding experiments were performed in triplicates.

Radioligand binding studies were also performed with adherent HEK293-AT1 cells grown on 6-well-plates. Prior to the experiment, HEK293-AT1 cells were kept for 3 h in DMEM supplemented with 0.2 % FCS. For radioligand binding, the culture medium was replaced by HEPES-buffered DMEM supplemented with protease inhibitors, and cells were incubated for 4 h at 4 °C with increasing concentrations of Sar^1[^{125}I] Tyr^4, Ile^8-angiotensin II in the presence and absence of losartan as detailed above. At the end of the incubation period, unbound radioligand was removed by three washing steps with DMEM. Thereafter cells were solubilized by 2 M sodium hydroxide (NaOH), the cell lysate was collected and cellular radioactivity was counted in a beta-counter.

For radiodioimmunohistochemistry studies, longitudinal heart cryosections of eight-month-old Tg-*SCD1* mice with low and high SCD1 contents and non-transgenic B6 controls were prepared. Hearts were isolated after intracardial perfusion of anesthetized mice, cryoprotected by sucrose infiltration with gradually increasing concentrations of sucrose (10 % to 30 % of sucrose in PBS), attached to the tissue holder with optimal cutting temperature (OCT) tissue freezing compound (TissueTek), and frozen on a dry ice methanol cool bath. Cryostat sections of 10 μm were cut (Microm, Zeiss), sections were collected, and air-dried. For radioimmunohistochemistry, cardiac cryosections were incubated in blocking buffer (PBS supplemented with 5 % BSA and 0.05 % Tween 20) for 1 h, followed by 2 h of incubation with affinity-purified anti-AGTR1 antibodies (dilution 1:200). After washing steps to remove unbound antibodies, and blocking with goat serum (10 % in PBST) for 1 h, incubation with [^{125}I]-labelled secondary antibodies (specific activity ~1400 Ci/mmol; [125I]-labelled, goat anti-rabbit IgG, NEX155250UC, Perkin Elmer) diluted in blocking buffer was performed for 1 h at room temperature. After additional washing steps with PBST and PBS to remove unbound antibody, sections were imaged by autoradiography by exposure to X-ray films.

5.8.3. Preparation of tissue sections

Preparation of formalin-fixed paraffin embedded (FFPE) heart tissue

After placing the mouse under deep anaesthesia, perfusion was performed for the purpose of removing the blood from the vasculature. The heart was rapidly dissected and fixed via immersion in 10% neutral buffered formalin (100 x tissue volume) for a minimum of 48 h under room temperature conditions. Subsequent to fixing the tissue, washing with water was performed, the heart specimens were dehydrated and paraffin was infiltrated through the application of a vacuum tissue processing system (Leica ASP200). Embedding of the heart specimens in paraffin was accomplished with a tissue embedding station (Leica EG1160). Longitudinal mouse heart sections with a thickness of 10 μm were cut using a microtome (Leica RM2265). These sections were placed in a water bath warmed to 37°C. Tissue sections were floated onto the surface of clean histological slides, placed on a warming block at 40 °C for 20 minutes for stretching (the paraffin sections) and then placed overnight in an incubator at 37°C for drying.

Dewaxing and rehydration procedure

To dewax the tissue sections, the wax was first melted by a heating step at 60°C. which was followed by two incubation steps in xylene (2-3 minutes). Dehydration was achieved by a graded series of incubations in ethanol/water with compositions of 100%, 95%, 90%, 80%, and 70% of ethanol diluted in water. Every step comprised two periods of incubation lasting 5 minutes each.

5.8.4. Haematoxylin and eosin (HE) staining of cardiac tissue sections

The haematoxylin and eosin (HE) stain was applied to the nuclei and cytosol of longitudinal heart tissue sections after dewaxing and rehydrating the tissue sections by incubation of the sections in filtered Mayer's hemalum solution (Sigma) for a period of 4 minutes followed by dipping into hydrochloric acid (0.1%) and the blueing step, which was permitted to continue for 5 minutes in flowing tap water. Subsequently, staining of the cytoplasm was performed with aqueous Eosin Y solution (0.5%), and the process was completed by an additional washing step.

5.8.5. Immunohistology procedure

Immunohistology was performed to detect the transgenic SCD1 protein on longitudinal heart sections of Tg-*SCD1* mice. Heart tissue sections were subjected to dewaxing and rehydration. Thereafter, antigen retrieval was performed by placing the tissue sections in antigen retrieval buffer (0.1 M citrate buffer pH 6, 0.1% (v/v) Triton X-100) with an uninterrupted source of heat provided by a microwave oven. This was followed by two washing steps with PBS followed by incubation in a 3% (v/v) hydrogen peroxide solution for 5 minutes for the purpose of inactivating any endogenous peroxidase activity. Residual hydrogen peroxide was removed by washing with PBS. Blocking of unspecific binding sites was performed using blocking solution [3% (w/v) BSA in PBST (0.05 % (v/v) Tween-20 in PBS)] for 1 h at 37°C, followed by incubation for 1 h at 37°C in blocking solution with the primary antibody (rabbit polyclonal anti-SCD1 antibody; dilution 1:200). Removal of the unbound antibody was achieved via three washing steps using PBST. Subsequently, the sections were placed in blocking buffer accompanied by the secondary POD-conjugated anti-rabbit antibody (peroxidase-conjugated AffiniPure F(ab)$_2$ fragment goat anti-rabbit IgG, Fc fragment specific with minimal cross-reaction to human

serum proteins) for 1 h at 37°C. This was followed by the removal of the antibody and three washing steps with PBST and then a last wash using PBS. A DAB (3,3'diaminobenzidine tetrahydrochloride) enhanced liquid substrate system was utilised for visualisation purposes in accordance with the guidelines provided by the manufacturer (Sigma). Water was applied to terminate the reaction, then slides were mounted with Poly-Mount Xylene (Polysciences).

5.8.6. Determination of the heart-to-body weight ratio of mice

After weighing the mice, an anaesthetic was applied by intraperitoneal (ip) injection (ketamine/xylazine 100/10 mg/kg) and the chest cavity was rapidly opened. Whole body perfusion was conducted using sterile PBS. The heart was dissected, any connective tissue was removed and then it was gently dried with tissue, and immediately weighed. Finally, the ratio of the heart-weight (mg) to the body-weight (g) was computed.

5.8.7. Measurement of left ventricular ejection fraction by echocardiography

The cardiac function of mice was determined with a Vivid 7 echocardiograph (GE Healthcare) equipped with a 12 MHz linear array transducer by transthoracic echocardiography of anesthetized mice (avertin anesthesia by i.p. injection of freshly prepared tribromoethanol). The Teichholz formula was applied to calculate the LVEF in the M-Mode of the parasternal long axis view. Analysis of the recordings was performed off-line with EchoPac Pc 3.0 software (GE Healthcare).

5.8.8. Microarray gene expression profiling

For microarray gene expression profiling, mice were weighed, and anesthetized by i.p. administration of tribromoethanol (100 mg/kg body weight; freshly prepared). After transcardial perfusion with sterile PBS, hearts were rapidly dissected on ice and immediately frozen in liquid nitrogen. For isolation of total RNA, hearts were pulverized under liquid nitrogen with a pestle and mortar. The pulverized hearts were transferred into an RNAse-free Eppendorf reaction vial, immediately lysed in lysis buffer provided by the RNeasy Mini kit (Qiagen). After a proteinase K digestion step, the heart lysate was processed for RNA isolation according to the protocol of the manufacturer (Qiagen). The isolated RNA was collected in 30 µL of RNAse-free H_2O and stored at -80 °C until further use.

In frame of this thesis, total cardiac RNA was prepared from eight-month-old, male Tg-*SCD1* mice and age-matched, non-transgenic B6 control mice. The total RNA concentration was determined by spectrophotometry with the absorption maximum at 260 nm, and RNA purity was controlled by measurement of the absorption ratio of A260/A280, which was ~2.0. Integrity of the total heart RNA was further controlled by denaturing formaldehyde-containing agarose gel electrophoresis by the absence of RNA degradation and the presence of two bright bands of the 18S and 28S ribosomal RNA.

For whole genome microarray gene expression profiling, the Affymetrix One-Cycle cDNA Synthesis kit was used. The protocol followed the Affymetrix GeneChip Expression Analysis Technical Manual (rev. 5, Affymetrix Inc., USA). In the first step, the mRNA was transcribed into single-stranded cDNA by oligo-dT priming by using Superscript II, which is an RNA-dependent T7-DNA polymerase, which synthesized the first cDNA strand. The second cDNA strand was synthesized by addition of *Escherichia coli* (*E. coli*) DNA ligase and *E. coli* DNA polymerase supplemented with ribonuclease (RNAse) for fragmentation of transfer ribonucleic acid (tRNA), ribosomal ribonucleic acid (rRNA) and residual messenger RNA (mRNA). The *E. Coli* DNA polymerase synthesized the second cDNA strand complementary to the first cDNA strand, and the *E. coli* DNA ligase ligated the cDNA fragments. Finally, by addition of T4-DNA polymerase, the synthesis of the two complementary strands of DNA was completed. The final synthesis product of this step was double-stranded cDNA. After a purification step with the Affymetrix Sample Cleanup Module, the purified cDNA was transcribed into complementary RNA (cRNA) by in vitro transcription (IVT) with the Affymetrix IVT-Labeling kit. During the in vitro transcription (IVT) step, biotin labelling of the newly transcribed cRNA was performed by incorporation of biotin-labelled nucleotides. The biotinylated cRNA was further purified and controlled for integrity by denaturing formaldehyde-containing agarose gel electrophoresis. Prior to hybridization with the gene chip, the biotinylated cRNA was fragmented by incubation in fragmentation buffer (part of the Affymetrix IVT-Labeling kit) for 35 minutes at 94 °C in a ThermoCycler. The cRNA fragmentation was stopped by incubation on ice. Complete fragmentation of the cRNA was controlled by denaturing formaldehyde-containing agarose gel electrophoresis. Biotin-labelled, fragmented cRNA (15 µg / gene chip) was hybridized to the gene chip (Affymetrix GeneChip MG430 2.0 Array with more than 45,000 probe sets) in 200 µl of hybridization solution in a Hybridization Oven 640 (Affymetrix) at 45 °C for 16 hours.

GeneChips were washed and stained with an Affymetrix Fluidics Station 450. Microarrays were scanned with the Affymetrix GeneChip Scanner 7G, and signals were processed to a target value of 300 using GCOS (version 1.4, Affymetrix). Gene ontology (GO) analyses of microarray data were performed with GCOS/RMA processed data using GeneSpring GX software (Agilent). Data were compared between groups using the unpaired two-tailed Student`s t-test. Probe sets with significant difference (i. e., $p \leq 0.01$ if not otherwise stated, ≤-2-fold or ≥+2-fold difference, with call present and/or signal intensity ≥100) between transgenic Tg-*SCD1* mice (or the other HF models) and their respective controls, were used for GO classification. Microarray data were deposited to the NCBI GEO database, accession number GSE120020. Microarray data of experimental HF models, which were used for GO analysis, are available at the NCBI GEO database with the accession numbers GSE25765, GSE25766, GSE25767, GSE25768.

Experimental heart failure models used for gene ontology (GO) analysis

The GO analysis was performed with GeneSpring GX software (Agilent), and applied cardiac whole genome microarray gene expression data from the following experimental HF models: six-month-old, male *Apoe-/-* mice with two months of AAC, age-matched, sham-operated *Apoe-/-* controls and age-matched, 6-month-old, non-transgenic B6 controls; 18-month-old, male *Apoe-/-* mice and age-matched, 18-month-old, male B6 controls; eight-month-old, male *Apoe-/-* mice with two months of treatment with the *PPARG* agonist, rosiglitazone (30 mg/kg/d in drinking water), age-matched, untreated male Apoe-/- controls, and age-matched, untreated male B6 controls; ten-month-old, male B6 mice with 6 months of AAC and age-matched, sham-operated B6 controls.

Abdominal aortic constriction

Abdominal aortic constriction was conducted in the Molecular Pharmacology Unit, ETH Zurich, Switzerland, by Dr. Said AbdAlla. The abdominal aorta was constricted under anesthesia (tribromoethanol 100 mg/kg body-weight; freshly prepared) of four-month-old, male B6 (C57Bl/6J) mice and four-month-old, male Apoe-/- mice with B6 background. For aortic constriction, the aorta was narrowed between the celiac and superior mesenteric artery through binding a 7-0 silk suture ligature against a blunt 28-gauge needle. Age-matched,

sham-operated mice served as controls, which underwent the same surgical procedure except for ligation of the aorta.

5.8.9. Statistical methods and data analysis

Analysis of the data acquired from the experiments was performed with GraphPad Prism 6. Microarray data were normalized to a target value of 300 by GCOS, and analysed by TIGR MeV. GCOS/RMA processed microarray data were analysed with GeneSpring GX software (Agilent). Unless otherwise stated, analysis of the groups was conducted by utilising the unpaired two-tailed student's t-test, where p-values < 0.05 were regarded as significant. Analysis of variance (ANOVA) was used to analyse the differences among multiple groups and then a post-test as indicated was applied. Data are displayed as means ± S.D.

6. RESULTS

6.1. Experimental models of heart failure used for GO analysis of whole genome gene expression data

The pathogenesis of HF is enhanced by major cardiovascular risk factors. The most frequent heart failure-enhancing cardiovascular risk factors are (i) long-term atherosclerotic vascular disease causing myocardial infarction, and (ii) high blood pressure with chronic pressure overload [60]. These major risk factors trigger cardiac adaptation and remodeling processes, which strongly accelerate the development of HF symptoms. To investigate pathomechanisms of HF, the study analyzed gene expression data from experimental mouse models, which mimic major cardiovascular risk factors (Figure 7).

Experimental heart failure model-1
Six-month-old Apoe-/- mice with heart failure symptoms induced by two months of chronic pressure overload imposed by abdominal aortic constriction (AAC).
Control group: age-matched, sham-operated Apoe-/- mice

Experimental heart failure model-2
Aged, 18-month-old Apoe-/- mice with symptoms of heart failure induced by aortic coarctation due to long-term atherosclerosis.
Control group: age-matched, non-transgenic B6 mice

Experimental heart failure model-3
Eight-month-old Apoe-/- mice with symptoms of heart failure triggered by two months of treatment with the heart failure-promoting *Pparg* agonist, rosiglitazone (30 mg/kg/d).
Control group: age-matched, untreated Apoe-/- mice

Figure 7: Overview of heart failure models, which were used for analysis of gene expression data obtained by whole genome microarray gene expression profiling.

Apolipoprotein E-deficient (Apoe-/-) mice with hypercholesterolemia were used, which develop atherosclerotic plaques starting at an age of 4-6 months. Chronic pressure overload was imposed by abdominal aortic constriction, AAC (Figure 7).

For the study, whole genome gene expression data from three different experimental models of HF were analyzed, which mimic the cardiovascular risk factors, atherosclerosis and chronic pressure overload (Figure 7). In the first model, HF was triggered in 4-month-old, male *Apoe-/-* mice with hypercholesterolemia at the onset of atherosclerosis, by chronic pressure overload imposed by 2 months of AAC. After 2 months of AAC, at an age of 6 months, these mice had developed symptoms of HF with a significantly decreased left ventricular cardiac ejection fraction of 27.8 ± 2.2 % compared to that of age-matched, sham-operated *Apoe-/-* mice, which had an ejection fraction of 51.1 ± 1.6 % (mean ± s.d., n=6; Figure 8A).

The second HF model used aged, 18-month-old, male *Apoe-/-* mice, in which symptoms of HF were caused by long-term atherosclerosis [124]. HF of aged *Apoe-/-* mice was documented by a significantly decreased left ventricular cardiac ejection fraction of 29.5 ± 2.9 % whereas the cardiac ejection fraction of age-matched, 18-month-old, non-transgenic B6 control mice was 47.5 ± 2.7 % (mean ± s.d., n=5; Figure 8B).

The third HF model used 8-month-old, male *Apoe-/-* mice, in which the development of HF was enhanced by chronic activation of the heart failure-promoting, adipogenic transcription factor, *Pparg* (peroxisome proliferator-activated receptor gamma). Chronic activation of *Pparg* either by transgenic expression of *Pparg* or treatment with the *Pparg* agonist, rosiglitazone, enhances the development of symptoms of HF in mice and patients [126, 264]. The study applied the *Pparg* agonist, rosiglitazone, to trigger symptoms of HF in *Apoe-/-* mice [130]. Chronic activation of *Pparg* was induced by treatment of *Apoe-/-* mice for two months with the *Pparg* agonist, rosiglitazone (30 mg/kg/d). After two months of rosiglitazone treatment, 8-month-old *Apoe-/-* mice had developed symptoms of HF, which was documented by a significantly decreased left ventricular cardiac ejection fraction of 30.2 ± 2.4 % whereas that of untreated, age-matched control *Apoe-/-* mice was 50.0 ± 2.3 % (mean ± s.d., n=5; Figure 8C).

In agreement with previous data [124, 130], the three different models of HF used for whole genome microarray gene expression data analysis showed a significantly impaired left ventricular cardiac ejection function indicative of HF [130].
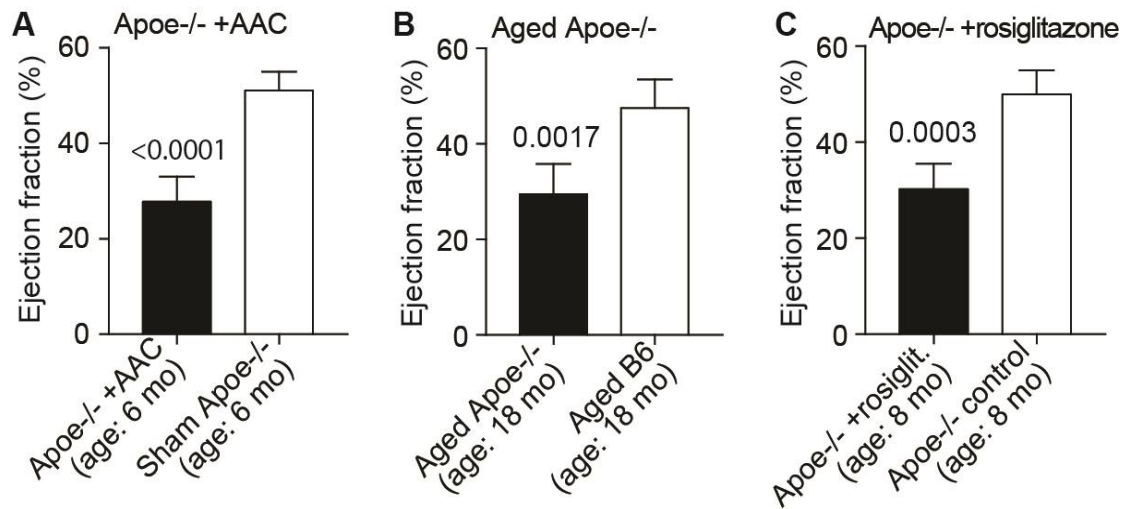
Figure 8: Decreased left ventricular cardiac ejection fraction of three different heart failure models. (**A**) Cardiac left ventricular ejection fraction of 6-month-old Apoe-/- mice with heart failure symptoms triggered by 2 months of AAC compared to age-matched, sham-operated Apoe-/- controls (mean ± s.d., n=6). (**B**) Cardiac left ventricular ejection fraction of aged, 18-month-old Apoe-/- mice with severe atherosclerosis and aged, 18-month-old, non-transgenic B6 controls (mean ± s.d., n=5). (**C**) Cardiac left ventricular ejection fraction of 8-month-old Apoe-/- mice with 2 months of treatment with the heart failure-enhancing Pparg agonist, rosiglitazone (30 mg/kg/d; mean ± s.d., n=5). P-values are indicated and were determined with the unpaired, two-tailed t-test.

6.2. The whole genome microarray gene expression data analysis of three different heart failure models

To investigate pathomechanisms underlying the development of HF in different experimental models, gene expression data were analyzed, which were obtained by whole genome gene expression profiling of heart specimens of the following three different HF models and their respective controls:

I. Six-month-old, male *Apoe-/-* mice with 2 months of AAC-induced chronic pressure overload, and age-matched, sham-operated Apoe-/- mice as controls.

II. Aged, 18-month-old, male *Apoe-/-* mice with severe atherosclerosis, and age-matched, non-transgenic B6 controls.

III. Eight-month-old, male *Apoe-/-* mice with 2 months of treatment with rosiglitazone (30 mg/kg/d), which is an agonist of the adipogenic and heart failure-enhancing transcription factor, *Pparg*. The control group consisted of age-matched, untreated *Apoe-/-* mice.

The different HF models reproduce major cardiovascular factors of HF patients, e.g. atherosclerotic vascular disease, and chronic pressure overload.

Whole genome gene expression data, which were analyzed in frame of this thesis, were generated by whole genome microarray gene expression profiling of cardiac RNA isolated from hearts that were dissected of the different HF models and their respective controls. The purity of the isolated total RNA was confirmed by the absorbance ratio A260/280 of ~2.0. Comparable RNA quality was controlled by the detection of bright bands of the 18S and 28S ribosomal RNA. After reverse transcription and processing according to the Affymetrix protocol, fragmented and biotin-labeled cRNA was hybridized to the gene chip with more than 45 000 probe sets covering the whole mouse genome (Mouse Genome MG430 2.0 Array, Affymetrix). Total cardiac RNA from four mice was pooled for one gene chip. This approach is feasible because intra-individual variability is negligible due to the use of inbred mouse lines [265]. After scanning of gene chips, signal intensities of all probe sets were recorded, and data normalization to a target value of 300 was performed by GeneChip® operating software (GCOS). Microarray data of experimental HF models, which were used for GO analysis, are deposited to the NCBI GEO database with the accession numbers GSE25765, GSE25766, GSE25767, GSE25768.

Probe sets with significantly different signal intensities between study groups were identified by TIGR Multiexperiment Viewer (MeV v. 4.0). After identification of significantly different probe sets between study groups, microarray data were subjected to stringent data filtering according to the following criteria: (i) significant difference from the control group ($p \leq 0.01$; just alpha), (ii) $\geq$ 2-fold up-regulation compared to the respective control group, and (iii) call present and/or signal intensity $\geq$100. For gene ontology (GO) analysis, GeneSpring Software (v. 5.4 and v11, Agilent) was used after data normalization.

6.3. GO analysis of whole genome microarray gene expression data identifies the cardiac lipid metabolic process as the predominant biological process up-regulated in experimental heart failure

Gene ontology analysis was performed of significantly different probe sets according to the above-defined stringent criteria. GO classification of microarray data identified "metabolic processes" as the top biological process with most up-regulated genes at the onset of HF of three different HF models (Figure 9). Among different metabolic processes, the "lipid metabolic process" was the category encompassing the highest number of up-regulated heart failure-related genes (Figure 9; Supplemental Table (Appendix 13.3)).

Data analysis of significantly up-regulated genes of six-month-old *Apoe-/-* hearts with HF induced by two months of AAC-induced chronic pressure overload showed that the "lipid metabolic process" encompassed 51.1 % of up-regulated genes of the category "metabolic processes" (Figure 9A). In failing hearts induced by long-term atherosclerosis of aged, 18-month-old *Apoe-/-* mice, 44.2 % of up-regulated genes of the "metabolic process" were sorted into the category "lipid metabolic processes" (Figure 9B). Finally, GO analysis detected that *Pparg* activation-induced HF of *Apoe-/-* mice induced the predominant up-regulation of genes from the cardiac "lipid metabolic process", which encompass 52.3 % of all up-regulated genes of "metabolic processes" (Figure 9C).

Taken together, GO analysis of whole genome microarray gene expression data identified that failing hearts from three different experimental heart failure models showed the predominant up-regulation of genes from the cardiac "lipid metabolic process".
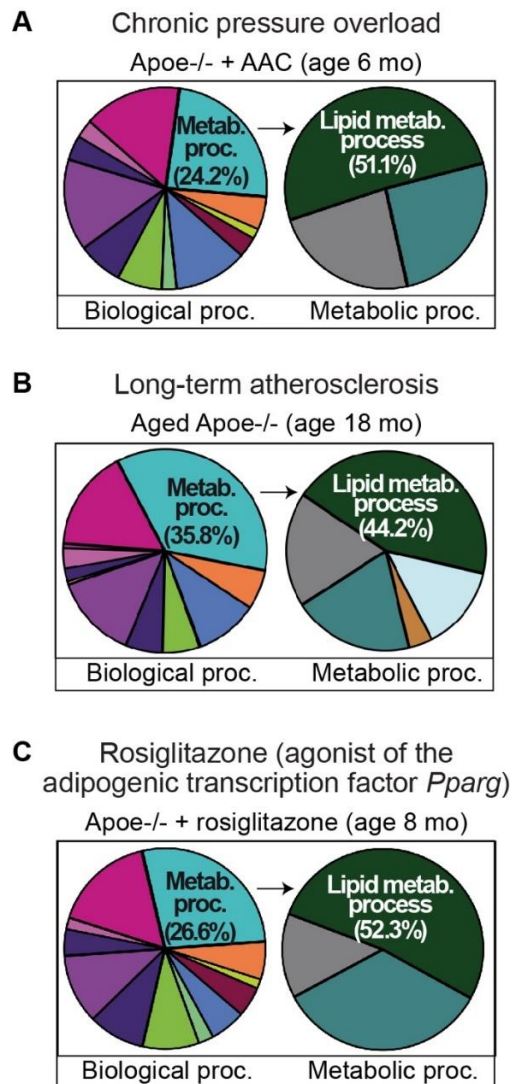
Figure 9: Gene ontology (GO) analysis of significantly up-regulated genes identifies the "lipid metabolic process" as the top biological process induced in different experimental heart failure models.

(**A**) GO analysis of significantly up-regulated genes in hearts of six-month-old Apoe-/- mice with heart failure induced by two months of AAC. The control group consisted of age-matched, sham-operated Apoe-/- mice. (**B**) GO analysis of significantly up-regulated genes of aged, 18-month-old Apoe-/- mice compared to 18-month-old, non-transgenic B6 mice. (**C**) GO analysis of significantly up-regulated genes of eight-month-old Apoe-/- mice with two months of rosiglitazone treatment. GO analysis was performed by GeneSpring. Significantly up-regulated genes in comparison to the respective control group (p ≤ 0.01, ≥ 2-fold difference, call present and/or intensity > 100) were used for data analysis.

6.4. Whole genome microarray gene expression profiling identifies *Scd1* as one of the most up-regulated lipid metabolism genes of failing hearts from *Apoe-/-* mice and non-transgenic B6 mice with chronic pressure overload

Cardiac lipid metabolism genes were up-regulated at the onset of HF of different HF models, which rely on atherosclerosis-prone *Apoe-/-* mice with hypercholesterolemia (Figure 9, and Supplemental Table (Appendix 13.3)). Moreover, these heart failure-related cardiac lipid metabolism genes were also up-regulated in non-transgenic B6 mice with symptoms of HF triggered by six months of chronic pressure overload imposed by AAC (Figure 10, and Supplemental Table (Appendix 13.3).

Comparative analysis of whole genome gene expression data identified these genes of the cardiac lipid metabolic process, which were up-regulated in failing hearts from six-month-old *Apoe-/-* mice with two months of AAC, and 10-month-old B6 mice with six months of AAC (Figure 10). The overview of up-regulated genes of the cardiac lipid metabolic process shows that chronic pressure overload-induced HF was accompanied by the up-regulation of genes involved in lipid synthesis, lipid storage and lipid oxidation (Figure 10).

Highly expressed genes involved in lipid synthesis include the gene *Scd1* (stearoyl-coenzyme A desaturase) and *Fasn* (fatty acid synthase). A lipid storage gene with high expression in failing hearts is *Cidea* (cell death inducing DFFA like effector a), and *Adipoq* (adiponectin) was identified as one of the genes involved in lipid oxidation with high expression in failing hearts (Figure 10).

As a control, whole genome gene expression profiling also documented the complete absence of apolipoprotein E (*Apoe*) in hearts from *Apoe-/-* mice with and without HF imposed by AAC whereas the expression of *Apoe* was prominent in B6 hearts with and without AAC-induced HF, e.g. the signal intensities of probe sets detecting *Apoe* (1432466_a_at) were 100.3 and 122.6 in hearts from *Apoe-/-* mice, and 4718.2, 4779.7, 6100.5, 6182.7, 5539.0 and 6020.7 in hearts from B6 mice (Figure 10).

Affymetrix ID	Gene	Pressure overload (Apoe$^{-/-}$)						Pressure overload (B6)			
		AAC-Apoe1	AAC-Apoe2	Apoe-sham1	Apoe-sham2	B6-1	B6-2	AAC-1	AAC-2	Sham-1	Sham-2
1415964_at	*Scd1*	10213.2	9825.8	807.8	841.9	972	1069.8	9983.6	9823.4	817.6	804.5
1415965_at	*Scd1*	782.6	776.4	49	55.9	73.3	80.8	627.1	533.8	59.7	38.7
1423828_at	***Fasn***	3458.4	3555.6	554.4	570.2	540.8	639.6	4586.4	4420.4	708.3	824.1
1420722_at	*Elovl3*	54.2	50.4	38.1	52.9	66.9	34.7	143	130.2	34.2	45.3
1417403_at	*Elovl6*	173.9	160.2	17.9	24.7	49.7	52.1	243.8	237.1	53.2	37.2
1417404_at	*Elovl6*	278.2	260.9	63.7	11.2	59	58.4	439.3	537.2	62.1	66.8
1416316_at	*Slc27a2*	140.7	142.6	36.1	4.9	34.1	5.9	236.8	217.5	11.9	13.8
1423439_at	*Pck1*	637.6	669.7	32.9	19.5	42.8	60.4	1260.7	1254.5	41.6	51.6
1439617_s_at	*Pck1*	229.2	199.4	55.2	27.4	45.4	35	360.7	434.8	42.5	27.4
1434185_at	*Acaca*	866.1	773.5	422.8	324.2	339.1	289.6	876.9	892.8	398.4	406.2
1434191_at	*Tmem195*	237.5	268.8	158.8	152.5	83	93.7	351.2	375.2	100	125.5
1428190_at	*Ctp*	781.2	736.3	249.3	239.6	254.1	274.4	793.9	767.8	368	308.8
1417561_at	*Apoc1*	373.5	317.3	48.5	51.2	65.4	42.2	621.3	670.6	42.1	22.8
1417956_at	***Cidea***	3022.8	2855.2	1390.5	1402.6	1448.1	1467.3	5317.7	5004.8	1214.8	1299.8
1452260_at	*Cidec*	694.9	684.4	51.6	56.9	65.1	29.4	825.7	754.4	64.5	26.5
1418190_at	*Pon1*	237.7	214.4	64.2	63.6	61.3	26.5	700.6	688	30	45
1418197_at	*Ucp1*	282.2	269.4	14.5	9	31.8	40.3	6319.5	6405.9	16.3	26.5
1424451_at	*Acaa1b*	46.6	65.5	9	16.5	37.7	8.8	242.3	198.9	17.4	1
1439459_x_at	*Acly*	1294.4	1319.7	591.6	570.5	650.6	662.8	1408.2	1353.5	846.4	768.2
1416468_at	*Aldh1a1*	2068.2	2037.3	785.3	797.3	768.4	734	2516.5	2394.5	699.3	688.5
1418601_at	*Aldh1a7*	191.2	187.4	48.6	53.7	37.4	54.9	387.9	435.9	45.2	63.8
1426225_at	*Rbp4*	327.1	272.7	65.9	53.7	42.8	63.3	744.6	828.3	48.9	70.4
1422651_at	***Adipoq***	4490.1	4373.5	232.7	240.2	215.3	261	6107.9	5880.6	269.5	198.1
1449182_at	*Retn*	538.9	617.9	108	61	10.1	78.6	314.2	303.3	44.3	55.6
1430640_a_at	*Prkar2b*	103.4	108.5	24.9	28.2	38.8	11.9	303.3	333.2	24.5	2
1438664_at	*Prkar2b*	342.4	328.2	32.6	52.1	45.3	45.3	981.5	1128.7	45.6	38.1
1456475_s_at	*Prkar2b*	243	229.3	51.1	44.6	60.2	44	709.5	741	53.7	42.4
1432466_a_at	*Apoe*	122.6	121.8	102.4	100.3	4718.2	4779.7	6100.5	6182.7	5539.9	6020.7

(Left-margin row group labels: Lipid synthesis — rows Scd1 through Elovl6; Lipid storage — rows Slc27a2 through Cidec; Lipid oxidation — rows Pon1 through Prkar2b.)

Figure 10: Overview of whole genome microarray gene expression data of significantly up-regulated genes of the cardiac lipid metabolic process of Apoe-/- and B6 mice with heart failure triggered by chronic pressure overload.
Six-month-old Apoe-/- mice with two months of AAC-induced heart failure were analyzed and compared to age-matched, sham-operated Apoe-/- and non-transgenic B6 mice. Ten-month-old B6 mice with six months of AAC-induced heart failure were compared to age-matched, sham-operated B6 mice. The list shows probe set intensities of significantly different genes between heart failure models and the respective controls (≥2-fold difference to the respective control group; p≤0.01; unpaired, two-tailed, t-test). Two-fold difference was not reached of probe set intensities detecting Elovl3 and Tmem195 (AAC-Apoe-/- vs. Sham Apoe-/-) and Acly (AAC-B6 vs. Sham B6).

Currently, it is not clear whether up-regulation of lipid metabolism genes is beneficial or detrimental for the heart. On one hand, the failing heart is considered an "engine out of fuel" [266], and consequently, the up-regulation of lipid genes could replenish the heart with fuel. On the other hand, it is well known, that excessive accumulation of lipids in the heart is toxic and causes symptoms of HF by triggering cardiolipotoxicity [264]. Moreover, under physiological conditions, the heart mainly controls the availability of lipids by lipid uptake while the cardiac synthesis of lipids is negligible [266].

Because excessive lipid accumulation could cause cardiolipotoxicity, the search of potential new targets involved in HF pathogenesis focused on genes involved in lipid synthesis. With this concept, *Scd1* was identified as one of the genes of the cardiac lipid metabolic process

with the highest up-regulation. The two different probes detecting *Scd1* (1415964_at; 1415965_at) showed more than 10-fold increased signal intensities in failing hearts with chronic pressure overload-induced symptoms of HF compared to those of the respective healthy controls (Figure 10). The increased signal intensities of the two *Scd1*-detecting probes reflect strongly increased *Scd1* expression levels in failing *Apoe*-/- and B6 hearts with HF triggered by AAC-induced chronic pressure overload compared to those of the respective control groups (Figure 10).

6.5. The generation of Tg-*SCD1* mice with myocardium-specific *SCD1* expression

In view of the strong up-regulation of *Scd1* in failing hearts of several experimental models of HF, the in vivo role of *SCD1* up-regulation in the heart was investigated. To this end, transgenic mouse lines were generated with myocardium-specific expression of *SCD1* under control of the alpha myosin heavy chain (alpha-MHC) promoter (Figure 11A) and Appendix 13.1 and 13.2. The alpha-MHC promoter directs the myocardium-specific expression of a transgene [132].

Transgenic mice were generated by injection of the linearized *SCD1*-transgene (1-2 ng/microL) into the pro-nucleus of fertilized oocytes from B6 (C57BL/6J) mice. After overnight incubation, two-cell stage embryos were implanted into the oviducts of pseudo-pregnant foster mice. After weaning, at an age of 3-4 weeks, offspring were analyzed for the stable insertion of the transgene into the genomic DNA by genotyping PCR of ear-punch biopsies (Figure 11B).

Genotyping PCR identified founder mice of the FO generation with stable integration of the *SCD1* transgene into the genomic DNA (Figure 11B). Founders number 5 and 6 with high and low *SCD1* gene dosages were used for further breeding.

.
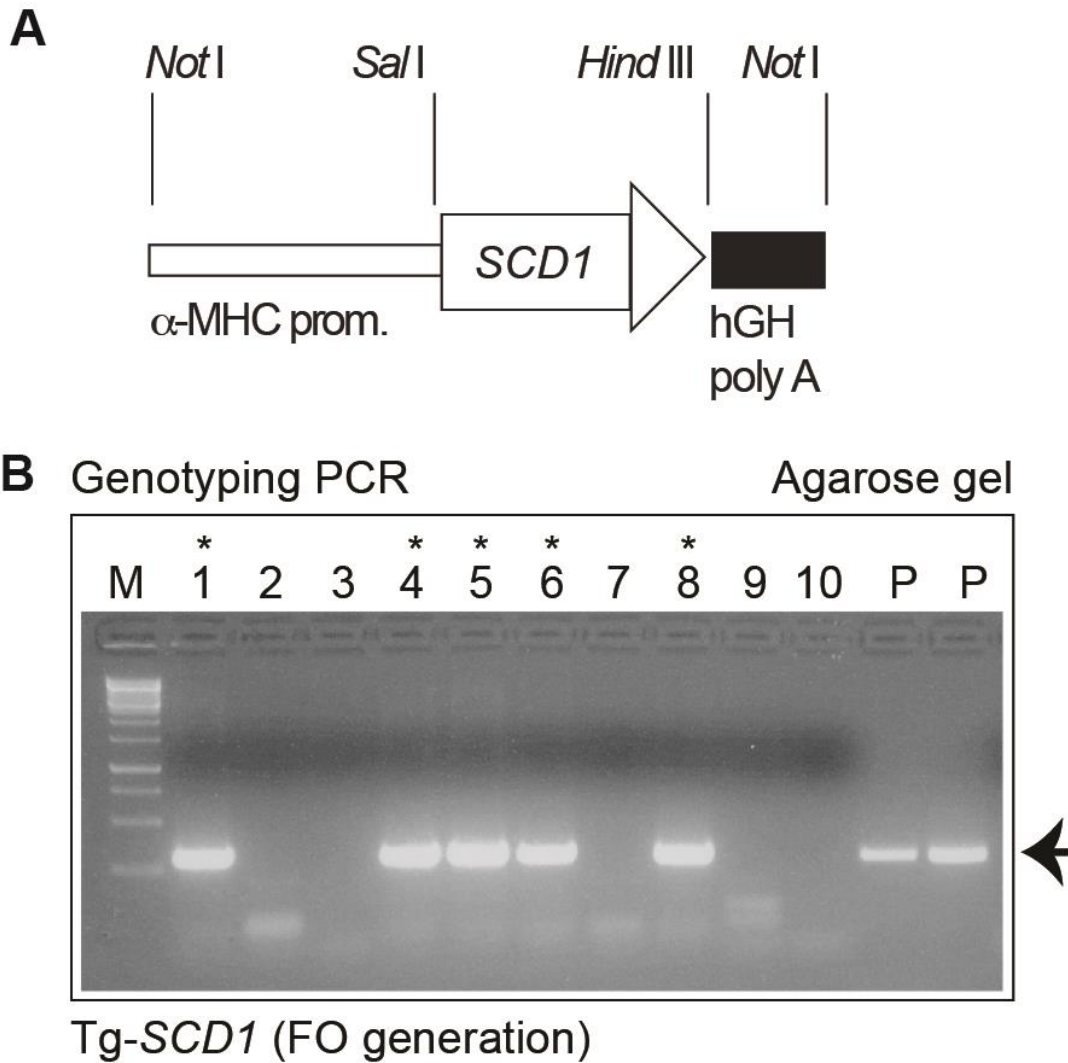
Figure 11: Generation of transgenic Tg-SCD1 mice with myocardium-specific expression of SCD1.
(A) Scheme of alpha-MHC promoter transgene used for generation of Tg-SCD1 mice. (**B**) Genotyping PCR of ear-punch biopsies identified Tg-SCD1 mice with stable integration of the SCD1 transgene into the genomic DNA. The amplification of the SCD1-plasmid DNA (P) was included as a positive control.

6.6. Immunoblot detection of the SCD1 protein in the hearts of Tg-*SCD1* mice

After the identification of founder mice with stable integration of the *SCD1* transgene into the genomic DNA, transgenic founder mice were used for further breeding and two different transgenic Tg-*SCD1* mouse lines were established.

Immunoblot detection of SCD1 of cardiac lysates was performed to analyze the presence of the SCD1 protein in the hearts of Tg-*SCD1* mice (Figure 12).

The immunoblot analysis showed that the two different Tg-*SCD1* mouse lines had increased cardiac SCD1/Scd1 protein levels compared to those of non-transgenic B6 control mice (Figure 12). The cardiac SCD1/Scd1 protein levels of Tg-*SCD1* mice with high cardiac SCD1 contents were increased 4.3 ± 0.8-fold compared to those of non-transgenic B6 mice, and the SCD1/Scd1 protein levels of Tg-*SCD1* mice with low SCD1 contents were increased 1.9 ± 0.6-fold (Figure 12).
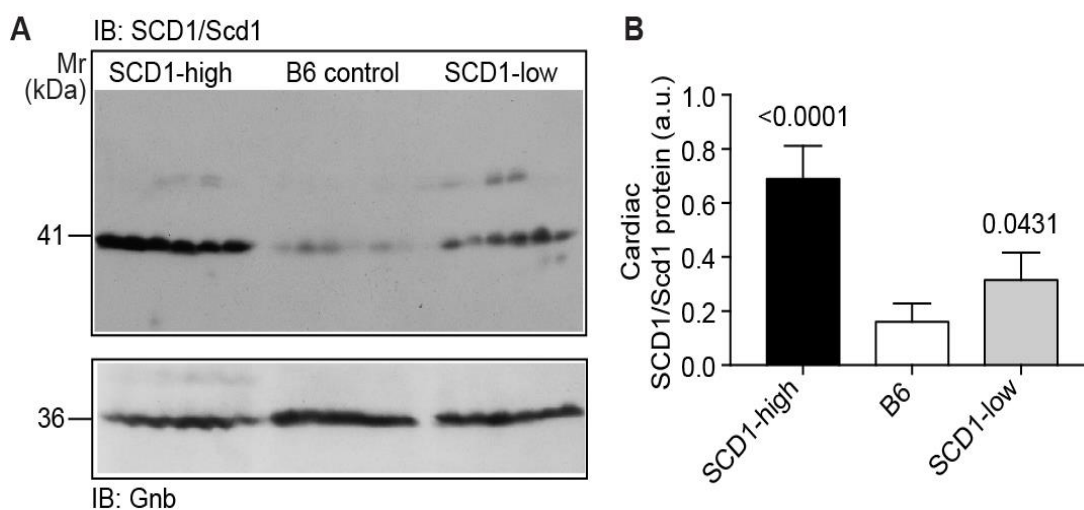
Figure 12: Immunoblot detection of SCD1/Scd1 protein in Tg-*SCD1* hearts.
(A) Representative immunoblot detection of SCD1/Scd1 proteins in the hearts of male, eight-month-old mice from two different Tg-*SCD1* mouse lines with high and low cardiac SCD1 protein levels (n=6 mice/group). As a control group, male, age-matched, non-transgenic B6 mice were used. The lower panel shows a control blot, which detects Gnb, the guanine nucleotide-binding protein subunit beta. (**B**) Panel (B) shows quantitative evaluation of immunoblot data by densitometric scanning analysis (mean ± s.d., n=6 mice/group; p-values vs. non-transgenic B6 mice are indicated and were determined by Tukey`s test).

These immunoblot data show the successful generation of two different Tg-*SCD1* mouse lines with 4.3- and 1.9-fold increased cardiac SCD1 protein levels compared to those of non-transgenic B6 mice.

6.7. Phenotyping of Tg-*SCD1* mice showed cardiac hypertrophy and dysfunction

After detection of the increased cardiac SCD1 levels, the two different Tg-*SCD1* mouse lines were further characterized by phenotyping to elucidate the impact of an increased cardiac SCD1 protein content on cardiac weight and cardiac function. The heart-to-body weight ratio of eight-month-old male Tg-*SCD1* mice was determined and compared to that of non-transgenic B6 mice. At an age of 8 months, the Tg-*SCD1* mice with high cardiac SCD1 protein levels showed a significantly increased heart-to-body-weight ratio, which was 6.22 ± 0.6 mg/g compared to 4.9 ± 0.2 mg/g of non-transgenic B6 mice (Figure 13A).

The SCD1-induced increase in the heart-to-body weight ratio was protein dosage-dependent because the heart-to-body weight ratio of Tg-*SCD1* mice with low cardiac SCD1 levels was increased to only 5.4 ± 0.3 mg/g but not significantly different from that of non-transgenic B6 control mice (Figure 13A). Thus, at an age of 8 months, Tg-*SCD1* mice with 4.3-fold increased cardiac SCD1 levels had an increased heart-to-body-weight ratio, which is indicative of cardiac hypertrophy. For comparison, Tg-*SCD1* mice with 1.9-fold increased SCD1 protein level showed a trend towards an increased heart-to-body-weight ratio.

The cardiac function of Tg-*SCD1* mice was investigated by echocardiography. At an age of 8 months, male Tg-*SCD1* mice with 4.3-fold increased cardiac SCD1 protein level and cardiac hypertrophy had a significantly decreased left ventricular cardiac ejection fraction of 35.2 ± 6.1 % compared to that of non-transgenic B6 mice, which had a cardiac ejection fraction of 52.7 ± 5.2 % (Figure 13B). Tg-*SCD1* mice with only 1.9-fold increased cardiac SCD1 protein contents showed a trend towards a decreased left ventricular cardiac ejection fraction, i.e. Tg-*SCD1* mice with low SCD1 levels had a cardiac ejection fraction of 47.0 ± 5.1 %, which was not significantly different from that of non-transgenic B6 control mice (Figure 13B).

Together these phenotyping results show that a 4.3-fold increased cardiac SCD1 protein level is sufficient to trigger cardiac hypertrophy and cardiac dysfunction.
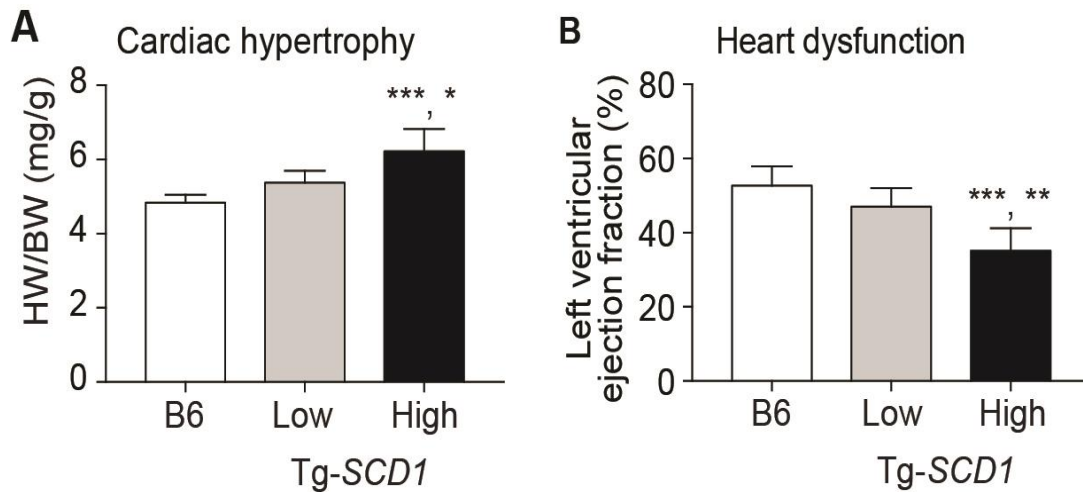
Figure 13: Phenotyping of Tg-*SCD1* mice showed cardiac hypertrophy and cardiac dysfunction.
(**A**) The heart-to-body-weight ratio of male Tg-*SCD1* mice with 4.3-fold increased cardiac SCD1 protein (high) and 1.9-fold increased SCD1 protein (low) was determined and compared to that of non-transgenic B6 mice (mean ± s.d. n=5 hearts/group; ***, p=0.0006 vs. B6 and *, p=0.0199 vs. Tg-*SCD1*-low; Tukey`s test). (**B**) The left ventricular cardiac ejection fraction was analyzed of Tg-*SCD1*-high and Tg-*SCD1*-low mice and compared to that of non-transgenic B6 mice (mean ± s.d., n=6 mice/group; ***, p = 0.0002 vs. B6 and **, p = 0.0052 vs. Tg-*SCD1*-low; Tukey`s test).

6.8. Histology analysis of Tg-*SCD1* hearts

The heart-to-body-weight ratio determination of Tg-*SCD1* hearts indicated that Tg-*SCD1* mice with 4.3-fold increased cardiac SCD1 protein levels, developed cardiac hypertrophy. Histology analysis was performed to further analyze the phenotype of Tg-*SCD1* mice.

Longitudinal paraffin-embedded heart sections were prepared of 8-month-old, male Tg-*SCD1* mice with high SCD1 levels. As a control group, male, age-matched, non-transgenic B6 mice were used. Cardiac sections were inspected under a light microscope after hematoxylin-eosin staining. The histology analysis of hematoxylin-eosin-stained longitudinal heart sections prepared from 8-month-old male Tg-*SCD1* mice confirmed the phenotype of cardiac hypertrophy with enlargement of the left ventricle of eight-month-old Tg-*SCD1* mice with 4.3-fold increased cardiac SCD1 protein levels compared to the normal heart morphology of age-matched, non-transgenic B6 mice (Figure 14, upper and lower panels).
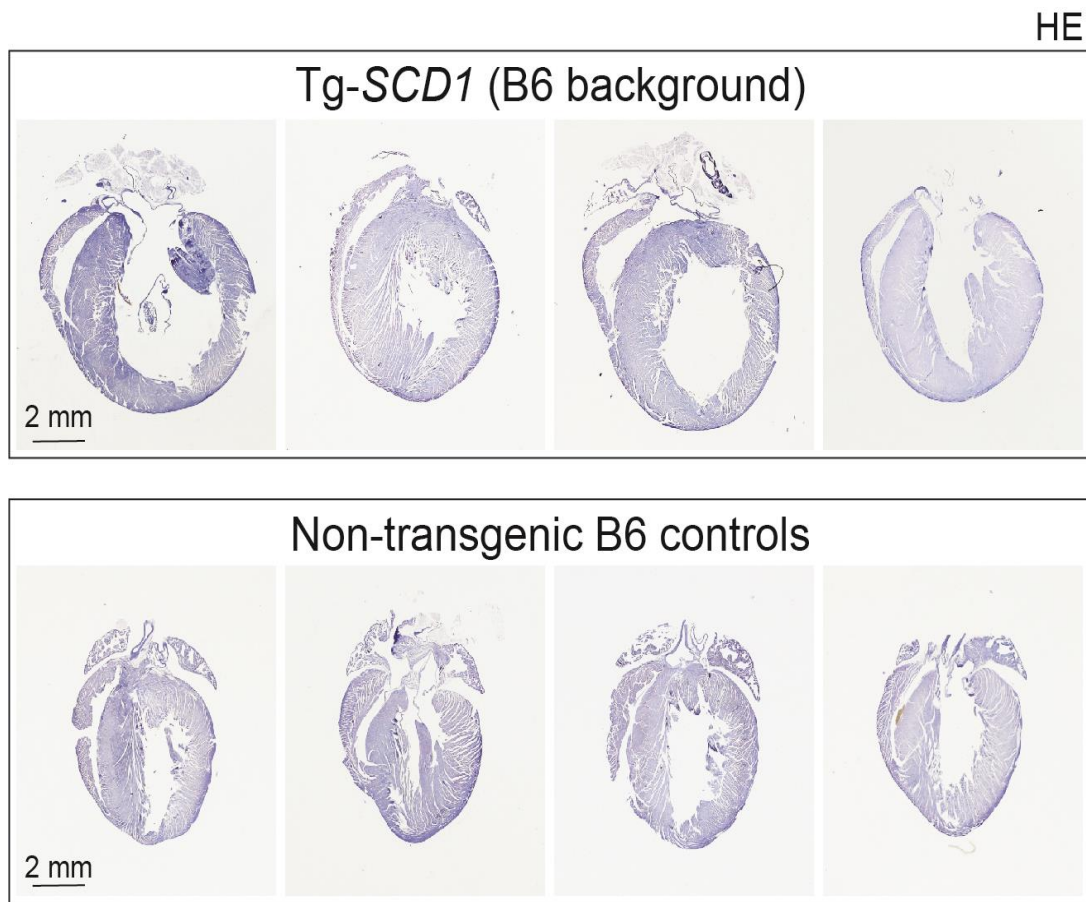
Figure 14: Histology analysis of Tg-*SCD1* hearts shows cardiac hypertrophy.
Longitudinal paraffin-embedded heart sections of eight-month-old, male Tg-*SCD1* mice with high SCD1 level were stained with hematoxylin-eosin (HE). As a control heart sections of age-matched, non-transgenic B6 mice were used. Histology analysis was performed of four mice/group.

6.9. The immunohistology analysis showed increased cardiac SCD1 protein contents of Tg-*SCD1* mice with cardiac hypertrophy

To further analyze the phenotype of Tg-*SCD1* mice, immunohistology detection of the cardiac SCD1 protein was performed of longitudinal heart sections of eight-month-old Tg-*SCD1* mice with 4.3-fold increased cardiac SCD1 protein levels as determined by immunoblot (cf. Figure 12). The staining of paraffin-embedded heart sections with polyclonal anti-SCD1 antibodies documented the increased cardiac SCD1 protein in the myocardium of Tg-*SCD1* mice compared to that of non-transgenic B6 mice (Figure 15 upper vs. lower panels).
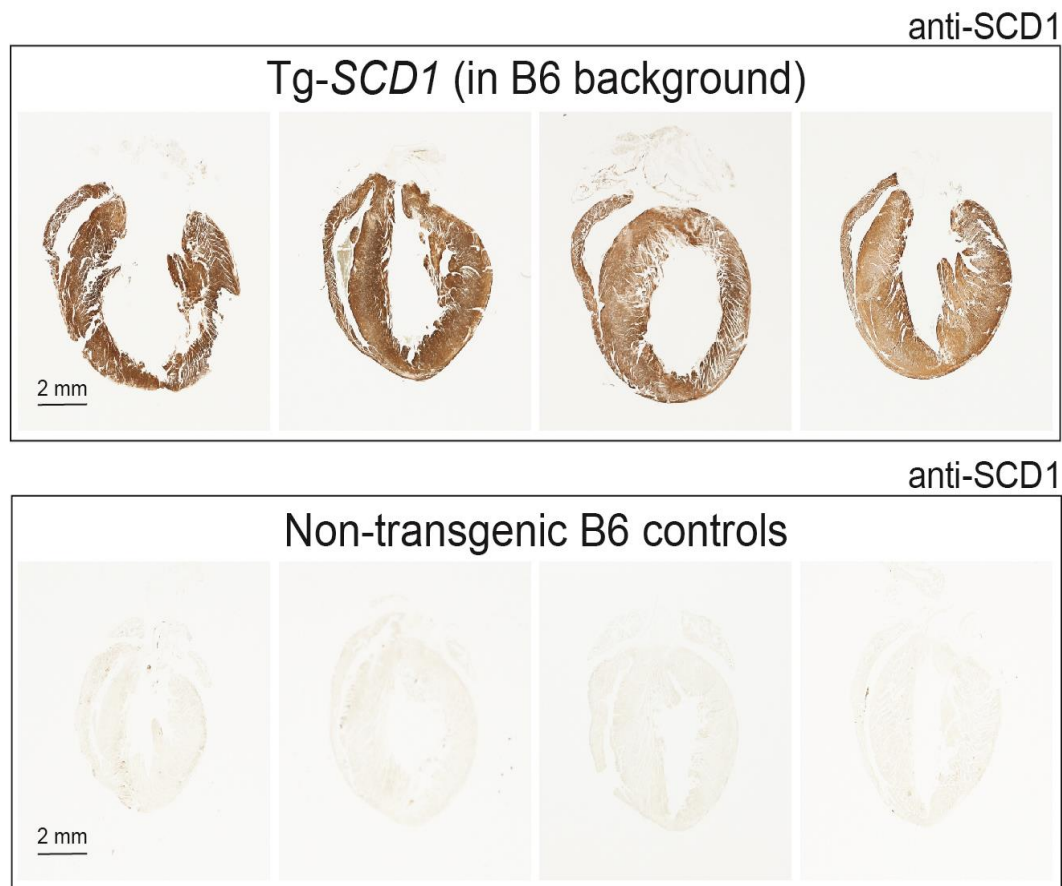
Figure 15: Immunohistology detection of SCD1 on longitudinal heart sections of Tg-*SCD1* mice. Longitudinal paraffin-embedded heart sections of eight-month-old Tg-*SCD1* mice were stained with polyclonal anti-SCD1 antibodies (upper panels). As a control heart sections of non-transgenic B6 mice were used. (lower panels). Immunohistology was performed of four mice/group.

For comparison, the anti-SCD1 antibody staining was largely absent in the ascending aorta and the aortic arch of Tg-*SCD1* mice (Figure 15, upper panels). These immunohistology data confirm the myocardium-specific expression of *SCD1* under control of the alpha-MHC promoter, which does not induce protein expression in vascular smooth muscle cells.

Immunohistology analysis further confirmed the phenotype of cardiac hypertrophy with predominant enlargement of the left ventricle of Tg-*SCD1* mice with increased cardiac SCD1 protein (Figure 15, upper panels) whereas eight-month-old non-transgenic B6 mice without increased cardiac SCD1 protein level did not develop cardiac hypertrophy (Figure 15, lower panels).

6.10. Whole genome microarray gene expression profiling identified up-regulated heart failure-related genes in Tg-*SCD1* hearts

The phenotype of Tg-*SCD1* mice was analyzed further by whole genome microarray gene expression profiling. Total RNA was isolated of heart specimens from eight-month-old, male Tg-*SCD1* mice with 4.3-fold increased cardiac SCD1 protein level. As a control group, total cardiac RNA from age-matched, male, non-transgenic B6 mice was used. After reverse transcription of mRNA into cDNA, and further processing according to the Affymetrix protocol, fragmented and biotin-labeled cRNA was hybridized to the gene chip (Mouse Genome MG430 2.0 Array, Affymetrix), which contains more than 45 000 probe sets and covers the whole mouse genome.

Probe set intensities were recorded, and after data normalization by GCOS to a target value of 300, data analysis was performed to identify probe sets with significantly different signal intensities indicative of differentially expressed genes between eight-month-old, male Tg-*SCD1* hearts and age-matched, non-transgenic B6 controls.

The following criteria were used for identification of probe sets detecting differentially expressed genes: (i) significant difference from the B6 control group (p ≤ 0.01; just alpha), (ii) ≥ 2-fold difference (up-regulation or down-regulation) compared to the B6 control group, and (iii) call present and/or signal intensity ≥100. Whole genome microarray gene expression data were deposited to the repository and are available at the NCBI GEO database (GSE 120020).

After data normalization and data analysis, microarray data were used to further investigate the HF phenotype of Tg-*SCD1* mice. To this end, the list of differentially expressed genes was searched manually for established heart failure-related genes of the cardiac lipid metabolic process [130, 267, 268]. Notably, for HF phenotyping, the focus was put on the expression level of fatty acid synthase, *Fasn*, adiponectin, *Adipoq* [268], and resistin, *Retn* [267], because the heart failure-enhancing and cardiac dysfunction-promoting functions of these lipid metabolism genes were previously established [130].
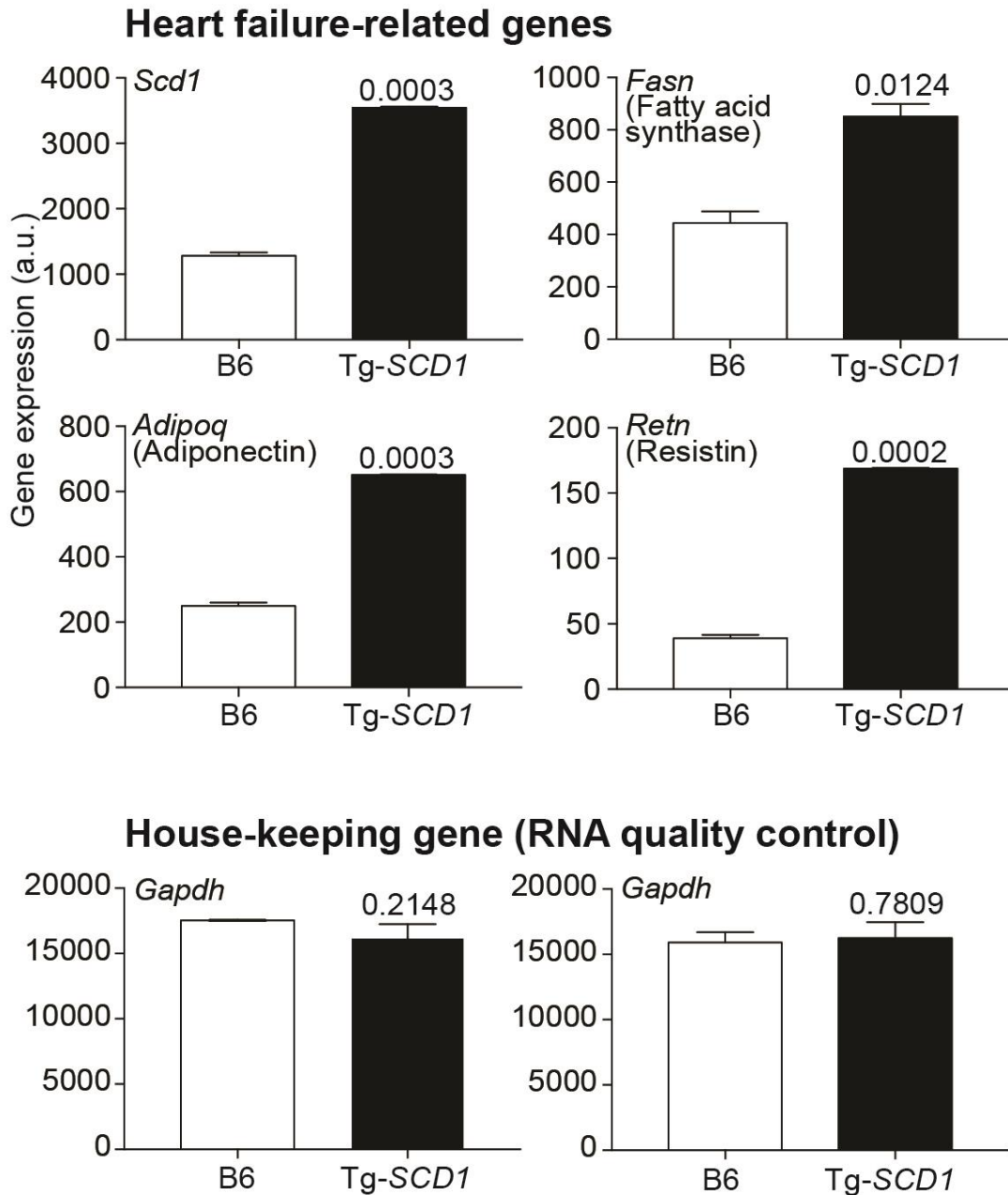
Figure 16: Whole genome microarray gene expression profiling shows up-regulation of heart failure-related genes in hearts of Tg-*SCD1* mice.
Differentially expressed genes between Tg-*SCD1* and B6 mice were identified by p≤0.01, just alpha, ≥ 2-fold up-regulation in Tg-*SCD1* hearts vs. B6 hearts and call present and/or signal intensity > 100 (mean ± s.d., n=2 gene chips/group with RNA pooled from n=4 hearts for one gene chip; p-values were determined by the unpaired, two-tailed t-test, and calculated by MEV). Signal intensities of the following probe sets are shown: 1415964_at (*Scd1*); 1423828_at (*Fasn*); 1422651_at (*Adipoq*); 1449182_at (*Retn*); AFFX-GapdhMur/M32599_5_at and AFFX-GapdhMur/M32599_3_at (*Gapdh*).

In addition to these established heart failure-enhancing lipid metabolism genes, the search of differentially expressed genes between Tg-*SCD1* and B6 mice also focused on the gene expression level *Scd1* because *Scd1* was highly up-regulated in different HF models (cf. Figure 10), and thus could also serve as an indicator and/or promoter of HF. In agreement with the HF phenotype of Tg-*SCD1* mice, whole genome gene expression profiling detected the significant up-regulation of the mouse *Scd1* gene expression levels in hearts of Tg-*SCD1* mice (Figure 16). The microarray gene expression analysis technique specifically detects the gene expression level of the endogenously expressed murine *Scd1* gene of Tg-*SCD1* mice because for detection of *Scd1* gene expression, the gene chip (Mouse Genome MG430 2.0 Array, Affymetrix) applies antisense probes, which hybridize to the non-coding 3`-end of the murine *Scd1* transcript (Figure 17). This non-coding region of the *Scd1* transcript is absent in the human *SCD1* cDNA, which was used for the generation of Tg-*SCD1* mice.

Probe set ID	probe x	probe y	probe interrogation position	probe sequence	target strandedness
1415964_at	187	508	4546	TTGTAACAAACCCACCCCAGAGATA	Antisense
1415964_at	635	58	4591	AAACTCCTGGGCTAAGTATCTGACA	Antisense
1415964_at	477	451	4607	TATCTGACAGTCTCACATCTCAACA	Antisense
1415964_at	197	156	4638	ATTAAGTGTCCATAGCATCAGCTCA	Antisense
1415964_at	278	522	4712	GACCTACTACTTCAAGGGCAGTTCT	Antisense
1415964_at	368	557	4788	AGGTATTCATACAGACTCCCAAAGA	Antisense
1415964_at	533	625	4819	TATGTTCCTGAGACCATCGTTTAGT	Antisense
1415964_at	294	547	4838	TTTAGTCTACATTGCTCTTCCCAGA	Antisense
1415964_at	110	683	4851	GCTCTTCCCAGAGACTGACAGATAT	Antisense
1415964_at	242	573	4884	AAAGTGCAAGACTACCTACCCACTG	Antisense
1415964_at	476	131	4929	AACCTTTCCCTTCCCTGAATGAGAT	Antisense

Figure 17: Antisense probes used for detection of murine *Scd1* gene expression by probe ID 1415964_at of the gene chip "Mouse Genome MG430 2.0 Array" (Affymetrix).
Antisense probes hybridize to the non-coding 3`-end of the murine *Scd1* transcript, which is absent in the transgenic *SCD1* cDNA used for generation of Tg-*SCD1* mice.

Tg-*SCD1* hearts showed the significant up-regulation of other well-established heart failure-enhancing genes of the cardiac lipid metabolic process, i.e. *Fasn* (fatty acid synthase), *Adipoq* (adiponectin) and *Retn* (resistin) (Figure 16). These three genes are not only up-regulated in

experimental models of HF (see also Figure 10) [267, 268] but also on biopsy specimens and/or peripheral blood of human patients with HF [124, 130, 269-272].

As a control, signal intensities of probe sets detecting the house-keeping gene, *Gapdh*, were comparable and not significantly different between Tg-*SCD1* and non-transgenic B6 hearts (Figure 16). Notably, signal intensities of two different probe sets with antisense nucleotides, which hybridize to the 5`- and 3`- ends of the *Gapdh* transcript, were comparable and not significantly different between Tg-*SCD1* mice and B6 hearts (Figure 16). The following 3`/5`-ratios of *Gapdh*-detecting probe sets were determined: 0.84 and 0.82 (Tg-*SCD1* hearts), and 0.94 and 0.87 (B6-controls). Together these data confirm the integrity of the cardiac RNA of Tg-*SCD1* and B6 control hearts used for microarray gene expression profiling.

Taken together, whole genome microarray gene expression analysis demonstrates that Tg-*SCD1* hearts with symptoms of HF showed up-regulation of heart failure-related target genes of the cardiac lipid metabolic process.

6.11. Immunoblot analysis confirmed microarray gene expression data and showed increased cardiac Fasn and Adipoq contents of Tg-*SCD1* mice

Differential gene expression data of the microarray study were validated by immunoblot analysis of cardiac Fasn and Adipoq protein levels of Tg-*SCD1* mice. In agreement with the microarray data, immunoblotting showed the significant up-regulation of cardiac Fasn protein contents, in hearts of eight-month-old Tg-*SCD1* mice compared to non-transgenic B6 controls (Figure 18A). In addition, the heart failure-related cardiac Adipoq contents were also significantly increased of Tg-*SCD1* mice (Figure 18B).
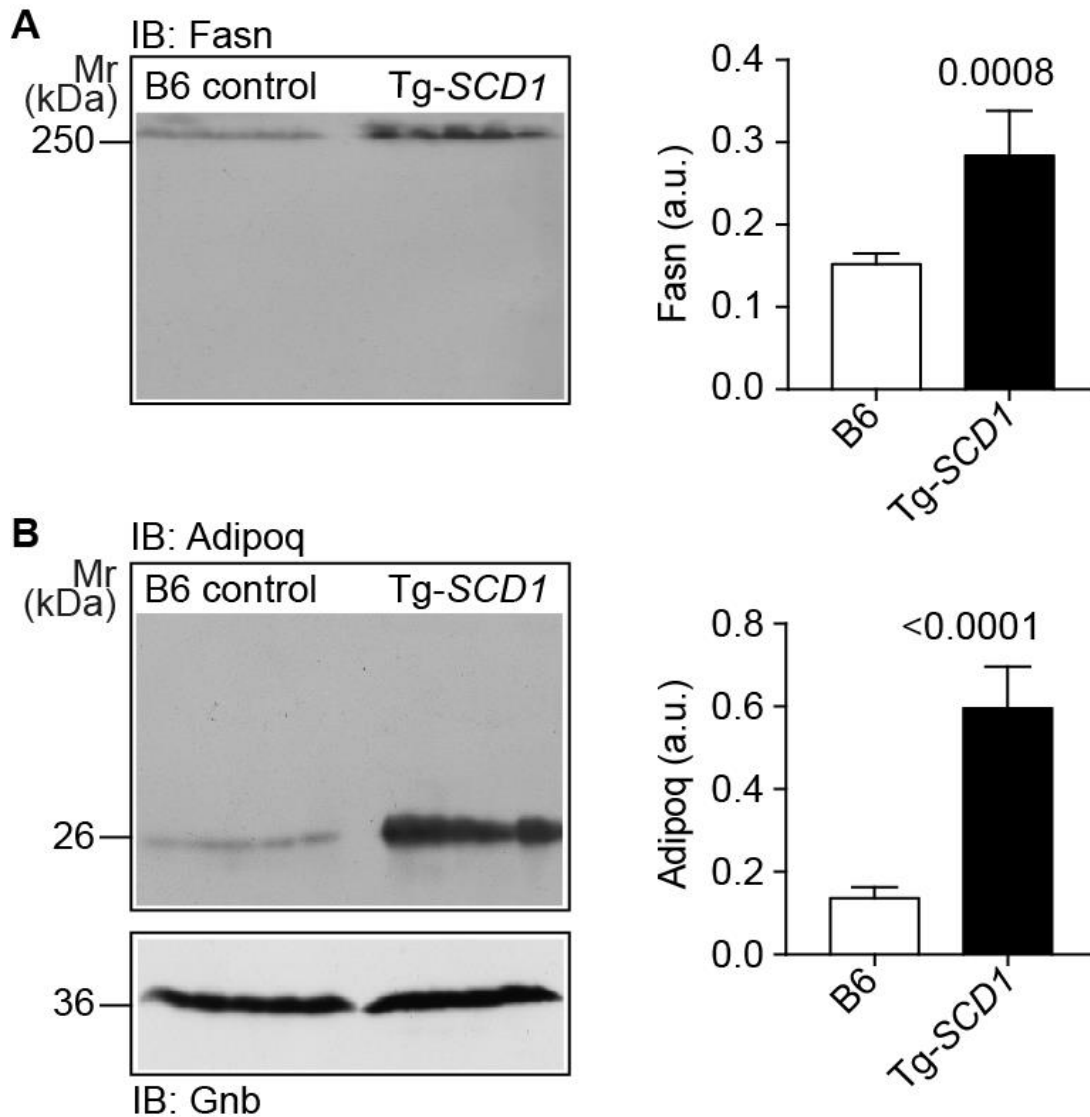
Figure 18: Immunoblot detection showed increased cardiac Fasn and Adipoq contents of Tg-*SCD1* mouse hearts.

(**A, B**) Immunoblot analysis (IB) of cardiac Fasn (**A**) and Adipoq (**B**) contents was performed of 8-month-old Tg-*SCD1* mice and non-transgenic B6 controls. The left panels show representative immunoblot images and the right panels show quantitative data (mean ± s.d.; n=5 hearts/group; p-values were determined with the unpaired, two-tailed t-test). The lower panel (**B**) is a control immunoblot, which detects Gnb.

6.12. Tg-*SCD1* mice displayed increased cardiac levels of the heart failure-promoting angiotensin II AT1 receptor

Phenotyping and gene expression profiling showed that an increased cardiac SCD1 level triggers cardiac hypertrophy and cardiac dysfunction of Tg-*SCD1* mice. However, the mechanism underlying this heart failure-enhancing function of SCD1 is not clear. Because SCD1 enhances

the membrane fluidity by catalyzing the delta-9 desaturation of 12-19 carbon SFAs [273], the

impact of SCD1 up-regulation on a heart failure-related transmembrane protein was investigated.
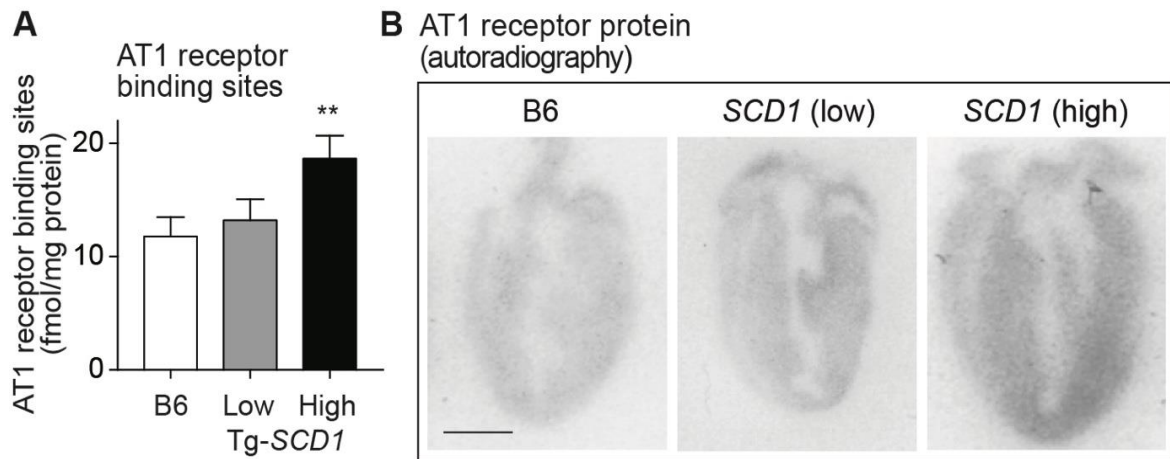
Figure 19: The heart failure-related angiotensin II AT1 receptor is increased in hearts of Tg-*SCD1* mice.
(**A**) Number of AT1 receptor binding sites were determined by radioligand binding with Sar^1,$[^{125}I]Tyr^4$,Ile^8-angiotensin II of eight-month-old B6, and Tg-*SCD1* myocardial membranes with 1.9-fold (Low) and 4.3-fold (High) increased cardiac *SCD1* protein contents (mean ± s.d., n=4 heart membrane preparations/group; **,p = 0.0015 and 0.0067 vs. B6 and Tg-*SCD1* low; Tukey`s test). (**B**). Representative autoradiography images of longitudinal heart sections of B6 and Tg-*SCD1* mice with 1.9-fold (low) and 4.3-fold (high) increased cardiac *SCD1* contents after autoradiography imaging of the AT1 receptor with anti-AT1 receptor antibodies. Autoradiography images are representative of three hearts/group, bar: 2 mm.

The angiotensin II AT1 receptor is one of the major transmembrane receptors, which

promotes cardiac hypertrophy, cardiac fibrosis and cardiac dysfunction and thereby enhances

HF pathogenesis [274]. Vice versa, AT1 receptor inhibition by an AT1 antagonist retards the

progression of HF, and reduces morbidity and mortality of HF patients [275]. To investigate

the impact of *SCD1* on cardiac AT1 receptors, the number of AT1 receptors was determined

on myocardial membranes of eight-month-old Tg-*SCD1* mice and compared to that of non-

transgenic B6 mice (Figure 19A). The radioligand binding studies showed that the number of

AT1 receptor binding sites of Tg-*SCD1* hearts with 4.3-fold increased SCD1 contents was

1.6±0.2-fold higher than of non-transgenic B6 hearts (Figure 19A). For comparison, the

number of AT1 receptor binding sites of Tg-*SCD1* hearts with only 1.9-fold increased SCD1

was not significantly different from B6 controls (Figure 19A).

To determine the AT1 receptor protein, detection of AT1 receptors was performed by autoradiography of longitudinal cardiac sections of Tg-*SCD1* hearts with 4.3-fold increased cardiac SCD1 levels. The control groups were non-transgenic B6 hearts and Tg-*SCD1* hearts with only 1.9-fold increased SCD1 levels. For imaging of cardiac AT1 receptors by autoradiography, affinity-purified, rabbit polyclonal, anti-AT1 receptor antibodies and [^{125}I]-labeled, secondary anti-rabbit antibodies were used. The autoradiography images revealed the location of the AT1 receptor in the myocardium of Tg-*SCD1* hearts. A strong binding of anti-AT1 receptor antibodies was detected in the left ventricle of Tg-*SCD1* hearts with cardiac hypertrophy whereas B6 control heart sections showed a much weaker optical density of the autoradiogram indicative of a smaller amount of bound anti-AT1 receptor antibodies (Figure 19B).

Taken together, radioligand binding showed a significantly higher number of AT1 receptor binding sites of Tg-*SCD1* hearts with 4.3-fold increased cardiac SCD1 protein. Complementary to the radioligand binding studies, autoradiography imaging with anti-AT1 receptor antibodies predominantly located the increased AT1 receptor protein in the hypertrophic left cardiac ventricle.

6.13. SCD1 up-regulated the heart failure-promoting angiotensin II AT1 receptor protein of transfected HEK-293 cells

In view of the increased AT1 receptor protein of Tg-*SCD1* hearts, the direct effect of *SCD1* on AT1 receptor protein levels was investigated in transfected HEK-293 cells. HEK-293 cells with stable expression of the AT1 receptor (*AGTR1*) were transiently transfected with low and high plasmid-DNA amounts encoding *SCD1*. The control cells were mock-transfected. Radioligand binding studies showed that *SCD1* expression led to an increased number of cell-surface AT1 receptor binding sites of HEK-293 cells compared to that of control cells without *SCD1* co-expression (Figure 20A). The number of AT1 receptor binding sites of HEK-293 cells with high *SCD1* co-expression was 2.2 ± 0.4-fold higher than that of control cells (Figure 20A). In HEK-293 cells with low *SCD1* co-expression, there was a trend towards an increased AT1 receptor level, which was not significantly different from that of control cells without co-expression of *SCD1* (Figure 20A).

Gene expression analysis of *SCD1* by real-time quantitative reverse transcription PCR (real-time qRT-PCR) confirmed the elevated *SCD1* expression levels of *SCD1*-transfected HEK-293 cells (Figure 20B).
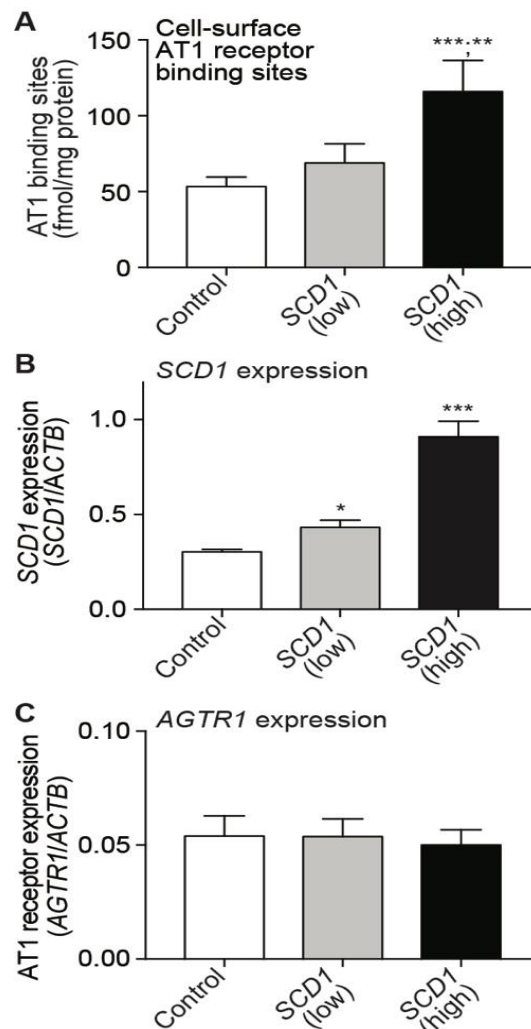
Figure 20: SCD1 increased the number of cell-surface AT1 receptor binding sites of transfected HEK-293 cells.
(A) Number of cell-surface AT1 receptor binding sites were determined by radioligand binding with Sar[1],[^{125}I]Tyr[4],Ile[8]-angiotensin II of AT1 receptor-expressing HEK-293 cells transfected with low and high amounts of *SCD1* expression plasmid. As a control, AT1 receptor-expressing HEK-293 cells were mock-transfected with plasmid pcDNA3.1 (mean ± s.d.; n=4 biological replicates performed in triplicates; ***,p = 0.0004 vs. control, and **,p = 0.0032 vs. *SCD1* low; Tukey`s test). (**B, C**) *SCD1* (**B**) and *AGTR1* (**C**) expression levels of AT1 receptor-expressing HEK-293 cells transfected with low and high amounts of *SCD1* expression plasmid (mean ± s.d.; n=4 biological replicates performed in quadruplicates; ***,p < 0.0001 vs. control and *SCD1* low, and *,p = 0.0137 vs. control; Tukey`s test).

The SCD1 expression levels of high and low SCD1-expressing cells were 3.0 ± 0.3-fold and 1.4 ± 0.1-fold increased, respectively, compared to those of mock-transfected, control cells (Figure 20B). As a control, the gene expression level of the AT1 receptor (AGTR1) was not significantly

altered by co-expression of SCD1 (Figure 20C). Thus, the increased expression of SCD1 led to an increased number of cell-surface AT1 receptor binding sites of HEK cells.

The effect of *SCD1* on total cellular AT1 receptor protein was analyzed with an AT1-Cerulean fusion protein. AT1-Cerulean is an AT1 receptor protein with a carboxyl-terminally fusion of Cerulean [263], which is an improved variant of the enhanced cyan fluorescent protein, ECFP, with 2.5-fold increased brightness [276].

Cellular fluorescence of AT1-Cerulean-expressing HEK-293 cells was recorded with a fluorescence spectrometer at an excitation wavelength of 430 nm, and emission spectra and peak fluorescence emission at 475 nm were determined. Fluorescence measurements were performed to quantify cellular AT1-Cerulean protein levels with the fluorescence emission peak at 475 nm. Cellular fluorescence intensity was recorded of HEK-293 cells expressing AT1-Cerulean without and with low and high amounts of *SCD1* (Figure 21A-C). Experiments showed that AT1-Cerulean-expressing HEK-293 cells with a high level of *SCD1* expression showed a significantly increased AT1-Cerulean fluorescence compared to that of AT1-Cerulean-expressing control cells without *SCD1* co-expression or AT1-Cerulean-expressing cells with low amounts of *SCD1* expression (Figure 21A-C). As a control, *SCD1* expression did not significantly alter the expression level of AT1-Cerulean (*AGTR1*-Cerulean) of transfected HEK-293 cells (Figure 21D).

Together these experiments with HEK-293 cells show that an increased expression level of *SCD1* increases the number of cell-surface AT1 receptor binding sites and the cellular AT1-Cerulean protein level in a gene dosage-dependent manner. *SCD1* could exert an effect on protein folding of the AT1 receptor because AGTR1 gene expression levels were not affected by *SCD1*.
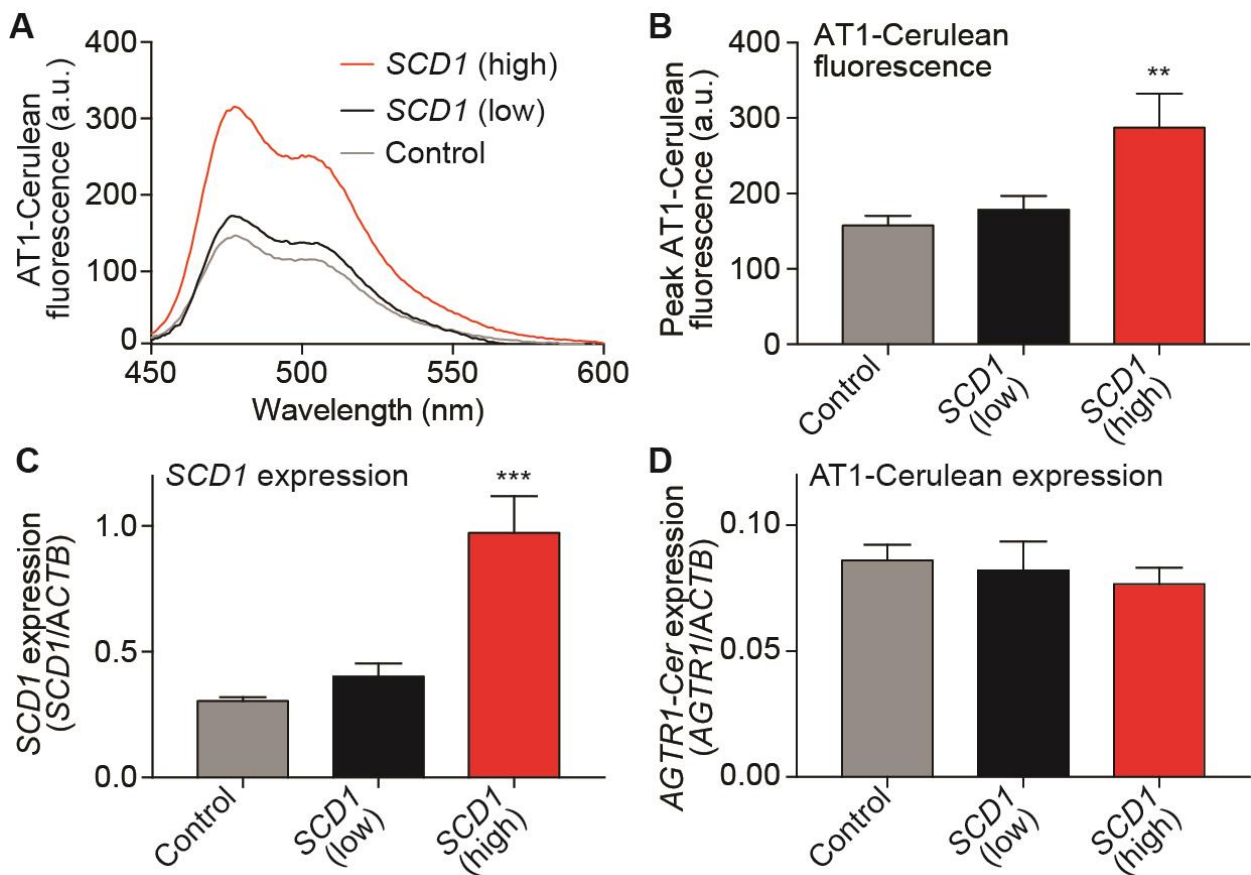
Figure 21: SCD1 increases the cellular AT1-Cerulean protein of HEK-293 cells.
(**A, B**) Fluorescence intensity of HEK-293 cells transiently transfected with a constant amount of AT1-Cerulean expression plasmid (5 microg/10^6 cells) and co-transfection without (Control) or with high (10 mcirog/10^6 cells) and low (3 microg/10^6 cells) amounts of *SCD1* expression plasmid. The panel (**A**) shows a representative experiment, and panel (**B**) shows quantitative evaluation of the peak emission fluorescence intensity of AT1-Cerulean at 475 nm (mean ± s.d.; n=3 biological replicates; **, p=0.040 and 0.0095 vs. Control and *SCD1* low, Tukey`s test; background fluorescence was subtracted). (**C, D**) *SCD1* (**C**) and *AGTR1*-Cerulean (**D**) expression levels of AT1-Cerulean-expressing HEK-293 cells transfected with low and high amounts of *SCD1* expression plasmid (mean ± s.d.; n=3 biological replicates performed in quadruplicates; ***,p = 0.0003 and 0.0006 and vs. control and *SCD1* low; Tukey`s test).

7. DISCUSSION

7.1. Search for pathomechanisms of heart failure in view of limited treatment options of heart failure with reduced ejection fraction (HFrEF)

CHF is still one of the major causes of world-wide morbidity and mortality, in the elderly population. Current pharmacological treatment options for symptomatic treatment of patients suffering from heart failure with reduced ejection fraction (HFrEF) are limited. According to current treatment guidelines of the European Society of Cardiology (ESC), treatment of HFrEF mainly relies on the combination of an ACE inhibitor with one of three beta-blockers (carvedilol, bisoprolol or metoprolol), which have shown to reduce cardiovascular and/or all-cause mortality [60]. If symptoms persist, a mineralcorticoid receptor antagonist (spironolactone or eplereone) could be added [60]. All drugs are titrated to the highest tolerated dose. Symptoms of congestion are usually treated with a diuretic. Since 2015, ARNI was introduced as another treatment option, which consists of the combination of the AT1 receptor antagonist valsartan with the neprilysin inhibitor sacubitril [60]. Under the brand name Entresto®, this combination can significantly reduce the risk of cardiovascular morbidity and mortality in patients with severe HF NYHA class IV and a LVEF of < 40 % when given instead of the ACE-inhibitor and in combination with the other aforementioned drugs [89]. However, despite optimum treatment, morbidity and mortality of HF with reduced ejection fraction are still (too) high.

In view of these limited treatment options, the major goal of the present thesis was focused on the investigation of pathomechanisms involved in the pathogenesis of HF. Identification of previously unrecognized pathomechansims and causative genes could eventually contribute to the identification of target genes suitable to improve the diagnosis and/or treatment of this devastating disease.

7.2. Human heart failure symptoms are reproduced by experimental heart failure models

By methods of basic research, this thesis aimed to identify previously unrecognized targets involved in heart failure pathogenesis, which could eventually be exploited in the future to improve diagnosis and/or treatment of heart failure with reduced ejection fraction, HFrEF. To identify genes up-regulated in frame of the development of heart failure, the study performed analysis of whole genome microarray gene expression profiling data of failing heart specimens from different experimental mouse models, which mimic major cardiovascular risk factors of heart failure pathogenesis.

7.2.1. Experimental model of chronic pressure overload-induced symptoms of cardiac hypertrophy, cardiac dysfunction, and heart failure

Longstanding hypertension accounting for chronic pressure overload ultimately leads to HF in patients [9]. Consequently, many experimental HF models apply chronic pressure overload to trigger symptoms of HF. In these experimental HF models, chronic pressure overload is often imposed by transverse aortic constriction, TAC [122, 277] or abdominal aortic constriction, AAC [121, 124].

Initially, chronic pressure overload in human patients and experimental models is compensated by an increase in cardiomyocyte size and augmentation of heart muscle mass accounting for enhanced contractility and compensated cardiac hypertrophy [278]. On the long term, the increased oxygen and energy consumption of the hypertrophic heart muscle becomes a major pathologic factor, which cannot be compensated anymore and finally leads to cardiomyocyte degeneration. Insufficient oxygen supply to major organs (e.g. heart, kidney, brain) triggers neuro-humoral activation of the sympathetic and renin-angiotensin aldosterone systems, which further increase the cardiac oxygen consumption by augmenting blood pressure, heart rate and contractility. Neuro-humoral activation is also a major contributing factor to maladaptive cardiac remodeling, during which dying cardiomyocytes are replaced by fibrotic scar tissue composed of fibroblasts. With continuous hemodynamic load, this maladaptive remodeling process finally culminates in cardiac dilatation and HF with insufficient cardiac output to meet the oxygen demand of the body [278]. Because the mouse heart is considered a miniaturized human heart regarding major physiological parameters [279], cardiac remodeling processes

are reproduced in experimental models of aortic constriction-induced pressure overload-induced heart failure [121, 122, 124, 277].

7.2.2. Aortic coarctation-induced cardiac hypertrophy and cardiac dysfunction of aged Apoe-/- mice with aortic atherosclerotic plaques

The second model applied apolipoprotein E-deficient (Apoe-/-) mice with hypercholesterolemia, which develop severe atherosclerotic plaques with increasing age and reproduce - at least partially - the risk factor atherosclerosis. At an age of 18 months, aged Apoe-/- mice show a significantly reduced cardiac ejection fraction of 29.5 ± 2.9 % (Figure 8), indicative of cardiac dysfunction [124], and aging-induced heart remodeling with cardiomyocyte hypertrophy [124, 280]. The development of cardiac hypertrophy and cardiac remodeling leading finally to symptoms of HF was attributed to an increased afterload due to aortic coarctation by atherosclerotic plaques, notably in Apoe-/- mice with Western-type diet-enhanced progression of atherosclerosis [281]. The phenotype is linked to aging-dependent atherosclerosis progression, because the cardiac phenotype of young Apoe-/- mice with less advanced atherosclerosis is not altered compared to that of non-transgenic B6 mice [124, 281]. A major difference between Apoe-/- mice and patients is the fact that hypercholesterolemic Apoe-/- mice do not develop significant features of CAD or overt myocardial infarction [281]. The dysfunctional heart phenotype of aged Apoe-/- mice consequently reproduces features of cardiovascular aging and aging-related heart dysfunction, which strongly enhance the susceptibility to HF in synergy with other age-related co-morbidities [282].

7.2.3. Synergistic enhancement of pathological processes leading to the heart failure of Apoe-/- mice with chronic pressure overload

By combination of ApoE deficiency-induced hypercholesterolemia with chronic pressure overload, processes culminating in atherosclerotic plaque formation, cardiac dysfunction, and HF are synergistically enhanced compared to mice with either ApoE deficiency or chronic pressure overload [121, 124]. As a consequence, two months of AAC-induced chronic pressure overload leads to severe symptoms of cardiac dysfunction and HF of Apoe-/- mice [121, 124] whereas without AAC, symptoms of cardiac dysfunction of Apoe-/- mice develop only at old age, in 18-month-old Apoe-/- mice [124].

7.2.4. Rosiglitazone-enhanced heart failure symptoms of Apoe-/- mice

As detailed above, the combination of different cardiovascular risk factors strongly enhances the pathogenesis of HF in experimental models [121, 124], and also in patients [9, 283]. The antidiabetic drug and *PPARG* agonist, rosiglitazone, was suspended from the market in many countries due to the promotion of HF symptoms [126, 127]. By fluid retention, rosiglitazone is considered to enhance volume overload and the pathogenesis of HF [126, 284]. In addition, rosiglitazone could exert a direct deleterious effect to the heart by activation of cardiac *PPARG* [264]. Cardiotoxicity of *PPARG* could be further enhanced in synergy with *PPARA* activation [285], and/or together with other cardiovascular risk factors such as atherosclerosis, CAD, advanced age, and obesity [130, 284].

7.3. Different experimental heart failure models showed a significant up-regulation of the cardiac lipid metabolic process

By using different HF models, which impose chronic pressure overload by AAC, aging-induced aortic coarctation by atherosclerotic plaques, and *Pparg* activation by rosiglitazone, the study identified that failing hearts are characterized by up-regulation of the cardiac lipid metabolic process. This finding is based on GO analysis of up-regulated genes of the following three experimental models of HF:

I. Chronic pressure overload-induced heart failure by AAC of 6-month-old Apoe-/- mice.

II. Aortic coarctation-induced heart failure by atherosclerotic plaques of aged, 18-month-old Apoe-/- mice.

III. Rosiglitazone-enhanced heart failure of 8-month-old Apoe-/- mice.

The up-regulation of the cardiac lipid metabolic process was not restricted to the hypercholesterolemic Apoe-/- background, because AAC-induced chronic pressure overload of non-transgenic B6 mice overload similarly triggered the up-regulation of heart failure-related genes of the lipid metabolic process (Figure 10 and Supplemental Table (Appendix 13.3)).

7.4. The up-regulated cardiac lipid metabolic process contributes to heart failure progression by inducing cardiolipotoxicity

Does the up-regulated cardiac lipid metabolic process contribute to HF pathogenesis? The up-regulated genes of the cardiac lipid metabolic process cover all steps of the lipid metabolism and are involved in lipid synthesis, lipid metabolism and lipid storage. In agreement with an enhanced lipid synthesis and/or enhanced lipid uptake, failing hearts from experimental models and biopsy specimens from HF patients were found to be characterized by lipid accumulation and lipid overload [124, 133, 286]. A multitude of experimental studies with different genetically modified mice have shown that the excessive accumulation of lipids in the heart leads to lipotoxic cardiomyopathy and finally HF [130, 264, 287, 288].

Studies with isolated cardiomyocytes complement these in vivo data and showed direct toxic and apoptosis-enhancing effects of SFAs such as palmitate, which strongly enhances cardiomyocyte death [289, 290]. Direct cardiomyocyte toxicity of palmitate could further be enhanced in vivo, because palmitate is a major source of de novo synthesis of cardiotoxic ceramides [290, 291]. In agreement with a cardiotoxic action of palmitate, transgenic mice, which recapitulate the heart failure-related up-regulation of *FASN* (fatty acid synthase) by myocardium-specific expression of this major palmitate-synthesizing enzyme, developed dilated lipotoxic cardiomyopathy and symptoms of HF [130]. Taken together, up-regulation of genes of the cardiac lipid metabolic process could enhance the progression of HF by induction of cardiolipotoxicity.

7.5. SCD1 is one of the most up-regulated genes of the cardiac lipid metabolic process of experimental heart failure models

Not all up-regulated genes of the cardiac lipid metabolic process are necessarily cardiotoxic. The documented toxicity of fatty acids in vitro is linked to SFAs (C16:0 or C18:0) whereas equimolar amounts of mono-unsaturated fatty acids (e.g. cis-C18:1), were not toxic to neonatal cardiomyocytes and even protected these cells against palmitate-induced cardiomyocyte death [289].

Analysis of whole genome gene expression data of experimental HF models, which was performed in frame of this thesis, identified *SCD1* as one of the most-up-regulated genes of

the cardiac lipid metabolic process of failing hearts. Notably, *SCD1* is the enzyme responsible for beneficial oleic acid (C18 n-9) synthesis in humans and generally for the synthesis of MUFAs [292]. In agreement with a possible cardioprotective role of *SCD1* in the heart, forced expression of *SCD1* in rats by feeding a high-sucrose diet was protective against saturated fatty acids- induced toxicity and SFA-induced generation of cardiotoxic ceramides, pro-apoptotic caspase-3 activation and apoptotic cell death [155]. In apparent contrast to the claimed protective role of *SCD1*, deficiency of *SCD1* in *SCD1*-knockout mice was also found to exert a protective role in vivo, i.e. *SCD1* deficiency rescued the leptin-deficiency-induced cardiomyopathy of obese (ob/ob) mice and led to a decreased lipid accumulation and cardiomyocyte apoptosis [293]. Thus, the in vivo function of *SCD1* in the heart and its impact on HF pathogenesis are incompletely understood.

7.6. Investigation of the role of *SCD1* up-regulation in the heart by generation of Tg-*SCD1* mice with myocardium-specific *SCD1* expression

In view of the strong up-regulation of cardiac *Scd1* in different HF models, this study investigated the impact of *SCD1* up-regulation in the heart by generation of *SCD1*-transgenic mice with myocardium-specific expression of *SCD1* under control of the alpha-MHC promoter. Two different transgenic mouse lines with 1.9±0.6-fold and 4.3±0.8 increased cardiac *SCD1* protein levels were generated and characterized in frame of the study. The study used the human *SCD1* cDNA for generation of transgenic mice, because *SCD1* is the major *SCD* gene in humans [139].

7.7. Up-regulation of *SCD1* in the heart expression triggered cardiac hypertrophy, cardiac dysfunction and up-regulation of heart failure-related genes

Phenotyping of Tg-*SCD1* mice revealed that an increased cardiac SCD1 protein level triggered cardiac hypertrophy and cardiac dysfunction in aged, eight-month-old Tg-*SCD1* mice in a gene dosage-dependent manner. Cardiac hypertrophy was documented by a significantly increased heart-to-body weight ratio of Tg-*SCD1* mice with 4.3±0.8 increased cardiac SCD1 protein levels. The heart-to-body weight ratio Tg-*SCD1* mice was 6.22 ± 0.6 mg/g compared to 4.9 ± 0.2 mg/g of non-transgenic B6 mice (Figure 13A). In addition, histology analysis of Tg-*SCD1*

hearts confirmed cardiac hypertrophy and showed a significant enlargement of the left ventricle (Figure 14).

Cardiac dysfunction of Tg-*SCD1* mice with 4.3±0.8-fold increased cardiac SCD1 protein levels was documented by echocardiography, which detected a significantly reduced cardiac LVEF of 35.2 ± 6.1 % compared to the cardiac ejection fraction of 52.7 ± 5.2 % of non-transgenic B6 mice (Figure 13B). Together these data support the notion, that an increased cardiac SCD1 protein is a sufficient cause of the onset of major HF symptoms, such as cardiac hypertrophy and cardiac dysfunction.

In agreement with the onset of HF symptoms of eight-month-old Tg-*SCD1* mice with 4.3±0.8-fold increased SCD1 protein levels, whole genome microarray gene expression profiling detected the significant up-regulation of heart failure-related genes, fatty acid synthase (*Fasn*), adiponectin (*Adipoq*) and resistin (*Retn*) in these mice (Figure 16). These heart failure-related genes are up-regulated during the course of HF pathogenesis of experimental HF models and patients with HF, and could also exert a direct heart failure-promoting activity [130, 269-272].

 Microarray data were confirmed by immunoblot analysis, which showed the significant up-regulation of the heart failure-related proteins, Fasn and Adipoq, in hearts of Tg-*SCD1* mice (Figure 18).

Moreover, the microarray data showed up-regulation of the endogenous *Scd1* of Tg-*SCD1* mice (Figure 16). This observation supports the notion, that cardiac *SCD1/Scd1* up-regulation in experimental models and patients with HF is directly related to HF pathogenesis.

7.8. SCD1 mediates posttranslational up-regulation of the heart failure-enhancing AT1 receptor protein

Pathomechanisms accounting for the heart failure-enhancing function of *SCD1* are not understood because major lipids synthesized by SCD1 are cardio-protective, such as oleic acid and protect against saturated fatty acid-induced apoptotic cell death [155, 292].

In search for the *SCD1*-mediated pathomechanism, the study switched its focus to the function of SCD1 as one of the major enzymes involved in the formation of membrane

phospholipids. Thereby SCD1 acts as an enhancer of membrane fluidity by catalyzing the delta-9 desaturation of 12-19 carbon SFAs [273]. Because membrane phospholipids exert an essential role in membrane protein folding, and enhanced lipid synthesis could promote GPCR folding [294], the study investigated whether SCD1 enhanced the protein level of the angiotensin II AT1 receptor, AGTR1, which is a major pro-hypertrophic and heart failure-enhancing membrane-spanning GPCR protein [274]. By radioligand binding studies and autoradiography with anti-AT1 receptor antibodies, the study found that Tg-*SCD1* hearts were characterized by an increased number of AT1 receptor binding sites, which were predominantly localized in the hypertrophic left ventricle of *SCD1*-transgenic hearts.

Further studies with HEK-293 cells documented a direct effect of *SCD1* on the AT1 receptor protein. *SCD1* led to an increased number of cell-surface AT1 receptors and increased the total cellular amount of the AT1 receptor protein, AT1-Cerulean. The AT1 receptor-inducing effect of *SCD1* was posttranslational because the expression level of the AT1 receptor (*AGTR1*) was not altered by *SCD1*.

The enhancing effect of *SCD1* could be specific for the AT1 receptor protein during HF pathogenesis because the function of the beta-adrenergic receptor, as another major player of HF pathogenesis, is impaired by lipids [295]. The deduced mechanism involves beta-receptor down-regulation by protein kinase C (PKC), which is activated by lipid metabolites. Taken together, *SCD1* could enhance the protein folding and synthesis of the major heart failure-promoting angiotensin II AT1 receptor.

Up-regulation of the AT1 receptor protein was reported in some studies of cardiac biopsy specimens from HF patients [296, 297]. The *SCD1*-mediated up-regulation of the AT1 receptor could be specifically relevant for the pathogenesis of diabetic cardiomyopathy of type 2 diabetic patients, who are characterized by increased contents of myocardial AT1 receptors [297, 298] and increased levels of SCD1-derived lipids [299]. In this context, the up-regulated AT1 receptor could enhance the progression of early cardiac dysfunction to overt diabetic cardiomyopathy and HF [298]. However, at end-stage HF, there is a substantial down-regulation of major heart failure-related GPCRs including the AT1 receptor, largely due to strongly increased levels of the GPCR-desensitizing kinase, GRK2 [300].

7.9. Up-regulation of *SCD1* could be triggered in frame of heart failure pathogenesis as a result of neuro-hormonal activation of the sympathetic nervous system

This study detected that different experimental HF models and Tg-*SCD1* mice with symptoms of HF were characterized by the significant up-regulation of *Scd1*. By which mechanism does HF pathogenesis trigger the up-regulation of *SCD1*? A major feature of patients with HF and experimental models is the chronic neuro-hormonal activation of the sympathetic nervous system and renin-angiotensin-aldosterone system. Neuro-hormonal activation is triggered as a compensatory response to the insufficient cardiac output to maintain oxygen supply to vital organs such as heart, liver and kidney [301]. The neuro-hormonal activation is causally linked to HF pathogenesis because the mortality of HF patients is directly associated with the circulating levels of norepinephrine, angiotensin II and aldosterone as executors of the sympathetic nervous system and renin-angiotensin-aldosterone system [301, 302].

In this context, neuro-hormonal activation of the sympathetic nervous system could directly promote the induction of *SCD1* expression and SCD1 protein levels. Notably *SCD1* expression is induced by the cAMP-response element-binding protein 1, *Creb1* [303], which is triggered by chronic activation of the sympathetic nervous system by norepinephrine-mediated stimulation of cAMP-inducing and heart failure-enhancing beta-adrenergic receptors [304-306].

Other factors related to HF pathogenesis could synergistically enhance the expression of *SCD1* such as SFAs, carbohydrates and insulin [155]. In patients with type 2 diabetes or obesity, these factors could trigger a vicious circle of (lipid) metabolism-induced *SCD1* up-regulation, which in turn aggravates symptoms of HF accounting for an even stronger *SCD1* increase by neuro-hormonal activation of the sympathetic nervous system.

7.10. Relevance of the study to human heart failure and outlook

The present study was performed with experimental HF models and transgenic mice. Nevertheless, data of the present study could be relevant to human HF. Notably, the accumulation of cardiotoxic lipids generated by SCD1 in concert with FASN enhances the pathogenesis of dilated lipotoxic cardiomyopathy and contributes to human HF, especially under conditions of diabetes and severe obesity[286]. The SCD1 protein was found to be up-regulated on biopsy specimens of human HF patients [124], and higher circulating levels of the major SCD1 lipid synthesis product, oleic acid, are associated with a greater risk of cardiovascular events and all-cause mortality [307]. The deduced heart failure-enhancing effect of SCD1 could be relevant for diabetic patients with increased risk of diabetic cardiomyopathy and increased circulating levels of SCD1-derived desaturated lipids [299]. In view of this study and data about the in vivo function of *SCD1*, inhibition of *SCD1* could be envisaged, especially in obese patients with diabetes [293].

SCD1 acts in synergy with other heart failure-promoting genes of the cardiac lipid metabolic process, such as the heart failure-enhancing fatty acid synthase (*Fasn*) and resistin (*Retn*). Consequently, a more efficient, potential treatment approach of HF (in combination with the standard HF therapy regimen including a beta-blocker and an ACE inhibitor) could aim at targeting the dysfunctional cardiac lipid metabolic process. Restoration of the impaired lipid metabolism could be achieved, e.g. with a cardioprotective inhibitor of the G-protein-coupled receptor kinase 2, GRK2 [308], which also improves associated conditions such as insulin resistance and diabetes [130, 309]. The development of this novel class of GRK2 inhibitors for human use is urgently awaited in the near future.

8. ACKNOWLEDGMENTS

9. CURRICULUM VITAE

YAHYA FAHAD M. JAMOUS

Date of birth: March 21st, 1980

Place of birth: Riyadh

Nationality: Saudi Arabia

EDUCATION:

2017 - 2020	Doctorate degree candidate of pharmaceutical sciences (Ph.D.), Molecular Pharmacology, Swiss Federal Institute of Technology (ETH) Zurich, Switzerland.
2007 – 2010	Master degree of sciences in pharmacy (pharmaceutics), King Saud University, Riyadh, Saudi Arabia
2000 – 2006	Bachelor degree in Pharmaceutical sciences in the field of general pharmacy, College of pharmacy, king Saud University, Riyadh, Saudi Arabia.

EXPERIENCE:

Feb.2017 – current	Doctorate student in molecular pharmacology in the group of professor Dr. Ursula Quitterer, Swiss Federal Institute of Technology in Zurich (ETH Zurich), Zurich, Switzerland.
Aug.2013 – current	Academic researcher, King Abdulaziz City for Science and Technology (KACST), Riyadh, Saudi Arabia.
Sep.2010 - Aug.2013	Senior pharmacist, King Khaled Eye Specialist Hospital (KKESH), Riyadh, Saudi Arabia.

- Responsible for narcotics and controlled drugs.
- In-charge of pharmaceutical planning.
- Member in the Pharmacy and Therapeutics (P & T) Committee.
- Member in the medical quality control committee.

Feb.2010 - Sep.2010   Pharmacist, King Fahad Medical City (KFMC), Riyadh, Saudi Arabia.

Feb.2006 - Dec.2009   Pharmacist, Prince Sultan Bin Abdulaziz Humanitarian City (SBAHC), Riyadh, Saudi Arabia.

- Out- patient and in- patient pharmacist.

- Intravenous (IV) preparations pharmacist.

10. PUBLICATIONS

Peer-reviewed publications

Perhal A, Wolf S, **Jamous YF**, Langer A, Abd Alla J and Quitterer U (2019). Increased Reactive Oxygen Species Generation Contributes to the Atherogenic Activity of the B2 Bradykinin Receptor. Front. Med. 6:32. doi: 10.3389/fmed.2019.00032**.**

Buthaina Salim, Monia Zghal, Mounir Salem-Bekhit, **Yahiya Jamous**, Faris Al-Anazi, brahim Al Sarra, M. Bayomi and Mohamed-Dahmani Fathallah (2012). Introducing Plasmid DNA Fingerprinting in the Quality Control of pDNA Vaccine. International Journal of Biotechnology and Biochemistry. 8:2, pp. 87-100.

Mounir M. Salem-Bekhit, **Y. Jamous**, Fars Al-Anazi, Mohsen Bayomi, Ibrahib Alsarrah and M. D. Fathallah (2012). Quality control of optimized hepatitis B plasmid DNA vaccine. African Journal of Biotechnology. 11:5, pp. 1231-1239. DOI: 10.5897/AJB11.2924

Other publications (not peer-reviewed)

Y.F. Jamous, A. Perhal, U. Quitterer, J. Abd Alla (2019). Transgenic mice with myocardium-specific expression of SCD1 develop symptoms of heart failure. Naunyn-Schmiedeber`s Arch Pharmacol, 392 (Supplement 1): 43. DOI 10.1007/s00210-019-01621-6

Poster presentations:

Y.F. Jamous, A. Perhal, U. Quitterer, J. Abd Alla (2019). Transgenic mice with myocardium-specific expression of SCD1 develop symptoms of heart failure. 21st Annual Meeting of the German Society of Experimental and Clinical Pharmacology and Toxicology, Stuttgart, Germany, February 25–28.

11. LIST OF FIGURES

12. LIST OF TABLES

13. REFERENCES

1.   Velagaleti, R.S. and R.S. Vasan, *Heart failure in the twenty-first century: is it a coronary artery disease or hypertension problem?* Cardiol Clin, 2007. **25**(4): p. 487-95; v.

2.   Ponikowski, P., Anker, S. D., AlHabib, K. F., Cowie, M. R., Force, T. L., Hu, S., Jaarsma, T., Krum, H., Rastogi, V., Rohde, L. E., Samal, U. C., Shimokawa, H., Budi Siswanto, B., Sliwa, K., Filippatos, G., *Heart failure: preventing disease and death worldwide.* ESC Heart Fail, 2014. **1**(1): p. 4-25.

3.   Savarese, G. and L.H. Lund, *Global Public Health Burden of Heart Failure.* Card Fail Rev, 2017. **3**(1): p. 7-11.

4.   Inamdar, A.A. and A.C. Inamdar, *Heart Failure: Diagnosis, Management and Utilization.* J Clin Med, 2016. **5**(7).

5.   Katholi, R.E. and D.M. Couri, *Left ventricular hypertrophy: major risk factor in patients with hypertension: update and practical clinical applications.* Int J Hypertens, 2011. **2011**: p. 495349.

6.   Ho, C.Y., *Hypertrophic cardiomyopathy.* Heart Fail Clin, 2010. **6**(2): p. 141-59.

7.   Franco, O.H., Peeters, A., Bonneux, L., de Laet, C., *Blood pressure in adulthood and life expectancy with cardiovascular disease in men and women: life course analysis.* Hypertension, 2005. **46**(2): p. 280-6.

8.   Ford, E.S., *Trends in mortality from all causes and cardiovascular disease among hypertensive and nonhypertensive adults in the United States.* Circulation, 2011. **123**(16): p. 1737-44.

9.   Messerli, F.H., S.F. Rimoldi, and S. Bangalore, *The Transition From Hypertension to Heart Failure: Contemporary Update.* JACC Heart Fail, 2017. **5**(8): p. 543-551.

10.   Gray, L., Lee, I. M., Sesso, H. D., Batty, G. D., *Blood pressure in early adulthood, hypertension in middle age, and future cardiovascular disease mortality: HAHS (Harvard Alumni Health Study).* J Am Coll Cardiol, 2011. **58**(23): p. 2396-403.

11.   American Diabetes, A., *Diagnosis and classification of diabetes mellitus.* Diabetes Care, 2014. **37 Suppl 1**: p. S81-90.

12.   Galtier, F., *Definition, epidemiology, risk factors.* Diabetes Metab, 2010. **36**(6 Pt 2): p. 628-51.

13.   Matheus, A.S., Tannus, L. R., Cobas, R. A., Palma, C. C., Negrato, C. A., Gomes, M. B., *Impact of diabetes on cardiovascular disease: an update.* Int J Hypertens, 2013. **2013**: p. 653789.

14.   Rivellese, A.A., G. Riccardi, and O. Vaccaro, *Cardiovascular risk in women with diabetes.* Nutr Metab Cardiovasc Dis, 2010. **20**(6): p. 474-80.

15.   Kenny, H.C. and E.D. Abel, *Heart Failure in Type 2 Diabetes Mellitus.* Circ Res, 2019. **124**(1): p. 121-141.

16.   Agence Francaise de Securite Sanitaire des Produits de, S., *[AFSSAPS guideline for the treatment of dyslipidemia].* Rev Prat, 2005. **55**(16): p. 1788-93.

17.   Dzau, V.J., *Atherosclerosis and hypertension: mechanisms and interrelationships.* J Cardiovasc Pharmacol, 1990. **15 Suppl 5**: p. S59-64.

18.   Bao, W., Srinivasan, S. R., Valdez, R., Greenlund, K. J., Wattigney, W. A., Berenson, G. S. *Longitudinal changes in cardiovascular risk from childhood to young adulthood in offspring of parents with coronary artery disease: the Bogalusa Heart Study.* JAMA, 1997. **278**(21): p. 1749-54.

19.   Ezzati, M. and A.D. Lopez, *Regional, disease specific patterns of smoking-attributable mortality in 2000.* Tob Control, 2004. **13**(4): p. 388-95.

20.   Barua, R.S., Ambrose, J. A., Eales-Reynolds, L. J., DeVoe, M. C., Zervas, J. G., Saha, D. C., *Dysfunctional endothelial nitric oxide biosynthesis in healthy smokers with impaired endothelium-dependent vasodilatation.* Circulation, 2001. **104**(16): p. 1905-10.

21.   Cross, C.E., Halliwell, B., Borish, E. T., Pryor, W. A., Ames, B. N., Saul, R. L., McCord, J. M., Harman, D., *Oxygen radicals and human disease.* Ann Intern Med, 1987. **107**(4): p. 526-45.

22.   FitzGerald, G.A., J.A. Oates, and J. Nowak, *Cigarette smoking and hemostatic function.* Am Heart J, 1988. **115**(1 Pt 2): p. 267-71.

23.   Mendall, M.A., Patel, P., Asante, M., Ballam, L., Morris, J., Strachan, D. P., Camm, A. J., Northfield, T. C., *Relation of serum cytokine concentrations to cardiovascular risk factors and coronary heart disease.* Heart, 1997. **78**(3): p. 273-7.

24.   Ambrose, J.A. and R.S. Barua, *The pathophysiology of cigarette smoking and cardiovascular disease: an update.* J Am Coll Cardiol, 2004. **43**(10): p. 1731-7.

25.   Cryer, P.E., Haymond, M. W., Santiago, J. V., Shah, S. D., *Norepinephrine and epinephrine release and adrenergic mediation of smoking-associated hemodynamic and metabolic events.* N Engl J Med, 1976. **295**(11): p. 573-7.

26.   Price, J.F., Mowbray, P. I., Lee, A. J., Rumley, A., Lowe, G. D., Fowkes, F. G., *Relationship between smoking and cardiovascular risk factors in the development of peripheral arterial disease and coronary artery disease: Edinburgh Artery Study.* Eur Heart J, 1999. **20**(5): p. 344-53.

27.   Unverdorben, M., K. von Holt, and B.R. Winkelmann, *Smoking and atherosclerotic cardiovascular disease: part II: role of cigarette smoking in cardiovascular disease development.* Biomark Med, 2009. **3**(5): p. 617-53.

28.   Panuganti, K.K. and R.K. Kshirsagar, *Obesity*, in *StatPearls*. 2020: Treasure Island (FL).

29.   Van Gaal, L.F., I.L. Mertens, and C.E. De Block, *Mechanisms linking obesity with cardiovascular disease.* Nature, 2006. **444**(7121): p. 875-80.

30.   Ritchie, S.A. and J.M. Connell, *The link between abdominal obesity, metabolic syndrome and cardiovascular disease.* Nutr Metab Cardiovasc Dis, 2007. **17**(4): p. 319-26.

31.   Din-Dzietham, R., Liu, Y., Bielo, M. V., Shamsa, F., *High blood pressure trends in children and adolescents in national surveys, 1963 to 2002.* Circulation, 2007. **116**(13): p. 1488-96.

32.   Drozdz, D. and K. Kawecka-Jaszcz, *Cardiovascular changes during chronic hypertensive states.* Pediatr Nephrol, 2014. **29**(9): p. 1507-16.

33.   Eisenmann, J.C., *Physical activity and cardiovascular disease risk factors in children and adolescents: an overview.* Can J Cardiol, 2004. **20**(3): p. 295-301.

34. Ilanne-Parikka, P., Laaksonen, D. E., Eriksson, J. G., Lakka, T. A., Lindstr, J., Peltonen, M., Aunola, S., Keinanen-Kiukaanniemi, S., Uusitupa, M., Tuomilehto, J., Finnish Diabetes Prevention Study, Group., *Leisure-time physical activity and the metabolic syndrome in the Finnish diabetes prevention study.* Diabetes Care, 2010. **33**(7): p. 1610-7.

35. Katzmarzyk, P.T., Leon, A. S., Wilmore, J. H., Skinner, J. S., Rao, D. C., Rankinen, T., Bouchard, C., *Targeting the metabolic syndrome with exercise: evidence from the HERITAGE Family Study.* Med Sci Sports Exerc, 2003. **35**(10): p. 1703-9.

36. Lakka, T.A. and D.E. Laaksonen, *Physical activity in prevention and treatment of the metabolic syndrome.* Appl Physiol Nutr Metab, 2007. **32**(1): p. 76-88.

37. Mancia, G., Fagard, R., Narkiewicz, K., Redon, J., Zanchetti, A., Bohm, M., Christiaens, T., Cifkova, R., De Backer, G., Dominiczak, A., Galderisi, M., Grobbee, D. E., Jaarsma, T., Kirchhof, P.,Kjeldsen, S. E., Laurent, S., Manolis, A. J., Nilsson, P. M., Ruilope, L. M., Schmieder, R. E., Sirnes, P. A., Sleight, P. Viigimaa, M., Waeber, B., Zannad, F., Task Force, Members, *2013 ESH/ESC Guidelines for the management of arterial hypertension: the Task Force for the management of arterial hypertension of the European Society of Hypertension (ESH) and of the European Society of Cardiology (ESC).* J Hypertens, 2013. **31**(7): p. 1281-357.

38. Chobanian, A.V., Bakris, G. L., Black, H. R., Cushman, W. C., Green, L. A., Izzo, J. L., Jr., Jones, D. W., Materson, B. J., Oparil, S., Wright, J. T., Jr., Roccella, E. J., National Heart, Lung, Blood Institute Joint National Committee on Prevention, Detection Evaluation, Treatment of High Blood, PressureNational High Blood Pressure Education Program Coordinating, Committee, *The Seventh Report of the Joint National Committee on Prevention, Detection, Evaluation, and Treatment of High Blood Pressure: the JNC 7 report.* JAMA, 2003. **289**(19): p. 2560-72.

39. Kim, Y. and S. Lee, *Physical activity and abdominal obesity in youth.* Appl Physiol Nutr Metab, 2009. **34**(4): p. 571-81.

40. Ekelund, U., Luan, J., Sherar, L. B., Esliger, D. W., Griew, P., Cooper, A., International Children's Accelerometry Database, Collaborators, *Moderate to vigorous physical activity and sedentary time and cardiometabolic risk factors in children and adolescents.* JAMA, 2012. **307**(7): p. 704-12.

41. Lachman, S., Boekholdt, S. M., Luben, R. N., Sharp, S. J., Brage, S., Khaw, K. T., Peters, R. J., Wareham, N. J., *Impact of physical activity on the risk of cardiovascular disease*

in middle-aged and older adults: EPIC Norfolk prospective population study. Eur J Prev Cardiol, 2018. **25**(2): p. 200-208.

42. Doukky, R., Mangla, A., Ibrahim, Z., Poulin, M. F., Avery, E., Collado, F. M., Kaplan, J., Richardson, D., Powell, L. H., *Impact of Physical Inactivity on Mortality in Patients With Heart Failure.* Am J Cardiol, 2016. **117**(7): p. 1135-43.

43. Tapsell, L.C., Neale, E. P., Satija, A., Hu, F. B., *Foods, Nutrients, and Dietary Patterns: Interconnections and Implications for Dietary Guidelines.* Adv Nutr, 2016. **7**(3): p. 445-54.

44. Briggs, M.A., K.S. Petersen, and P.M. Kris-Etherton, *Saturated Fatty Acids and Cardiovascular Disease: Replacements for Saturated Fat to Reduce Cardiovascular Risk.* Healthcare (Basel), 2017. **5**(2).

45. Bowen, K.J., Sullivan, V. K., Kris-Etherton, P. M., Petersen, K. S., *Nutrition and Cardiovascular Disease-an Update.* Curr Atheroscler Rep, 2018. **20**(2): p. 8.

46. Abshire, M., Xu, J., Baptiste, D., Almansa, J. R., Xu, J., Cummings, A., Andrews, M. J., Dennison Himmelfarb, C., *Nutritional Interventions in Heart Failure: A Systematic Review of the Literature.* J Card Fail, 2015. **21**(12): p. 989-99.

47. Sutton, M.G. and N. Sharpe, *Left ventricular remodeling after myocardial infarction: pathophysiology and therapy.* Circulation, 2000. **101**(25): p. 2981-8.

48. Eichhorn, E.J. and M.R. Bristow, *Medical therapy can improve the biological properties of the chronically failing heart - A new era in the treatment of heart failure.* Circulation, 1996. **94**(9): p. 2285-2296.

49. Pfeffer, M.A. and E. Braunwald, *Ventricular remodeling after myocardial infarction. Experimental observations and clinical implications.* Circulation, 1990. **81**(4): p. 1161-72.

50. Reddy, H.K., Koshy, S. K., Wasson, S., Aggarwal, K. B., Tejwani, L., Ovechkin, A. V., Tyagi, S. C., *Echocardiography predicts adverse cardiac remodelling in heart failure.* Exp Clin Cardiol, 2004. **9**(2): p. 112-6.

51. Jessup, M. and S. Brozena, *Heart failure.* N Engl J Med, 2003. **348**(20): p. 2007-18.

52. Khattar, R.S., *Effects of ACE-inhibitors and beta-blockers on left ventricular remodeling in chronic heart failure.* Minerva Cardioangiol, 2003. **51**(2): p. 143-54.

53. Reis Filho, J.R., Cardoso, J. N., Cardoso, C. M., Pereira-Barretto, A. C., *Reverse Cardiac Remodeling: A Marker of Better Prognosis in Heart Failure.* Arq Bras Cardiol, 2015. **104**(6): p. 502-6.

54. Freemantle, N., Cleland, J., Young, P., Mason, J., Harrison, J., *beta Blockade after myocardial infarction: systematic review and meta regression analysis.* BMJ, 1999. **318**(7200): p. 1730-7.

55. James, P.A., Oparil, S., Carter, B. L., Cushman, W. C., Dennison-Himmelfarb, C., Handler, J., Lackland, D. T., LeFevre, M. L., MacKenzie, T. D., Ogedegbe, O., Smith, S. C., Jr., Svetkey, L. P., Taler, S. J., Townsend, R. R., Wright, J. T., Jr., Narva, A. S., Ortiz, E., *2014 evidence-based guideline for the management of high blood pressure in adults: report from the panel members appointed to the Eighth Joint National Committee (JNC 8).* JAMA, 2014. **311**(5): p. 507-20.

56. Farzam, K. and A. Jan, *Beta Blockers*, in *StatPearls*. 2020: Treasure Island (FL).

57. *Effect of metoprolol CR/XL in chronic heart failure: Metoprolol CR/XL Randomised Intervention Trial in Congestive Heart Failure (MERIT-HF).* Lancet, 1999. **353**(9169): p. 2001-7.

58. Packer, M., Coats, A. J., Fowler, M. B., Katus, H. A., Krum, H., Mohacsi, P., Rouleau, J. L., Tendera, M., Castaigne, A., Roecker, E. B., Schultz, M. K., DeMets, D. L., Carvedilol Prospective Randomized Cumulative Survival Study, Group, *Effect of carvedilol on survival in severe chronic heart failure.* N Engl J Med, 2001. **344**(22): p. 1651-8.

59. *The Cardiac Insufficiency Bisoprolol Study II (CIBIS-II): a randomised trial.* Lancet, 1999. **353**(9146): p. 9-13.

60. Ponikowski, P., Voors, A. A., Anker, S. D., Bueno, H., Cleland, J. G. F., Coats, A. J. S., Falk, V., Gonzalez-Juanatey, J. R., Harjola, V. P., Jankowska, E. A., Jessup, M., Linde, C., Nihoyannopoulos, P., Parissis, J. T.Pieske, B., Riley, J. P., Rosano, G. M. C., Ruilope, L. M., Ruschitzka, F., Rutten, F. H, van der Meer, P., E. S. C. Scientific Document Group, *2016 ESC Guidelines for the diagnosis and treatment of acute and chronic heart failure: The Task Force for the diagnosis and treatment of acute and chronic heart failure of the European Society of Cardiology (ESC)Developed with the special contribution of the Heart Failure Association (HFA) of the ESC.* Eur Heart J, 2016. **37**(27): p. 2129-2200.

61. Doughty, R.N., Rodgers, A., Sharpe, N., MacMahon, S., *Effects of beta-blocker therapy on mortality in patients with heart failure., A systematic overview of randomized controlled trials.* Eur Heart J, 1997. **18**(4): p. 560-5.

62. Heidenreich, P.A., T.T. Lee, and B.M. Massie, *Effect of beta-blockade on mortality in patients with heart failure: a meta-analysis of randomized clinical trials.* J Am Coll Cardiol, 1997. **30**(1): p. 27-34.

63. Bristow, M.R., Larrabee, P., Minobe, W., Roden, R., Skerl, L., Klein, J., Handwerger, D., Port, J. D., Muller-Beckmann, B., *Receptor pharmacology of carvedilol in the human heart.* J Cardiovasc Pharmacol, 1992. **19 Suppl 1**: p. S68-80.

64. Gilbert, E.M., Abraham, W. T., Olsen, S., Hattler, B. White., M., Mealy, P., Larrabee, P., Bristow, M. R., *Comparative hemodynamic, left ventricular functional, and antiadrenergic effects of chronic treatment with metoprolol versus carvedilol in the failing heart.* Circulation, 1996. **94**(11): p. 2817-25.

65. Macdonald, P.S., Keogh, A. M., Aboyoun, C. L., Lund, M., Amor, R., McCaffrey, D. J., *Tolerability and efficacy of carvedilol in patients with New York Heart Association class IV heart failure.* J Am Coll Cardiol, 1999. **33**(4): p. 924-31.

66. Krum, H., Sackner-Bernstein, J. D., Goldsmith, R. L., Kukin, M. L., Schwartz, B., Penn, J., Medina, N., Yushak, M., Horn, E., Katz, S. D., *Double-blind, placebo-controlled study of the long-term efficacy of carvedilol in patients with severe chronic heart failure.* Circulation, 1995. **92**(6): p. 1499-506.

67. Messaoudi, S., Azibani, F., Delcayre, C., Jaisser, F., *Aldosterone, mineralocorticoid receptor, and heart failure.* Mol Cell Endocrinol, 2012. **350**(2): p. 266-72.

68. Mihailidou, A.S., *Aldosterone in heart disease.* Curr Hypertens Rep, 2012. **14**(2): p. 125-9.

69. Okoshi, M.P., Yan, X., Okoshi, K., Nakayama, M., Schuldt, A. J., O'Connell, T. D., Simpson, P. C., Lorell, B. H., *Aldosterone directly stimulates cardiac myocyte hypertrophy.* J Card Fail, 2004. **10**(6): p. 511-8.

70. Nolly, M.B., Caldiz, C. I., Yeves, A. M., Villa-Abrille, M. C., Morgan, P. E., Amado Mondaca, N., Portiansky, E. L., Chiappe de Cingolani, G. E., Cingolani, H. E., Ennis, I. L.,

The signaling pathway for aldosterone-induced mitochondrial production of superoxide anion in the myocardium. J Mol Cell Cardiol, 2014. **67**: p. 60-8.

71.   Cheema, Y., Zhao, W., Zhao, T., Khan, M. U., Green, K. D., Ahokas, R. A., Gerling, I. C., Bhattacharya, S. K., Weber, K. T., *Reverse remodeling and recovery from cachexia in rats with aldosteronism.* Am J Physiol Heart Circ Physiol, 2012. **303**(4): p. H486-95.

72.   Mano, A., Tatsumi, T., Shiraishi, J., Keira, N., Nomura, T., Takeda, M., Nishikawa, S., Yamanaka, S., Matoba, S., Kobara, M., Tanaka, H., Shirayama, T., Takamatsu, T., Nozawa, Y., Matsubara, H., *Aldosterone directly induces myocyte apoptosis through calcineurin-dependent pathways.* Circulation, 2004. **110**(3): p. 317-23.

73.   Struthers, A.D. and T.M. MacDonald, *Review of aldosterone- and angiotensin II-induced target organ damage and prevention.* Cardiovasc Res, 2004. **61**(4): p. 663-70.

74.   Fraccarollo, D., Galuppo, P., Schraut, S., Kneitz., S.van Rooijen, N., Ertl, G., Bauersachs, J., *Immediate mineralocorticoid receptor blockade improves myocardial infarct healing by modulation of the inflammatory response.* Hypertension, 2008. **51**(4): p. 905-14.

75.   Kuster, G.M., Kotlyar, E., Rude, M. K.Siwik, D. A., Liao, R., Colucci, W. S., Sam, F., *Mineralocorticoid receptor inhibition ameliorates the transition to myocardial failure and decreases oxidative stress and inflammation in mice with chronic pressure overload.* Circulation, 2005. **111**(4): p. 420-7.

76.   Martin-Fernandez, B., de las Heras, N., Miana, M., Ballesteros, S., Valero-Munoz, M., Vassallo, D., Davel, A., P.Rossoni, L. V.Cachofeiro, V., Lahera, V., *Spironolactone prevents alterations associated with cardiac hypertrophy produced by isoproterenol in rats: involvement of serum- and glucocorticoid-regulated kinase type 1.* Exp Physiol, 2012. **97**(6): p. 710-8.

77.   *Interlaboratory variability in drug assay: a comparison of quality control data with reanalysis of routine patient samples. II: Digoxin. Clinical Pharmacology and Toxicology Study Group, Italian Society for Clinical Biochemistry.* Ther Drug Monit, 1991. **13**(2): p. 140-5.

78.   Kobayashi, N., Yoshida, K., Nakano, S., Ohno, T., Honda, T., Tsubokou, Y., Matsuoka, H., *Cardioprotective mechanisms of eplerenone on cardiac performance and remodeling in failing rat hearts.* Hypertension, 2006. **47**(4): p. 671-9.

79. Pitt, B., Remme, W., Zannad, F., Neaton, J.,Martinez, F.,Roniker, B., Bittman, R., Hurley, S., Kleiman, J., Gatlin, M., Eplerenone Post-Acute Myocardial Infarction Heart Failure, Efficacy Survival Study, Investigators., *Eplerenone, a selective aldosterone blocker, in patients with left ventricular dysfunction after myocardial infarction.* N Engl J Med, 2003. **348**(14): p. 1309-21.

80. Pitt, B., Zannad, F., Remme, W. J., Cody, R., Castaigne, A., Perez, A., Palensky, J., Wittes, J., *The effect of spironolactone on morbidity and mortality in patients with severe heart failure. Randomized Aldactone Evaluation Study Investigators.* N Engl J Med, 1999. **341**(10): p. 709-17.

81. Zannad, F., McMurray, J. J., Krum, H., van Veldhuisen, D. J., Swedberg, K., Shi, H., Vincent, J., Pocock, S. J., Pitt, B., Emphasis-Hf Study Group, *Eplerenone in patients with systolic heart failure and mild symptoms.* N Engl J Med, 2011. **364**(1): p. 11-21.

82. Vizzardi, E., Nodari, S., Caretta, G., D'Aloia, A., Pezzali, N., Faden, G., Lombardi, C., Raddino, R., Metra, M., Dei Cas, L., *Effects of spironolactone on long-term mortality and morbidity in patients with heart failure and mild or no symptoms.* Am J Med Sci, 2014. **347**(4): p. 271-6.

83. Gilbert, B.W., *Ace Inhibitors and Regression of Left-Ventricular Hypertrophy.* Clinical Cardiology, 1992. **15**(10): p. 711-714.

84. Anguita-Sanchez, M., Castillo-Dominguez, J. C., Mesa-Rubio, D., Ruiz-Ortiz, M., Lopez-Granados, A., de Lezo, J., *[Should Angiotensin-converting enzyme inhibitors be continued over the long term in patients whose left ventricular ejection fraction normalizes after an episode of acute myocarditis?].* Rev Esp Cardiol, 2006. **59**(11): p. 1199-201.

85. Quitterer, U. and AbdAlla, S., *Vasopressor meets vasodepressor: The AT1-B2 receptor heterodimer.* Biochem Pharmacol, 2014. **88**(3): p. 284-90.

86. Flather, M.D., Yusuf, S.Kober, L.Pfeffer, M.Hall, A.Murray, G.Torp-Pedersen, C.Ball, S.Pogue, J.Moye, L., Braunwald, E., *Long-term ACE-inhibitor therapy in patients with heart failure or left-ventricular dysfunction: a systematic overview of data from individual patients. ACE-Inhibitor Myocardial Infarction Collaborative Group.* Lancet, 2000. **355**(9215): p. 1575-81.

87. Konstam, M.A., Patten, R. D., Thomas, I., Ramahi, T., La Bresh, K., Goldman, S., Lewis, W.Gradman, A., Self, K. S., Bittner, V., Rand, W., Kinan, D., Smith, J. J., Ford, T., Segal,

R., Udelson, J. E, *Effects of losartan and captopril on left ventricular volumes in elderly patients with heart failure: results of the ELITE ventricular function substudy.* Am Heart J, 2000. **139**(6): p. 1081-7.

88.   Granger, C.B., McMurray, J. J., Yusuf, S., Held, P., Michelson, E. L., Olofsson, B., Ostergren, J. Pfeffer, M. A., Swedberg, K., Charm Investigators,,Committees., *Effects of candesartan in patients with chronic heart failure and reduced left-ventricular systolic function intolerant to angiotensin-converting-enzyme inhibitors: the CHARM-Alternative trial.* Lancet, 2003. **362**(9386): p. 772-6.

89.   McMurray, J.J., Packer, M., Desai, A., SGong, J., Lefkowitz, M. P., Rizkala, A. R.Rouleau, J. L., Shi, V. C., Solomon, S. D., Swedberg, K.Zile, M. R., Paradigm-Hf InvestigatorsCommittees., *Angiotensin-neprilysin inhibition versus enalapril in heart failure.* N Engl J Med, 2014. **371**(11): p. 993-1004.

90.   Tsouli, S.G., Liberopoulos, E. N.Goudevenos, J. A., Mikhailidis, D. P., Elisaf, M. S., *Should a statin be prescribed to every patient with heart failure?* Heart Fail Rev, 2008. **13**(2): p. 211-25.

91.   Fukuta, H., Sane, D. C., Brucks, S., Little, W. C., *Statin therapy may be associated with lower mortality in patients with diastolic heart failure: a preliminary report.* Circulation, 2005. **112**(3): p. 357-63.

92.   Kjekshus, J., Apetrei, E., Barrios, V., Bohm, M., Cleland, J. G., Cornel, J. H., Dunselman, P., Fonseca, C., Goudev, A., Grande, P., Gullestad, L., Hjalmarson, A.,Hradec, J., Janosi, A., Kamensky, G., Komajda, M., Korewicki, J., Kuusi, T., Mach, F., Mareev, V., McMurray, J. J., Ranjith, N., Schaufelberger, M., Vanhaecke, J., van Veldhuisen, D. J., Waagstein, F., Wedel, H., Wikstrand, J.Corona Group, *Rosuvastatin in older patients with systolic heart failure.* N Engl J Med, 2007. **357**(22): p. 2248-61.

93.   Tavazzi, L., Maggioni, A. P., Marchioli, R., Barlera, S., Franzosi, M. G., Latini, R., Lucci, D., Nicolosi, G. L., Porcu, M., Tognoni, G., Gissi, H. F., investigators., *Effect of rosuvastatin in patients with chronic heart failure (the GISSI-HF trial): a randomised, double-blind, placebo-controlled trial.* Lancet, 2008. **372**(9645): p. 1231-9.

94.   Rehsia, N.S. and N.S. Dhalla, *Potential of endothelin-1 and vasopressin antagonists for the treatment of congestive heart failure.* Heart Fail Rev, 2010. **15**(1): p. 85-101.

95.   Gheorghiade, M., Konstam, M. A., Burnett, J. C., Jr., Grinfeld, L., Maggioni, A. P., Swedberg, K., Udelson, J. E., Zannad, F., Cook, T., Ouyang, J., Zimmer, C., Orlandi, C.,

Efficacy of Vasopressin Antagonism in Heart Failure Outcome Study With Tolvaptan, Investigators., *Short-term clinical effects of tolvaptan, an oral vasopressin antagonist, in patients hospitalized for heart failure: the EVEREST Clinical Status Trials.* JAMA, 2007. **297**(12): p. 1332-43.

96.   Konstam, M.A., Gheorghiade, M., Burnett, J. C., Jr., Grinfeld, L., Maggioni, A. P., Swedberg, K., U., delson, J. E., Zannad, F., Cook, T., Ouyang, J., Zimmer, C., Orlandi, C., Efficacy of Vasopressin Antagonism in Heart Failure Outcome Study With Tolvaptan, Investigators., *Effects of oral tolvaptan in patients hospitalized for worsening heart failure: the EVEREST Outcome Trial.* JAMA, 2007. **297**(12): p. 1319-31.

97.   Sugden, P.H., *An overview of endothelin signaling in the cardiac myocyte.* J Mol Cell Cardiol, 2003. **35**(8): p. 871-86.

98.   Louis, A., Cleland, J. G., Crabbe, S., Ford, S., Thackray, S., Houghton, T., Clark, A., *Clinical Trials Update: CAPRICORN, COPERNICUS, MIRACLE, STAF, RITZ-2, RECOVER and RENAISSANCE and cachexia and cholesterol in heart failure. Highlights of the Scientific Sessions of the American College of Cardiology, 2001.* Eur J Heart Fail, 2001. **3**(3): p. 381-7.

99.   Anand, I., McMurray, J., Cohn, J. N., Konstam, M. A., Notter, T., Quitzau, K., Ruschitzka, F., Luscher, T. F., Earth investigators, *Long-term effects of darusentan on left-ventricular remodelling and clinical outcomes in the EndothelinA Receptor Antagonist Trial in Heart Failure (EARTH): randomised, double-blind, placebo-controlled trial.* Lancet, 2004. **364**(9431): p. 347-54.

100.   O'Connor, C.M., Gattis, W. A., Adams, K. F., Jr., Hasselblad, V., Chandler, B., Frey, A., Kobrin, I., Rainisio, M., Shah, M. R., Teerlink, J., Gheorghiade, M., Randomized Intravenous Tezosentan Study, Investigators, *Tezosentan in patients with acute heart failure and acute coronary syndromes: results of the Randomized Intravenous TeZosentan Study (RITZ-4).* J Am Coll Cardiol, 2003. **41**(9): p. 1452-7.

101.   Epelman, S. and D.L. Mann, *Communication in the heart: the role of the innate immune system in coordinating cellular responses to ischemic injury.* J Cardiovasc Transl Res, 2012. **5**(6): p. 827-36.

102.   Fildes, J.E., Shaw, S., M., Yonan, N., Williams, S. G., *The immune system and chronic heart failure: is the heart in control?* J Am Coll Cardiol, 2009. **53**(12): p. 1013-20.

103. Cacciapaglia, F., Navarini, L., Menna, P., Salvatorelli, E., Minotti, G., Afeltra, A., *Cardiovascular safety of anti-TNF-alpha therapies: facts and unsettled issues.* Autoimmun Rev, 2011. **10**(10): p. 631-5.

104. Battiprolu, P.K., Lopez-Crisosto, C.Wang, Z. V., Nemchenko, A., Lavandero, S., Hill, J. A.., *Diabetic cardiomyopathy and metabolic remodeling of the heart.* Life Sci, 2013. **92**(11): p. 609-15.

105. Fields, A.V., Patterson, B., Karnik, A., A.Shannon, R. P., *Glucagon-like peptide-1 and myocardial protection: more than glycemic control.* Clin Cardiol, 2009. **32**(5): p. 236-43.

106. Nauck, M.A. and J.J. Meier, *Incretin hormones: Their role in health and disease.* Diabetes Obes Metab, 2018. **20 Suppl 1**: p. 5-21.

107. Kreymann, B., Williams, G., Ghatei, M., A.Bloom, S. R., *Glucagon-like peptide-1 7-36: a physiological incretin in man.* Lancet, 1987. **2**(8571): p. 1300-4.

108. Bhashyam, S., Fields, A. V., Patterson, B., Testani, J. M., Chen, L.Shen, Y. T.S, hannon, R. P., *Glucagon-like peptide-1 increases myocardial glucose uptake via p38alpha MAP kinase-mediated, nitric oxide-dependent mechanisms in conscious dogs with dilated cardiomyopathy.* Circ Heart Fail, 2010. **3**(4): p. 512-21.

109. Poornima, I., Brown, S. B., Bhashyam, S., Parikh, P.Bolukoglu, H., Shannon, R. P. *Chronic glucagon-like peptide-1 infusion sustains left ventricular systolic function and prolongs survival in the spontaneously hypertensive, heart failure-prone rat.* Circ Heart Fail, 2008. **1**(3): p. 153-60.

110. Marso, S.P., Daniels, G. H.Brown-Frandsen, K.Kristensen, P Mann, J. F Nauck, M. A. Nissen, S. E., Pocock, S., Poulter, N. R., Ravn, L. S., Steinberg, W., M.Stockner, M.Zinman, B Bergenstal, R. M.Buse, J. B.Leader Steering CommitteeLeader Trial Investigators., *Liraglutide and Cardiovascular Outcomes in Type 2 Diabetes.* N Engl J Med, 2016. **375**(4): p. 311-22.

111. Verma, S., Bain, S. C., Buse, J. B., Idorn, T., Rasmussen, S., Orsted, D. D., Nauck, M. A., *Occurence of First and Recurrent Major Adverse Cardiovascular Events With Liraglutide Treatment Among Patients With Type 2 Diabetes and High Risk of Cardiovascular Events: A Post Hoc Analysis of a Randomized Clinical Trial.* JAMA Cardiol, 2019.

112. Guazzi, M., Vicenzi, M., Arena, R., Guazzi, M. D., *PDE5 inhibition with sildenafil improves left ventricular diastolic function, cardiac geometry, and clinical status in patients with stable systolic heart failure: results of a 1-year, prospective, randomized, placebo-controlled study.* Circ Heart Fail, 2011. **4**(1): p. 8-17.

113. Redfield, M.M., Chen, H. H., Borlaug, B. A., Semigran, M. J., Lee, K. L., Lewis, G., LeWinter, M. M., Rouleau, J. L., Bull, D. A., Mann, D. L., Deswal, A., Stevenson, L. W., Givertz, M. M., Ofili, E. O., O'Connor, C. M., Felker, G. M., Goldsmith, S. R., Bart, B. A., McNulty, S. E., Ibarra, J. C., Lin, G., Oh, J. K., Patel, M. R., Kim, R. J.Tracy, R. P., Velazquez, E. J., Anstrom, K. J., Hernandez, A. F., Mascette, A. M., Braunwald, E., Relax Trial, *Effect of phosphodiesterase-5 inhibition on exercise capacity and clinical status in heart failure with preserved ejection fraction: a randomized clinical trial.* JAMA, 2013. **309**(12): p. 1268-77.

114. Prabhu, S.D., *Nitric oxide protects against pathological ventricular remodeling: reconsideration of the role of NO in the failing heart.* Circ Res, 2004. **94**(9): p. 1155-7.

115. Fraccarollo, D., Widder, J. D., Galuppo, P., Thum, T., Tsikas, D., Hoffmann, M., Ruetten, H.Ertl, G., Bauersachs, J., *Improvement in left ventricular remodeling by the endothelial nitric oxide synthase enhancer AVE9488 after experimental myocardial infarction.* Circulation, 2008. **118**(8): p. 818-27.

116. Malik, F.I., Hartman, J. J., Elias, K. A., Morgan, B. P., Rodriguez, H., Brejc, K.Anderson, R. L., Sueoka, S. H., Lee, K. H., Finer, J. T., Sakowicz, R., Baliga, R., Cox, D. R., Garard, M., Godinez, G., Kawas, R., Kraynack, E., Lenzi, D., Lu, P. P., Muci, A., Niu, C., Qian, X, .Pierce, D. W., Pokrovskii, M., Suehiro, I., Sylvester, S., Tochimoto, T., Valdez, C., Wang, W., Katori, T., Kass, D. A., Shen, Y. T., Vatner, S. F., Morgans, D. J., *Cardiac myosin activation: a potential therapeutic approach for systolic heart failure.* Science, 2011. **331**(6023): p. 1439-43.

117. Cleland, J.G., Teerlink, J. R., Senior, R., Nifontov, E. M., Mc Murray, J. J., Lang, C. C., Tsyrlin, V. A., Greenberg, B. H., Mayet, J., Francis, D. P., Shaburishvili, T., Monaghan, M., Saltzberg, M., Neyses, L., Wasserman, S. M., Lee, J. H., Saikali, K. G., Clarke, C. P., Goldman, J. H., Wolff, A. A., Malik, F. I., *The effects of the cardiac myosin activator, omecamtiv mecarbil, on cardiac function in systolic heart failure: a double-blind, placebo-controlled, crossover, dose-ranging phase 2 trial.* Lancet, 2011. **378**(9792): p. 676-83.

118. Teerlink, J.R., Felker, G. M., McMurray, J. J., Solomon, S. D., Adams, K. F., Jr., Cleland, J. G., Ezekowitz, J. A., Goudev, A., Macdonald, P., Metra, M., Mitrovic, V., Ponikowski, P., Serpytis, P., Spinar, J., Tomcsanyi, J., Vandekerckhove, H. J., Voors, A. A., Monsalvo,

M. L., Johnston, J., Malik, F. I., Honarpour, N., Cosmic-Hf Investigators, *Chronic Oral Study of* Myosin *Activation to Increase Contractility in Heart Failure (COSMIC-HF): a phase 2, pharmacokinetic, randomised, placebo-controlled trial.* Lancet, 2016. **388**(10062): p. 2895-2903.

119. Azevedo, P.S., Polegato, B. F., Minicucci, M. F., Paiva, S. A., Zornoff, L. A., *Cardiac Remodeling: Concepts, Clinical Impact, Pathophysiological Mechanisms and Pharmacologic Treatment.* Arq Bras Cardiol, 2016. **106**(1): p. 62-9.

120. Braunwald, E., *Heart failure.* JACC Heart Fail, 2013. **1**(1): p. 1-20.

121. Wu, J.H., Hagaman, J., Kim, S., Reddick, R. L., Maeda, N., *Aortic constriction exacerbates atherosclerosis and induces cardiac dysfunction in milacking apolipoprotein E.* Arterioscler Thromb Vasc Biol, 2002. **22**(3): p. 469-75.

122. Rockman, H.A., Ross, R. S., Harris, A. N., Knowlton, K. U., Steinhelper, M. E., Field, L. J., Ross, J., Jr., Chien, K. R., *Segregation of atrial-specific and inducible expression of an atrial natriuretic factor transgene in an in vivo murine model of cardiac hypertrophy.* Proc Natl Acad Sci U S A, 1991. **88**(18): p. 8277-81.

123. Lo Sasso, G., Schlage, W. K., Boue, S., Veljkovic, E., Peitsch, M. C., Hoeng, J., *The Apoe(-/-) mouse model: a suitable model to study cardiovascular and respiratory diseases in the context of cigarette smoke exposure and harm reduction.* J Transl Med, 2016. **14**(1): p. 146.

124. Abdalla, S., Fu, X., Elzahwy, S. S., Klaetschke, K., Streichert, T., Quitterer, U., *Up-regulation of the cardiac lipid metabolism at the onset of heart failure.* Cardiovasc Hematol Agents Med Chem, 2011. **9**(3): p. 190-206.

125. Meir, K.S. and E. Leitersdorf, *Atherosclerosis in the apolipoprotein-E-deficient mouse: a decade of progress.* Arterioscler Thromb Vasc Biol, 2004. **24**(6): p. 1006-14.

126. Graham, D.J., Ouellet-Hellstrom, R., MaCurdy, T. E.. Ali, F., Sholley, C., Worrall, C., Kelman, J. A., *Risk of acute myocardial infarction, stroke, heart failure, and death in elderly Medicare patients treated with rosiglitazone or pioglitazone.* JAMA, 2010. **304**(4): p. 411-8.

127. Krentz, A.J., *Rosiglitazone: trials, tribulations and termination.* Drugs, 2011. **71**(2): p. 123-30.

128. Seidman, J.G. and C. Seidman, *The genetic basis for cardiomyopathy: from mutation identification to mechanistic paradigms.* Cell, 2001. **104**(4): p. 557-67.

129. Rajan, S., Pena, J. R., Jegga, A. G., Aronow, B. J., Wolska, B. M., Wieczorek, D. F., *Microarray analysis of active cardiac remodeling genes in a familial hypertrophic cardiomyopathy mouse model rescued by a phospholamban knockout.* Physiol Genomics, 2013. **45**(17): p. 764-73.

130. Abd Alla, J., Graemer, M., Fu, X., Quitterer, U., *Inhibition of G-protein-coupled Receptor Kinase 2 Prevents the Dysfunctional Cardiac Substrate Metabolism in Fatty Acid Synthase Transgenic Mice.* J Biol Chem, 2016. **291**(6): p. 2583-600.

131. Nagy, A., Gertsenstein, M., Vintersten, K., Behringer, R, *Manipulating the mouse embryo. A laboratory manual.* Cold Spring Harbor Laboratory Press, Cold Spring Harbor NY, USA 2003.

132. Gulick, J. Subramaniam, A., Neumann, J., Robbins, J., *Isolation and characterization of the mouse cardiac myosin heavy chain genes.* J Biol Chem, 1991. **266**(14): p. 9180-5.

133. Wolf, S., J. Abd Alla., and U. Quitterer., *Sensitization of the Angiotensin II AT1 Receptor Contributes to RKIP-Induced Symptoms of Heart Failure.* Front Med (Lausanne), 2018. **5**: p. 359.

134. Moran, C.M., Thomson, A. J., Rog-Zielinska, E., Gray, G. A., *High-resolution echocardiography in the assessment of cardiac physiology and disease in preclinical models.* Exp Physiol, 2013. **98**(3): p. 629-44.

135. Ramos-Vara, J.A., *Technical aspects of immunohistochemistry.* Vet Pathol, 2005. **42**(4): p. 405-26.

136. Hodson, L. and B.A. Fielding, *Stearoyl-CoA desaturase: rogue or innocent bystander?* Prog Lipid Res, 2013. **52**(1): p. 15-42.

137. Paton, C.M. and J.M. Ntambi, *Biochemical and physiological function of stearoyl-CoA desaturase.* Am J Physiol Endocrinol Metab, 2009. **297**(1): p. E28-37.

138. Sampath, H. and J.M. Ntambi, *The role of stearoyl-CoA desaturase in obesity, insulin resistance, and inflammation.* Ann N Y Acad Sci, 2011. **1243**: p. 47-53.

139.   Sampath, H. and J.M. Ntambi, *Role of stearoyl-CoA desaturase-1 in skin integrity and whole body energy balance.* J Biol Chem, 2014. **289**(5): p. 2482-8.

140.   Flowers, M.T. and J.M. Ntambi, *Role of stearoyl-coenzyme A desaturase in regulating lipid metabolism.* Curr Opin Lipidol, 2008. **19**(3): p. 248-56.

141.   Castro, L.F., Wilson, J. M., Goncalves, O., Galante-Oliveira, S., Rocha, E., Cunha, I., *The evolutionary history of the stearoyl-CoA desaturase gene family in vertebrates.* BMC Evol Biol, 2011. **11**: p. 132.

142.   Wang, J., Yu, L., Schmidt, R. E., Su, C., Huang, X., Gould, K., Cao, G., *Characterization of HSCD5, a novel human stearoyl-CoA desaturase unique to primates.* Biochem Biophys Res Commun, 2005. **332**(3): p. 735-42.

143.   Miyazaki, M., Dobrzyn, A., Elias, P. M., Ntambi, J. M., *Stearoyl-CoA desaturase-2 gene expression is required for lipid synthesis during early skin and liver development.* Proceedings of the National Academy of Sciences of the United States of America, 2005. **102**(35): p. 12501-12506.

144.   Zheng, Y., Prouty, S. M., Harmon, A., Sundberg, J. P., Stenn, K. S., Parimoo, S., *Scd3--a novel gene of the stearoyl-CoA desaturase family with restricted expression in skin.* Genomics, 2001. **71**(2): p. 182-91.

145.   Miyazaki, M., F.E. Gomez, and J.M. Ntambi, *Lack of stearoyl-CoA desaturase-1 function induces a palmitoyl-CoA Delta6 desaturase and represses the stearoyl-CoA desaturase-3 gene in the preputial glands of the mouse.* J Lipid Res, 2002. **43**(12): p. 2146-54.

146.   Miyazaki, M., Jacobson, M. J., Man, W. C., Cohen, P., Asilmaz, E., Friedman, J. M., Ntambi, J. M., *Identification and characterization of murine SCD4, a novel heart-specific stearoyl-CoA desaturase isoform regulated by leptin and dietary factors.* J Biol Chem, 2003. **278**(36): p.3390411.

147.   Mauvoisin, D. and C. Mounier, *Hormonal and nutritional regulation of SCD1 gene expression.* Biochimie, 2011. **93**(1): p. 78-86.

148.   Christy, R.J., Yang, V. W., Ntambi, J. M., Geiman, D. E., Landschulz, W. H., Friedman, A. D. Nakabeppu, Y., Kelly, T. J., Lane, M. D., *Differentiation-induced gene expression in 3T3-L1 preadipocytes: CCAAT/enhancer binding protein interacts with and activates the promoters of two adipocyte-specific genes.* Genes Dev, 1989. **3**(9): p. 1323-35.

149. Biddinger, S.B., Almind, K., Miyazaki, M., Kokkotou, E., Ntambi, J. M., Kahn, C. R., *Effects of diet and genetic background on sterol regulatory element-binding protein-1c, stearoyl CoA desaturase 1, and the development of the metabolic syndrome.* Diabetes, 2005. **54**(5): p. 1314-23.

150. Sampath, H., Miyazaki, M., Dobrzyn, A., Ntambi, J. M., *Stearoyl-CoA desaturase-1 mediates the pro-lipogenic effects of dietary saturated fat.* J Biol Chem, 2007. **282**(4): p. 2483-93.

151. Lin, J., Yang, R., Tarr, P. T., Wu, P. H., Handschin, C., Li, S., Yang, W., Pei, L., Uldry, M., Tontonoz, P., Newgard, C. B., *Hyperlipidemic effects of dietary saturated fats mediated through PGC-1beta coactivation of SREBP.* Cell, 2005. **120**(2): p. 261-73.

152. Jump, D.B. and S.D. Clarke, *Regulation of gene expression by dietary fat.* Annu Rev Nutr, 1999. **19**: p. 63-90.

153. Sessler, A.M., Kaur, N., Palta, J. P., Ntambi, J. M., *Regulation of stearoyl-CoA desaturase 1 mRNA stability by polyunsaturated fatty acids in 3T3-L1 adipocytes.* J Biol Chem, 1996. **271**(47): p. 29854-8.

154. Sampath, H. and J.M. Ntambi, *Polyunsaturated fatty acid regulation of genes of lipid metabolism.* Annu Rev Nutr, 2005. **25**: p. 317-40.

155. Matsui, H., Yokoyama, T., Sekiguchi, K., Iijima, D., Sunaga, H., Maniwa, M., Ueno, M., Iso, T., Arai, M., Kurabayashi, M., *Stearoyl-CoA desaturase-1 (SCD1) augments saturated fatty acid-induced lipid accumulation and inhibits apoptosis in cardiac myocytes.* PLoS One, 2012. **7**(3): p. e33283.

156. Ntambi, J.M., *Dietary regulation of stearoyl-CoA desaturase 1 gene expression in mouse liver.* J Biol Chem, 1992. **267**(15): p. 10925-30.

157. Miyazaki, M., Y.C. Kim, and J.M. Ntambi, *A lipogenic diet in mice with a disruption of the stearoyl-CoA desaturase 1 gene reveals a stringent requirement of endogenous monounsaturated fatty acids for triglyceride synthesis.* J Lipid Res, 2001. **42**(7): p. 1018-24.

158. Iizuka, K., Bruick, R. K., Liang, G., Horton, J. D., Uyeda, K., *Deficiency of carbohydrate response element-binding protein (ChREBP) reduces lipogenesis as well as glycolysis.* Proc Natl Acad Sci U S A, 2004. **101**(19): p. 7281-6.

159. Mauvoisin, D., Rocque, G., Arfa, O., Radenne, A., Boissier, P., Mounier, C., *Role of the PI3-kinase/mTor pathway in the regulation of the stearoyl CoA desaturase (SCD1) gene expression by insulin in liver.* J Cell Commun Signal, 2007. **1**(2): p. 113-25.

160. Jeffcoat, R., Roberts, P. A., Ormesher, J., James, A. T., *Stearolyl-CoA desaturase: a control enzyme in hepatic lipogenesis.* Eur J Biochem, 1979. **101**(2): p. 439-45.

161. Waters, K.M. and J.M. Ntambi, *Insulin and dietary fructose induce stearoyl-CoA desaturase 1 gene expression of diabetic mice.* J Biol Chem, 1994. **269**(44): p. 27773-7.

162. Singh, M.V. and J.M. Ntambi, *Nuclear factor 1 is essential for the expression of stearoyl-CoA desaturase 1 gene during preadipocyte differentiation.* Biochim Biophys Acta, 1998. **1398**(2): p. 148-56.

163. Tabor, D.E., Kim, J. B., Spiegelman, B. M., Edwards, P. A., *Identification of conserved cis-elements and transcription factors required for sterol-regulated transcription of stearoyl-CoA desaturase 1 and 2.* J Biol Chem, 1999. **274**(29): p. 20603-10

164. Zhang, W., Della-Fera, M. A., Hartzell, D. L., Hausman, D., Baile, C. A., *Adipose tissue gene expression profiles in ob/ob mice treated with leptin.* Life Sci, 2008. **83**(1-2): p. 35-42.

165. Mauvoisin, D., Prevost, M., Ducheix, S., Arnaud, M. P., Mounier, C., *Key role of the ERK1/2 MAPK pathway in the transcriptional regulation of the Stearoyl-CoA Desaturase (SCD1) gene expression in response to leptin.* Mol Cell Endocrinol, 2010. **319**(1-2): p. 116-28.

166. Lundholm, L., Zang, H., Hirschberg, A. L., Gustafsson, J. A., Arner, P., Dahlman-Wright, K., *Key lipogenic gene expression can be decreased by estrogen in human adipose tissue.* Fertility and Sterility, 2008. **90**(1): p. 44-48.

167. Bryzgalova, G., Lundholm, L., Portwood, N., Gustafsson, J. A., Khan, A., Efendic, S., Dahlman-Wright, K., *Mechanisms of antidiabetogenic and body weight-lowering effects of estrogen in high-fat diet-fed mice.* Am J Physiol Endocrinol Metab, 2008. **295**(4): p. E904-12.

168. Bryzgalova, G., Gao, H., Ahren, B., Zierath, J. R., Galuska, D., Steiler, T. L., Dahlman-Wright, K., Nilsson, S., Gustafsson, J. A., Efendic, S., Khan, A., *Evidence that oestrogen*

receptor-alpha plays an important role in the regulation of glucose homeostasis in mice: insulin sensitivity in the liver. Diabetologia, 2006. **49**(3): p. 588-597.

169. Gao, H., Bryzgalova, G., Hedman, E., Khan, A., Efendic, S., Gustafsson, J. A., Dahlman-Wright, K., *Long-term administration of estradiol decreases expression of hepatic lipogenic genes and improves insulin sensitivity in ob/ob mice: a possible mechanism is through direct regulation of signal transducer and activator of transcription 3.* Mol Endocrinol, 2006. **20**(6): p. 1287-99.

170. Waters, K.M., C.W. Miller, and J.M. Ntambi, *Localization of a negative thyroid hormone-response region in hepatic Stearoyl-CoA desaturase gene 1.* Biochemical and Biophysical Research Communications, 1997. **233**(3): p. 838-843.

171. Stone, R.L. and D.A. Bernlohr, *The molecular basis for inhibition of adipose conversion of murine 3T3-L1 cells by retinoic acid.* Differentiation, 1990. **45**(2): p. 119-27.

172. Miller, C.W., K.M. Waters, and J.M. Ntambi, *Regulation of hepatic stearoyl-CoA desaturase gene 1 by vitamin A.* Biochem Biophys Res Commun, 1997. **231**(1): p. 206-10.

173. Mar-Heyming, R., Miyazaki, M., Weissglas-Volkov, D., Kolaitis, N. A., Sadaat, N., Plaisier, C., Pajukanta, P., Cantor, R. M., de Bruin, T. W., Ntambi, J. M., Lusis, A. J., *Association of stearoyl-CoA desaturase 1 activity with familial combined hyperlipidemia.* Arterioscler Thromb Vasc Biol, 2008. **28**(6): p. 1193-9.

174. Flowers, M.T., Groen, A. K., Oler, A. T., Keller, M. P., Choi, Y., Schueler, K. L., Richards, O. C., Lan, H., Miyazaki, M., Kuipers, F., Kendziorski, C. M., Ntambi, J. M., Attie, A. D., *Cholestasis and hypercholesterolemia in SCD1-deficient mice fed a low-fat, high-carbohydrate diet.* J Lipid Res, 2006. **47**(12): p. 2668-80.

175. Ntambi, J.M., Miyazaki, M., Stoehr, J. P., Lan, H., Kendziorski, C. M., Yandell, B. S., Song, Y., Cohen, P., Friedman, J. M., Attie, A. D., *Loss of stearoyl-CoA desaturase-1 function protects mice against adiposity.* Proc Natl Acad Sci U S A, 2002. **99**(17): p. 11482-6.

176. Rahman, S.M., Dobrzyn, A., Dobrzyn, P., Lee, S. H., Miyazaki, M., Ntambi, J. M., *Stearoyl-CoA desaturase 1 deficiency elevates insulin-signaling components and down-regulates protein-tyrosine phosphatase 1B in muscle.* Proc Natl Acad Sci U S A, 2003. **100**(19): p. 11110-5.

177. Ide, Y., Waki, M., Hayasaka, T., Nishio, T., Morita, Y., Tanaka, H., Sasaki, T., Koizumi, K., Matsunuma, R., Hosokawa, Y., Ogura, H., Shiiya, N., *Human breast cancer tissues contain abundant phosphatidylcholine(36ratio1) with high stearoyl-CoA desaturase-1 expression.* PLoS One, 2013. **8**(4): p. e61204.

178. Dobrzyn, A. and J.M. Ntambi, *The role of stearoyl-CoA desaturase in body weight regulation.* Trends Cardiovasc Med, 2004. **14**(2): p. 77-81.

179. Barouch, L.A., Gao, D. Q., Chen, L., Miller, K. L., Xu, W. H., Phan, A. C., Kittleson, M. M., Minhas, K. M., Berkowitz, D. E., Wei, C. M., *Cardiac myocyte apoptosis is associated with increased DNA damage and decreased survival in murine models of obesity.* Circulation Research, 2006. **98**(1): p. 119-124.

180. Szczepaniak, L.S., *Forgotten but not gone: the rediscovery of fatty heart, the most common unrecognized disease in America.* Circ Res, 2007. **101**(8): p. 759-67.

181. Bielawska, A.E., Shapiro, J. P., Jiang, L., Melkonyan, H. S., Piot, C., Wolfe, C. L., Tomei, L. D., Hannun, Y. A., Umansky, S. R., *Ceramide is involved in triggering of cardiomyocyte apoptosis induced by ischemia and reperfusion.* Am J Pathol, 1997. **151**(5): p. 1257-63.

182. Dobrzyn, A., Dobrzyn, P., Lee, S. H., Miyazaki, M., Cohen, P., Asilmaz, E., Hardie, D. G., Friedman, J. M., Ntambi, J. M., *Stearoyl-CoA desaturase-1 deficiency reduces ceramide synthesis by downregulating serine palmitoyltransferase and increasing beta-oxidation in skeletal muscle.* Am J Physiol Endocrinol Metab, 2005. **288**(3): p. E599-607.

183. Cohen, P., Miyazaki, M., Socci, N. D., Hagge-Greenberg, A., Liedtke, W., Soukas, A. A., Sharma, R., Hudgins, L. C., Ntambi, J. M., Friedman, J. M., *Role for stearoyl-CoA desaturase-1 in leptin-mediated weight loss.* Science, 2002. **297**(5579): p. 240-3.

184. Dobrzyn, P., Sampath, H., Dobrzyn, A., Miyazaki, M., Ntambi, J. M., *Loss of stearoyl-CoA desaturase 1 inhibits fatty acid oxidation and increases glucose utilization in the heart.* Am J Physiol Endocrinol Metab, 2008. **294**(2): p. E357-64.

185. Miyazaki, M., W.C. Man, and J.M. Ntambi, *Targeted disruption of stearoyl-CoA desaturase1 gene in mice causes atrophy of sebaceous and meibomian glands and depletion of wax esters in the eyelid.* J Nutr, 2001. **131**(9): p. 2260-8.

186. Miyazaki, M., Kim, H. J., Man, W. C., Ntambi, J. M., *Oleoyl-CoA is the major de novo product of stearoyl-CoA desaturase 1 gene isoform and substrate for the biosynthesis*

of the Harderian gland 1-alkyl-2,3-diacylglycerol. J Biol Chem, 2001. **276**(42): p. 39455-61.

187. Miyazaki, M., Kim, Y. C., Gray-Keller, M. P., Attie, A. D., Ntambi, J. M., *The biosynthesis of hepatic cholesterol esters and triglycerides is impaired in mice with a disruption of the gene for stearoyl-CoA desaturase 1.* J Biol Chem, 2000. **275**(39): p. 30132-8.

188. Man, W.C., Miyazaki, M., Chu, K., Ntambi, J., *Colocalization of SCD1 and DGAT2: implying preference for endogenous monounsaturated fatty acids in triglyceride synthesis.* J Lipid Res, 2006. **47**(9): p. 1928-39.

189. Harris, C.A., Haas, J. T., Streeper, R. S., Stone, S. J., Kumari, M., Yang, K., Han, X., Brownell, N., Gross, R. W., Zechner, R., Farese, R. V., Jr., *DGAT enzymes are required for triacylglycerol synthesis and lipid droplets in adipocytes.* J Lipid Res, 2011. **52**(4): p. 657-67.

190. Zammit, V.A., *Hepatic triacylglycerol synthesis and secretion: DGAT2 as the link between glycaemia and triglyceridaemia.* Biochem J, 2013. **451**(1): p. 1-12.

191. Weiss, S.B., E.P. Kennedy, and J.Y. Kiyasu, *The enzymatic synthesis of triglycerides.* J Biol Chem, 1960. **235**: p. 40-4.

192. Nilsson, A., R. Sundler, and B. Akesson, *Effect of different albumin-bound fatty acids on fatty acid and cholesterol biosynthesis in rat hepatocytes.* FEBS Lett, 1974. **45**(1): p. 282-5.

193. Dobrzyn, P., Dobrzyn, A., Miyazaki, M., Cohen, P., Asilmaz, E., Hardie, D. G., Friedman, J. M., Ntambi, J. M., *Stearoyl-CoA desaturase 1 deficiency increases fatty acid oxidation by activating AMP-activated protein kinase in liver.* Proc Natl Acad Sci U S A, 2004. **101**(17): p. 6409-14.

194. Cowherd, R.M., R.E. Lyle, and R.E. McGehee, Jr., *Molecular regulation of adipocyte differentiation.* Semin Cell Dev Biol, 1999. **10**(1): p. 3-10.

195. Kim, Y.C. and J.M. Ntambi, *Regulation of stearoyl-CoA desaturase genes: role in cellular metabolism and preadipocyte differentiation.* Biochem Biophys Res Commun, 1999. **266**(1): p. 1-4.

196.   Querfurth, H.W. and F.M. LaFerla, *Alzheimer's disease.* N Engl J Med, 2010. **362**(4): p. 329-44.

197.   Finch, C.E., *Developmental origins of aging in brain and blood vessels: an overview.* Neurobiol Aging, 2005. **26**(3): p. 281-91.

198.   Launer, L.J., *The epidemiologic study of dementia: a life-long quest?* Neurobiol Aging, 2005. **26**(3): p. 335-40.

199.   Whalley, L.J., F.D. Dick, and G. McNeill, *A life-course approach to the aetiology of late-onset dementias.* Lancet Neurol, 2006. **5**(1): p. 87-96.

200.   Saunders, A.M., Strittmatter, W. J., Schmechel, D., George-Hyslop, P. H., Pericak-Vance, M. A., Joo, S. H., Rosi, B. L., Gusella, J. F., Crapper-MacLachlan, D. R., Alberts, M. J., *Association of apolipoprotein E allele epsilon 4 with late-onset familial and sporadic Alzheimer's disease.* Neurology, 1993. **43**(8): p. 1467-72.

201.   Cutler, R.G., Kelly, J., Storie, K., Pedersen, W. A., Tammara, A., Hatanpaa, K., Troncoso, J. C., Mattson, M. P., *Involvement of oxidative stress-induced abnormalities in ceramide and cholesterol metabolism in brain aging and Alzheimer's disease.* Proc Natl Acad Sci U S A, 2004. **101**(7): p. 2070-5.

202.   Lukiw, W.J., Pappolla, M., Pelaez, R. P., Bazan, N. G., *Alzheimer's disease--a dysfunction in cholesterol and lipid metabolism.* Cell Mol Neurobiol, 2005. **25**(3-4): p. 475

203.   Astarita, G., Jung, K. M., Berchtold, N. C., Nguyen, V. Q., Gillen, D. L., Head, E., Cotman, C. W., Piomelli, D., *Deficient liver biosynthesis of docosahexaenoic acid correlates with cognitive impairment in Alzheimer's disease.* PLoS One, 2010. **5**(9): p. e12538.

204.   Sanchez-Mejia, R.O., Newman, J. W., Toh, S., Yu, G. Q., Zhou, Y., Halabisky, B., Cisse, M., Scearce-Levie, K., Cheng, I. H., Gan, L., Palop, J. J., Bonventre, J. V., Mucke, L., *Phospholipase A2 reduction ameliorates cognitive deficits in a mouse model of Alzheimer's disease.* Nat Neurosci, 2008. **11**(11): p. 1311-8.

205.   Grimm, M.O., Grimm, H. S., Patzold, A. J., Zinser, E. G., Halonen, R., Duering, M., Tschape, J. A., De Strooper, B., Muller, U., Shen, J., Hartmann, T., *Regulation of cholesterol and sphingomyelin metabolism by amyloid-beta and presenilin.* Nat Cell Biol, 2005. **7**(11): p. 1118-23.

206. Cottet, V., Collin, M., Gross, A. S., Boutron-Ruault, M. C., Morois, S., Clavel-Chapelon, F., Chajes, V., *Erythrocyte membrane phospholipid fatty acid concentrations and risk of colorectal adenomas: a case-control nested in the French E3N-EPIC cohort study.* Cancer Epidemiol Biomarkers Prev, 2013. **22**(8): p. 1417-27.

207. Chavarro, J.E., Kenfield, S. A., Stampfer, M. J., Loda, M., Campos, H., Sesso, H. D., Ma, J., *Blood levels of saturated and monounsaturated fatty acids as markers of de novo lipogenesis and risk of prostate cancer.* Am J Epidemiol, 2013. **178**(8): p. 1246-55.

208. Chajes, V., Thiebaut, A. C., Rotival, M., Gauthier, E., Maillard, V., Boutron-Ruault, M. C., Joulin, V., Lenoir, G. M., Clavel-Chapelon, F., *Association between serum trans-monounsaturated fatty acids and breast cancer risk in the E3N-EPIC Study.* Am J Epidemiol, 2008. **167**(11): p. 1312-20.

209. Pala, V., Krogh, V., Muti, P., Chajes, V., Riboli, E., Micheli, A., Saadatian, M., Sieri, S., Berrino, F., *Erythrocyte membrane fatty acids and subsequent breast cancer: a prospective Italian study.* J Natl Cancer Inst, 2001. **93**(14): p. 1088-95.

210. Wood, C.B. Habib, N. A., Thompson, A., Bradpiece, H., Smadja, C., Hershman, M., Barker, W., Apostolov, K., *Increase of oleic acid in erythrocytes associated with malignancies.* Br Med J (Clin Res Ed), 1985. **291**(6489): p. 163-5.

211. Mohammadzadeh, F., Mosayebi, G., Montazeri, V., Darabi, M., Fayezi, S., Shaaker, M., Rahmati, M., Baradaran, B., Mehdizadeh, A., Darabi, M., *Fatty Acid Composition of Tissue Cultured Breast Carcinoma and the Effect of Stearoyl-CoA Desaturase 1 Inhibition.* J Breast Cancer, 2014. **17**(2): p. 136-42.

212. Scaglia, N., J.M. Caviglia, and R.A. Igal, *High stearoyl-CoA desaturase protein and activity levels in simian virus 40 transformed-human lung fibroblasts.* Biochim Biophys Acta, 2005. **1687**(1-3): p. 141-51.

213. Budhu, A., Roessler, S., Zhao, X., Yu, Z., Forgues, M., Ji, J., Karoly, E., Qin, L. X., Ye, Q. H., Jia, H. L., Fan, J., Sun, H. C., Tang, Z. Y., Wang, X. W., *Integrated metabolite and gene expression profiles identify lipid biomarkers associated with progression of hepatocellular carcinoma and patient outcomes.* Gastroenterology, 2013. **144**(5): p. 1066-1075 e1.

214. Ruggieri, S., R. Roblin, and P.H. Black, *Lipids of whole cells and plasma membrane fractions from Balb/c3T3, SV3T3, and concanavalin A-selected revertant cells.* J Lipid Res, 1979. **20**(6): p. 760-71.

215. Guo, S., Wang, Y., Zhou, D., Li, Z., *Significantly increased monounsaturated lipids relative to polyunsaturated lipids in six types of cancer microenvironment are observed by mass spectrometry imaging.* Sci Rep, 2014. **4**: p. 5959.

216. Yahagi, N., Shimano, H., Hasegawa, K., Ohashi, K., Matsuzaka, T., Najima, Y., Sekiya, M., Tomita, S., Okazaki, H., Tamura, Y., Iizuka, Y., Ohashi, K., Nagai, R., Ishibashi, S., Kadowaki, T., Makuuchi, M., Ohnishi, S., Osuga, J., Yamada, N., *Co-ordinate activation of lipogenic enzymes in hepatocellular carcinoma.* Eur J Cancer, 2005. **41**(9): p. 1316-22.

217. Wang, J., Xu, Y., Zhu, L., Zou, Y., Kong, W., Dong, B., Huang, J., Chen, Y., Xue, W., Huang, Y., Zhang, J., *High Expression of Stearoyl-CoA Desaturase 1 Predicts Poor Prognosis in Patients with Clear-Cell Renal Cell Carcinoma.* PLoS One, 2016. **11**(11): p. e0166231.

218. Holder, A.M., Gonzalez-Angulo, A. M., Chen, H., Akcakanat, A., Do, K. A., Fraser Symmans, W., Pusztai, L., Hortobagyi, G. N., Mills, G. B., Meric-Bernstam, F., *High stearoyl-CoA desaturase 1 expression is associated with shorter survival in breast cancer patients.* Breast Cancer Res Treat, 2013. **137**(1): p. 319-27.

219. Presler, M., Wojtczyk-Miaskowska, A., Schlichtholz, B., Kaluzny, A., Matuszewski, M., Mika, A., Sledzinski, T., Swierczynski, J., *Increased expression of the gene encoding stearoyl-CoA desaturase 1 in human bladder cancer.* Mol Cell Biochem, 2018. **447**(1-2): p. 217-224.

220. Peck, B. and A. Schulze, *Lipid desaturation - the next step in targeting lipogenesis in cancer?* FEBS J, 2016. **283**(15): p. 2767-78.

221. von Roemeling, C.A., Marlow, L. A., Pinkerton, A. B., Crist, A., Miller, J., Tun, H. W., Smallridge, R. C., Copland, J. A., *Aberrant lipid metabolism in anaplastic thyroid carcinoma reveals stearoyl CoA desaturase 1 as a novel therapeutic target.* J Clin Endocrinol Metab, 2015. **100**(5): p. E697-709.

222. Bansal, S., Berk, M., Alkhouri, N., Partrick, D. A., Fung, J. J., Feldstein, A., *Stearoyl-CoA desaturase plays an important role in proliferation and chemoresistance in human hepatocellular carcinoma.* J Surg Res, 2014. **186**(1): p. 29-38.

223. Liu, G., Feng, S., Jia, L., Wang, C., Fu, Y., Luo, Y., et al., *Lung fibroblasts promote metastatic colonization through upregulation of stearoyl-CoA desaturase 1 in tumor cells.* Oncogene, 2018. **37**(11): p. 1519-1533.

224. MacDonald, M.L., van Eck, M., Hildebrand, R. B., Wong, B. W., Bissada, N., Ruddle, P., Kontush, A., Hussein, H., Pouladi, M. A., Chapman, M. J., Fievet, C., van Berkel, T. J., Staels, B., McManus, B. M., Hayden, M. R *Despite antiatherogenic metabolic characteristics, SCD1-deficient mice have increased inflammation and atherosclerosis.* Arterioscler Thromb Vasc Biol, 2009. **29**(3): p. 341-7.

225. James, M.J., R.A. Gibson, and L.G. Cleland, *Dietary polyunsaturated fatty acids and inflammatory mediator production.* Am J Clin Nutr, 2000. **71**(1 Suppl): p. 343S-8S.

226. Calder, P.C., *Polyunsaturated fatty acids and inflammation.* Prostaglandins Leukot Essent Fatty Acids, 2006. **75**(3): p. 197-202.

227. Shi, H., Kokoeva, M. V., Inouye, K., Tzameli, I., Yin, H., Flier, J. S., *TLR4 links innate immunity and fatty acid-induced insulin resistance.* J Clin Invest, 2006. **116**(11): p. 3015-25.

228. Feldstein, A.E., Werneburg, N. W., Canbay, A., Guicciardi, M. E., Bronk, S. F., Rydzewski, R., Burgart, L. J., Gores, G. J., *Free fatty acids promote hepatic lipotoxicity by stimulating TNF-alpha expression via a lysosomal pathway.* Hepatology, 2004. **40**(1): p. 185-94.

229. Kadotani, A., Tsuchiya, Y., Hatakeyama, H., Katagiri, H., Kanzaki, M., *Different impacts of saturated and unsaturated free fatty acids on COX-2 expression in C(2)C(12) myotubes.* Am J Physiol Endocrinol Metab, 2009. **297**(6): p. E1291-303.

230. Nguyen, M.T., Favelyukis, S., Nguyen, A. K., Reichart, D., Scott, P. A., Jenn, A., Liu-Bryan, R., Glass, C. K., Neels, J. G., Olefsky, J. M., *A subpopulation of macrophages infiltrates hypertrophic adipose tissue and is activated by free fatty acids via Toll-like receptors 2 and 4 and JNK-dependent pathways.* J Biol Chem, 2007. **282**(48): p. 35279-92.

231. Rizki, G., Arnaboldi, L., Gabrielli, B., Yan, J., Lee, G. S., Ng, R. K., Turner, S. M., Badger, T. M., Pitas, R. E., Maher, J. J., *Mice fed a lipogenic methionine-choline-deficient diet develop hypermetabolism coincident with hepatic suppression of SCD-1.* J Lipid Res, 2006. **47**(10): p. 2280-90.

232. Li, Z.Z., Berk, M., McIntyre, T. M., Feldstein, A. E., *Hepatic lipid partitioning and liver damage in nonalcoholic fatty liver disease: role of stearoyl-CoA desaturase.* J Biol Chem, 2009. **284**(9): p. 5637-44.

233. Flowers, M.T., Keller, M. P., Choi, Y., Lan, H., Kendziorski, C., Ntambi, J. M., Attie, A. D., *Liver gene expression analysis reveals endoplasmic reticulum stress and metabolic dysfunction in SCD1-deficient mice fed a very low-fat diet.* Physiol Genomics, 2008. **33**(3): p. 361-72.

234. Thorn, K., M. Hovsepyan, and P. Bergsten, *Reduced levels of SCD1 accentuate palmitate-induced stress in insulin-producing beta-cells.* Lipids Health Dis, 2010. **9**: p. 108.

235. Hellemans, K.H., Hannaert, J. C., Denys, B., Steffensen, K. R., Raemdonck, C., Martens, G. A., Van Veldhoven, P. P., Gustafsson, J. A., Pipeleers, D., *Susceptibility of pancreatic beta cells to fatty acids is regulated by LXR/PPARalpha-dependent stearoyl-coenzyme A desaturase.* PLoS One, 2009. **4**(9): p. e7266.

236. Lupi, R., Dotta, F., Marselli, L., Del Guerra, S., Masini, M., Santangelo, C., Patane, G., Boggi, U., Piro, S., Anello, M., Bergamini, E., Mosca, F., Di Mario, U., Del Prato, S., Marchetti, P., *Prolonged exposure to free fatty acids has cytostatic and pro-apoptotic effects on human pancreatic islets: evidence that beta-cell death is caspase mediated, partially dependent on ceramide pathway, and Bcl-2 regulated.* Diabetes, 2002. **51**(5): p. 1437-42.

237. Brown, J.M. and L.L. Rudel, *Stearoyl-coenzyme A desaturase 1 inhibition and the metabolic syndrome: considerations for future drug discovery.* Curr Opin Lipidol, 2010. **21**(3): p. 192-7.

238. Busch, A.K., Gurisik, E., Cordery, D. V., Sudlow, M., Denyer, G. S., Laybutt, D. R., Hughes, W. E., Biden, T. J., *Increased fatty acid desaturation and enhanced expression of stearoyl coenzyme A desaturase protects pancreatic beta-cells from lipoapoptosis.* Diabetes, 2005. **54**(10): p. 2917-24.

239. Maedler, K., Oberholzer, J., Bucher, P., Spinas, G. A., Donath, M. Y., *Monounsaturated fatty acids prevent the deleterious effects of palmitate and high glucose on human pancreatic beta-cell turnover and function.* Diabetes, 2003. **52**(3): p. 726-33.

240. Ntambi, J.M. and M. Miyazaki, *Regulation of stearoyl-CoA desaturases and role in metabolism.* Prog Lipid Res, 2004. **43**(2): p. 91-104.

241. Flowers, M.T. and J.M. Ntambi, *Stearoyl-CoA desaturase and its relation to high-carbohydrate diets and obesity.* Biochim Biophys Acta, 2009. **1791**(2): p. 85-91.

242. Miyazaki, M., Sampath, H., Liu, X., Flowers, M. T., Chu, K., Dobrzyn, A., Ntambi, J. M.., *Stearoyl-CoA desaturase-1 deficiency attenuates obesity and insulin resistance in leptin-resistant obese mice.* Biochem Biophys Res Commun, 2009. **380**(4): p. 818-22.

243. Flowers, J.B., Rabaglia, M. E., Schueler, K. L, Flowers, M. T., Lan, H., Keller, M. P., Ntambi, J. M., *Loss of stearoyl-CoA desaturase-1 improves insulin sensitivity in lean mice but worsens diabetes in leptin-deficient obese mice.* Diabetes, 2007. **56**(5): p. 1228-39.

244. Liu, X., Miyazaki, M., Flowers, M. T., Sampath, H., Zhao, M., Chu, K., Paton, C. M., Joo, D. S., Ntambi, J. M., *Loss of Stearoyl-CoA desaturase-1 attenuates adipocyte inflammation: effects of adipocyte-derived oleate.* Arterioscler Thromb Vasc Biol, 2010. **30**(1): p. 31-8.

245. Menghini, R., Menini, S., Amoruso, R., Fiorentino, L., Casagrande, V., Marzano, V., Tornei, F., Bertucci, P., Iacobini, C., Serino, M., Porzio, O., Hribal, M. L., Folli, F., Khokha, R., Urbani, A., Lauro, R., Pugliese, G., Federici, M., *Tissue inhibitor of metalloproteinase 3 deficiency causes hepatic steatosis and adipose tissue inflammation in mice.* Gastroenterology, 2009. **136**(2): p. 663-72 e4.

246. Petersson, H., Lind, L., Hulthe, J., Elmgren, A., Cederholm, T., Riserus, U., *Relationships between serum fatty acid composition and multiple markers of inflammation and endothelial function in an elderly population.* Atherosclerosis, 2009. **203**(1): p. 298-303.

247. Petersson, H., Basu, S., Cederholm, T., Riserus, U., *Serum fatty acid composition and indices of stearoyl-CoA desaturase activity are associated with systemic inflammation: longitudinal analyses in middle-aged men.* Br J Nutr, 2008. **99**(6): p. 1186-9.

248. Boden, G., *Obesity and free fatty acids.* Endocrinol Metab Clin North Am, 2008. **37**(3): p. 635-46, viii-ix.

249. Kearney, M.T., Duncan, E. R., Kahn, M., Wheatcroft, S. B., *Insulin resistance and endothelial cell dysfunction: studies in mammalian models.* Exp Physiol, 2008. **93**(1): p. 158-63.

250. Cersosimo, E. and R.A. DeFronzo, *Insulin resistance and endothelial dysfunction: the road map to cardiovascular diseases.* Diabetes Metab Res Rev, 2006. **22**(6): p. 423-36.

251.   Bakker, W., Eringa, E. C., Sipkema, P., van Hinsbergh, V. W., *Endothelial dysfunction and diabetes: roles of hyperglycemia, impaired insulin signaling and obesity.* Cell Tissue Res, 2009. **335**(1): p. 165-89.

252.   Duncan, E.R., Crossey, P. A., Walker, S., Anilkumar, N., Poston, L., Douglas, G., Ezzat, V. A., Wheatcroft, S. B., Shah, A. M., Kearney, M., *Effect of endothelium-specific insulin resistance on endothelial function in vivo.* Diabetes, 2008. **57**(12): p. 3307-14.

253.   Peter, A., Weigert, C., Staiger, H., Rittig, K., Cegan, A., Lutz, P., Machicao, F., Haring, H. U., Schleicher, E., *Induction of stearoyl-CoA desaturase protects human arterial endothelial cells against lipotoxicity.* Am J Physiol Endocrinol Metab, 2008. **295**(2): p. E339-49.

254.   Hulver, M.W. Berggren, J. R., Carper, M. J., Miyazaki, M., Ntambi, J. M., Hoffman, E. P., Thyfault, J. P., Stevens, R., Dohm, G. L., Houmard, J. A., *Elevated stearoyl-CoA desaturase-1 expression in skeletal muscle contributes to abnormal fatty acid partitioning in obese humans.* Cell Metab, 2005. **2**(4): p. 251-61.

255.   Schenk, S. and J.F. Horowitz, *Acute exercise increases triglyceride synthesis in skeletal muscle and prevents fatty acid-induced insulin resistance.* J Clin Invest, 2007. **117**(6): p. 1690-8.

256.   Pinnamaneni, S.K., Southgate, R. J., Febbraio, M. A., Watt, M. J., *Stearoyl CoA desaturase 1 is elevated in obesity but protects against fatty acid-induced skeletal muscle insulin resistance in vitro.* Diabetologia, 2006. **49**(12): p. 3027-37.

257.   Peter, A., Weigert, C., Staiger, H., Machicao, F., Schick, F., Machann, J., Stefan, N., Thamer, C, Haring, H. U., Schleicher, E., *Individual stearoyl-coa desaturase 1 expression modulates endoplasmic reticulum stress and inflammation in human myotubes and is associated with skeletal muscle lipid storage and insulin sensitivity in vivo.* Diabetes, 2009. **58**(8): p. 1757-65.

258.   Miyazaki, M. and J.M. Ntambi, *Role of stearoyl-coenzyme A desaturase in lipid metabolism.* Prostaglandins Leukot Essent Fatty Acids, 2003. **68**(2): p. 113-21.

259.   Sampath, H., Flowers, M. T., Liu, X., Paton, C. M., Sullivan, R., Chu, K., Zhao, M., Ntambi, J. M., *Skin-specific deletion of stearoyl-CoA desaturase-1 alters skin lipid composition and protects mice from high fat diet-induced obesity.* J Biol Chem, 2009. **284**(30): p. 19961-73.

260. Zheng, Y. Eilertsen, K. J., Ge, L., Zhang, L., Sundberg, J. P., Prouty, S. M., Stenn, K. S., Parimoo, S., *Scd1 is expressed in sebaceous glands and is disrupted in the asebia mouse.* Nat Genet, 1999. **23**(3): p. 268-70.

261. Chen, C., et Shah, Y. M., Morimura, K., Krausz, K. W., Miyazaki, M., Richardson, T. A., Morgan, E. T., Ntambi, J. M., Idle, J. R., Gonzalez, F. J., *Metabolomics reveals that hepatic stearoyl-CoA desaturase 1 downregulation exacerbates inflammation and acute colitis.* Cell Metab, 2008. **7**(2): p. 135-47.

262. Macdonald, M.L. Bissada, N., Vallance, B. A., Hayden, M. R., *Absence of stearoyl-CoA desaturase-1 does not promote DSS-induced acute colitis.* Biochim Biophys Acta, 2009. **1791**(12): p. 1166-72.

263. Quitterer, U., Pohl, A., Langer, A., Koller, S., Abdalla, S., *A cleavable signal peptide enhances cell surface delivery and heterodimerization of Cerulean-tagged angiotensin II AT1 and bradykinin B2 receptor.* Biochem Biophys Res Commun, 2011. **409**(3): p. 544-9.

264. Son, N.H., Yu, S., Tuinei, J., Arai, K., Hamai, H., Homma, S., Shulman, G. I., Abel, E. D., Goldberg, I. J., *PPARgamma-induced cardiolipotoxicity in mice is ameliorated by PPARalpha deficiency despite increases in fatty acid oxidation.* J Clin Invest, 2010. **120**(10): p. 3443-54.

265. AbdAlla, S., Langer, A., Fu, X., Quitterer, U., *ACE inhibition with captopril retards the development of signs of neurodegeneration in an animal model of Alzheimer's disease.* Int J Mol Sci, 2013. **14**(8): p. 16917-42.

266. Neubauer, S., *The failing heart--an engine out of fuel.* N Engl J Med, 2007. **356**(11): p. 1140-51.

267. Chemaly, E.R., Hadri, L., Zhang, S., Kim, M., Kohlbrenner, E., Sheng, J., Liang, L., Chen, J., K. Raman P, Hajjar, R. J., Lebeche, D., *Long-term in vivo resistin overexpression induces myocardial dysfunction and remodeling in rats.* J Mol Cell Cardiol, 2011. **51**(2): p. 144-55.

268. O'Shea, K.M., Chess, D. J., Khairallah, R. J., Rastogi, S., Hecker, P. A., Sabbah, H. N., Walsh, K., Stanley, W. C., *Effects of adiponectin deficiency on structural and metabolic remodeling in mice subjected to pressure overload.* Am J Physiol Heart Circ Physiol, 2010. **298**(6): p. H1639-45.

269. Frankel, D.S., Vasan, R. S., D'Agostino, R. B., Sr., Benjamin, E. J., Levy, D., Wang, T. J., Meigs, J. B., *Resistin, adiponectin, and risk of heart failure the Framingham offspring study.* J Am Coll Cardiol, 2009. **53**(9): p. 754-62.

270. George, J., Patal, S., Wexler, D., Sharabi, Y., Peleg, E., Kamari, Y., Grossman, E., Sheps, D., Keren, G., Roth, A., *Circulating adiponectin concentrations in patients with congestive heart failure.* Heart, 2006. **92**(10): p. 1420-4.

271. Norman, G., Norton, G. R., Peterson, V., Gomes, M., Libhaber, C. D., Sareli, P., Woodiwiss, A. J., *Associations between circulating resistin concentrations and left ventricular mass are not accounted for by effects on aortic stiffness or renal dysfunction.* BMC Cardiovasc Disord, 2020. **20**(1): p. 35.

272. Razani, B., Zhang, H., Schulze, P. C., Schilling, J. D., Verbsky, J., Lodhi, I. J., Topkara, V. K., Feng, C., Coleman, T., Kovacs, A., Kelly, D. P., Saffitz, J. E., Dorn, G. W., 2nd, Nichols, C. G., Semenkovich, C. F., *Fatty acid synthase modulates homeostatic responses to myocardial stress.* J Biol Chem, 2011. **286**(35): p. 30949-61.

273. Rodriguez-Cuenca, S., Whyte, L., Hagen, R., Vidal-Puig, A, Fuller, M., *Stearoyl-CoA Desaturase 1 Is a Key Determinant of Membrane Lipid Composition in 3T3-L1 Adipocytes.* PLoS One, 2016. **11**(9): p. e0162047.

274. Ainscough, J.F., Drinkhill, M. J., Sedo, A., Turner, N. A., Brooke, D. A., Balmforth, A. J., Ball, S. G., *Angiotensin II type-1 receptor activation in the adult heart causes blood pressure-independent hypertrophy and cardiac dysfunction.* Cardiovasc Res, 2009. **81**(3): p. 592-600.

275. Young, J.B., Dunlap, M. E., Pfeffer, M. A., Probstfield, J. L., Cohen-Solal, A., Dietz, R., Granger, C. B., Hradec, J., Kuch, J., McKelvie, R. S., McMurray, J. J., Michelson, E. L., Olofsson, B., Ostergren, J., Held, P., Solomon, S. D., Yusuf, S., Swedberg, K., Candesartan in Heart Failure Assessment of Reduction in, Mortality, morbidity, Investigators, Committees, *Mortality and morbidity reduction with Candesartan in patients with chronic heart failure and left ventricular systolic dysfunction: results of the CHARM low-left ventricular ejection fraction trials.* Circulation, 2004. **110**(17): p. 2618-26.

276. Rizzo, M.A., Springer, G. H., Granada, B., Piston, D. W., *An improved cyan fluorescent protein variant useful for FRET.* Nat Biotechnol, 2004. **22**(4): p. 445-9.

277. deAlmeida, A.C., R.J. van Oort, and X.H. Wehrens, *Transverse aortic constriction in mice.* J Vis Exp, 2010(38).

278. Burchfield, J.S., M. Xie, and J.A. Hill, *Pathological ventricular remodeling: mechanisms: part 1 of 2.* Circulation, 2013. **128**(4): p. 388-400.

279. Doevendans, P.A., Daemen, M. J., de Muinck, E. D., Smits, J. F., *Cardiovascular phenotyping in mice.* Cardiovasc Res, 1998. **39**(1): p. 34-49.

280. Wang, Y.X., *Cardiovascular functional phenotypes and pharmacological responses in apolipoprotein E deficient mice.* Neurobiol Aging, 2005. **26**(3): p. 309-16.

281. Vasquez, E.C., Peotta, V. A., Gava, A. L., Pereira, T. M., Meyrelles, S. S., *Cardiac and vascular phenotypes in the apolipoprotein E-deficient mouse.* J Biomed Sci, 2012. **19**: p. 22.

282. Singam, N.S.V., C. Fine, and J.L. Fleg, *Cardiac changes associated with vascular aging.* Clin Cardiol, 2020. **43**(2): p. 92-98.

283. Shah, S., Henry, A., Roselli, C., Lin, H., Sveinbjornsson, G., Fatemifar, G., Hedman, A. K., Wilk, J. B., Morley, M. P., Chaffin, M. D., Helgadottir, A., Verweij, N., Dehghan, A., Almgren, P., Andersson, C., Aragam, K. G., Arnlov, J., Backman, J. D., Biggs, M. L., Bloom, H. L., Brandimarto, J., Brown, M. R., Buckbinder, L., Carey, D. J., Chasman, D. I., Chen, X., Chen, X., Chung, J., Chutkow, W. et al., *Genome-wide association and Mendelian randomisation analysis provide insights into the pathogenesis of heart failure.* Nat Commun, 2020. **11**(1): p. 163.

284. Arnold, S.V., Inzucchi, S. E., Echouffo-Tcheugui, J. B., Tang, F., Lam, C. S. P., Sperling, L. S., Kosiborod, M.., *Understanding Contemporary Use of Thiazolidinediones.* Circ Heart Fail, 2019. **12**(6): p. e005855.

285. Kalliora, C., Kyriazis, I. D., Oka, S. I., Lieu, M. J., Yue, Y., Area-Gomez, E., Pol, C. J., Tian, Y., Mizushima, W., Chin, A., Scerbo, D., Schulze, P. C., Civelek, M., Sadoshima, J., Madesh, M., Goldberg, I. J., Drosatos, K., *Dual peroxisome-proliferator-activated-receptor-alpha/gamma activation inhibits SIRT1-PGC1alpha axis and causes cardiac dysfunction.* JCI Insight, 2019. **5**.

286. Goldberg, I.J., Reue, K., Abumrad, N. A., Bickel, P. E., Cohen, S., Fisher, E. A., Galis, Z. S., Granneman, J. G., Lewandowski, E. D., Murphy, R., Olive, M., Schaffer, J. E., Schwartz-Longacre, L., Shulman, G. I., Walther, T. C., Chen, J., *Deciphering the Role of*

Lipid Droplets in Cardiovascular Disease: A Report From the 2017 National Heart, Lung, and Blood Institute Workshop. Circulation, 2018. **138**(3): p. 305-315.

287.   Cheng, L., Ding, G., Qin, Q., Huang, Y., Lewis, W., He, N., Evans, R. M., Schneider, M. D., Brako, F. A., Xiao, Y., Chen, Y. E., Yang, Q., *Cardiomyocyte-restricted peroxisome proliferator-activated receptor-delta deletion perturbs myocardial fatty acid oxidation and leads to cardiomyopathy.* Nat Med, 2004. **10**(11): p. 1245-50.

288.   Chiu, H.C., Kovacs, A., Ford, D. A., Hsu, F. F., Garcia, R., Herrero, P., Saffitz, J. E., Schaffer, J. E.., *A novel mouse model of lipotoxic cardiomyopathy.* J Clin Invest, 2001. **107**(7): p. 813-22.

289.   de Vries, J.E., Vork, M. M., Roemen, T. H., de Jong, Y. F., Cleutjens, J. P., van der Vusse, G. J. van Bilsen, M., *Saturated but not mono-unsaturated fatty acids induce apoptotic cell death in neonatal rat ventricular myocytes.* J Lipid Res, 1997. **38**(7): p. 1384-94.

290.   Dyntar, D., Eppenberger-Eberhardt, M., Maedler, K., Pruschy, M., Eppenberger, H. M., Spinas, G. A., Donath, M. Y., *Glucose and palmitic acid induce degeneration of myofibrils and modulate apoptosis in rat adult cardiomyocytes.* Diabetes, 2001. **50**(9): p. 2105-13.

291.   Park, T.S., Hu, Y., Noh, H. L., Drosatos, K., Okajima, K., Buchanan, J., Tuinei, J., Homma, S., Jiang, X. C., Abel, E. D., Goldberg, I. J., *Ceramide is a cardiotoxin in lipotoxic cardiomyopathy.* J Lipid Res, 2008. **49**(10): p. 2101-12.

292.   Piccinin, E., Cariello, M., De Santis, S., Ducheix, S., Sabba, C., Ntambi, J. M., Moschetta, A., *Role of Oleic Acid in the Gut-Liver Axis: From Diet to the Regulation of Its Synthesis via Stearoyl-CoA Desaturase 1 (SCD1).* Nutrients, 2019. **11**(10).

293.   Dobrzyn, P., Dobrzyn, A., Miyazaki, M., Ntambi, J. M.., *Loss of stearoyl-CoA desaturase 1 rescues cardiac function in obese leptin-deficient mice.* J Lipid Res, 2010. **51**(8): p. 2202-10.

294.   Mitchell, D.C., *Progress in understanding the role of lipids in membrane protein folding.* Biochim Biophys Acta, 2012. **1818**(4): p. 951-6.

295.   Drosatos, K., Bharadwaj, K. G., Lymperopoulos, A., Ikeda, S., Khan, R., Hu, Y., Agarwal, R., Yu, S., Jiang, H., Steinberg, S. F., Blaner, W. S., Koch, W. J., Goldberg, I. J., *Cardiomyocyte lipids impair beta-adrenergic receptor function via PKC activation.* Am J Physiol Endocrinol Metab, 2011. **300**(3): p. E489-99.

296. Kaprielian, R.R., Dupont, E., Hafizi, S., Poole-Wilson, P. A., Khaghani, A., Yacoub, M. H., Severs, N. J., *Angiotensin II receptor type 1 mRNA is upregulated in atria of patients with end-stage heart failure.* J Mol Cell Cardiol, 1997. **29**(8): p. 2299-304.

297. Reuter, H., Adam, C., Gronke, S., Zobel, C., Frank, K. F., Muller-Ehmsen, J., Brabender, J., Schwinger, R. H., *The increased angiotensin II (type 1) receptor density in myocardium of type 2 diabetic patients is prevented by blockade of the renin-angiotensin system.* Diabetologia, 2006. **49**(12): p. 3067-74.

298. Miki, T., Yuda, S., Kouzu, H., Miura, T., *Diabetic cardiomyopathy: pathophysiology and clinical features.* Heart Fail Rev, 2013. **18**(2): p. 149-66.

299. Qureshi, W., Santaren, I. D., Hanley, A. J., Watkins, S. M., Lorenzo, C., Wagenknecht, L. E., *Risk of diabetes associated with fatty acids in the de novo lipogenesis pathway is independent of insulin sensitivity and response: the Insulin Resistance Atherosclerosis Study (IRAS).* BMJ Open Diabetes Res Care, 2019. **7**(1): p. e000691.

300. Regitz-Zagrosek, V., Friedel, N., Heymann, A., Bauer, P., Neuss, M., Rolfs, A., Steffen, C., Hildebrandt, A., Hetzer, R., Fleck, E, *Regulation, chamber localization, and subtype distribution of angiotensin II receptors in human hearts.* Circulation, 1995. **91**(5): p. 1461-71.

301. Hartupee, J. and D.L. Mann, *Neurohormonal activation in heart failure with reduced ejection fraction.* Nat Rev Cardiol, 2017. **14**(1): p. 30-38.

302. Swedberg, K., Eneroth, P., Kjekshus, J., Wilhelmsen, L., *Hormones regulating cardiovascular function in patients with severe congestive heart failure and their relation to mortality. CONSENSUS Trial Study Group.* Circulation, 1990. **82**(5): p. 1730-6.

303. Antony, N., Weir, J. R., McDougall, A. R., Mantamadiotis, T., Meikle, P. J., Cole, T. J., Bird, A. D., *cAMP response element binding protein1 is essential for activation of steroyl co-enzyme a desaturase 1 (Scd1) in mouse lung type II epithelial cells.* PLoS One, 2013. **8**(4): p. e59763.

304. Mougenot, N., Mika, D., Czibik, G., Marcos, E., Abid, S., Houssaini, A., Vallin, B., Guellich, A., Mehel, H., Sawaki, D., Vandecasteele, G., Fischmeister, R., Hajjar, R. J., Dubois-Rande, J. L., Limon, I., Adnot, S., Derumeaux, G., Lipskaia, L., *Cardiac adenylyl*

cyclase overexpression precipitates and aggravates age-related myocardial dysfunction. Cardiovasc Res, 2019. **115**(12): p. 1778-1790.

305.   Pinilla-Vera, M., V.S. Hahn, and D.A. Kass, *Leveraging Signaling Pathways to Treat Heart Failure With Reduced Ejection Fraction.* Circ Res, 2019. **124**(11): p. 1618-1632.

306.   Chruscinski, A.J., Singh, H., Chan, S. M., Utz, P. J., *Broad-scale phosphoprotein profiling of beta adrenergic receptor (beta-AR) signaling reveals novel phosphorylation and dephosphorylation events.* PLoS One, 2013. **8**(12): p. e82164.

307.   Steffen, B.T., Duprez, D., Szklo, M., Guan, W., Tsai, M. Y., *Circulating oleic acid levels are related to greater risks of cardiovascular events and all-cause mortality: The Multi-Ethnic Study of Atherosclerosis.* J Clin Lipidol, 2018. **12**(6): p. 1404-1412.

308.   Pfleger, J. Gross, P., Johnson, J., Carter, R. L., Gao, E., Tilley, D. G., Houser, S. R., Koch, W. J., *G protein-coupled receptor kinase 2 contributes to impaired fatty acid metabolism in the failing heart.* J Mol Cell Cardiol, 2018. **123**: p. 108-117.

309.   Murga, C., Arcones, A. C., Cruces-Sande, M., Briones, A. M., Salaices, M., Mayor, F., Jr., *G Protein-Coupled Receptor Kinase 2 (GRK2) as a Potential Therapeutic Target in Cardiovascular and Metabolic Diseases.* Front Pharmacol, 2019. **10**: p. 112.

14. APPENDIX

14.1. Oligonucleotides used for cloning of the alpha-MHC-promoter-SCD1 plasmid

```
SCD1-forward: 5'- TAC GTC GAC ACC ATG CCG GCC CAC TTG CTG CAG GAC -3'
SCD1-reverse: 5'- A TAC AAG CTT TCA GCC ACT CTT GTA GTT TCC ATC TC -3'
```

14.2. DNA sequencing data of the alpha-MHC-promoter-SCD1 plasmid

Sequencing data part 1: SalI site and startcodon of SCD1

```
NCTCTATCTCCNNANAAGAGTTTGAGTCGACACCATGCCGGCCCACTTGCTGCAGGACGATATCTCTAGCTCCTATACCACCA
CCACCACCATTACAGCGCCTCCCTCCAGGGTCCTGCAGAATGGAGGAGATAAGTTGGAGACGATGCCCCTCTACTTGGAAGAC
GACATTCGCCCTGATATAAAAGATGATATATATGACCCCACCTACAAGGATAAGGAAGGCCCAAGCCCCAAGGTTGAATATGT
CTGGAGAAACATCATCCTTATGTCTCTGCTACACTTGGGAGCCCTGTATGGGATCACTTTGATTCCTACCTGCAAGTTCTACA
CCTGGCTTTGGGGGGTATTCTACTATTTTGTCAGTGCCCTGGGCATAACAGCAGGAGCTCATCGTCTGTGGAGCCACCGCTCT
TACAAAGCTCGGCTGCCCCTACGGCTCTTTCTGATCATTGCCAACACAATGGCATTCCAGAATGATGTCTATGAATGGGCTCG
TGACCACCGTGCCCACCACAAGTTTTCAGAAACACATGCTGATCCTCATAATTCCCGACGTGGCTTTTTCTTCTCACGTGG
GTTGGCTGCTTGTGCGCAAACACCCAGCTGTCAAAGAGAAGGGGAGTACGCTAGACTTGTCTGACCTAGAAGCTGAGAAACTG
GTGATGTTCCAGAGGAGGTACTACAAACCTGGCTTGCTGCTGATGTGCTTCATCCTGCCCACGCTTGTGCCCTGGTATTTCTG
GGGTGAAACTTTTCAAAACAGTGTGTTCGTTGCCACTTTCTTGCGATATGCTGTGGTGCTTAATGCCACCTGGCTGGTGAACA
GTGCTGCCCACCTCTTCGGATATCGTCCTTATGACAAGAACATTAGCCNCCGGGAGAATATCCTGGTTTCACTTGGAGCTGTG
GGTGAGGGCTTCCACAACTACCACCACTCCTTTCCCTATGACTACTCTGCCAGTGAGTACCGCTGGCACATCAACTTCACCAC
ATTCTTCATTGATTGC
```

ATG: **Startcodon of SCD1**

SalI: GTCGAC

```
Query   6068    CTATCTCCCCCATAAGAGTTTGAGTCGACACCATGCCGGCCCACTTGCTGCAGGACGATA    6127
                ||||||  ||    |  |||||||||||||||||||||||||||||||||||||||||||
Sbjct   4       CTATCT-CCNNANAAGAGTTTGAGTCGACACCATGCCGGCCCACTTGCTGCAGGACGATA    62

Query   6128    TCTCTAGCTCCTATACCACCACCACCACCATTACAGCGCCTCCCTCCAGGGTCCTGCAGA    6187
                ||||||||||||||||||||||||||||||||||||||||||||||||||||||||||||
Sbjct   63      TCTCTAGCTCCTATACCACCACCACCACCATTACAGCGCCTCCCTCCAGGGTCCTGCAGA    122

Query   6188    ATGGAGGAGATAAGTTGGAGACGATGCCCCTCTACTTGGAAGACGACATTCGCCCTGATA    6247
                ||||||||||||||||||||||||||||||||||||||||||||||||||||||||||||
Sbjct   123     ATGGAGGAGATAAGTTGGAGACGATGCCCCTCTACTTGGAAGACGACATTCGCCCTGATA    182

Query   6248    TAAAAGATGATATATATGACCCCACCTACAAGGATAAGGAAGGCCCAAGCCCCAAGGTTG    6307
                ||||||||||||||||||||||||||||||||||||||||||||||||||||||||||||
Sbjct   183     TAAAAGATGATATATATGACCCCACCTACAAGGATAAGGAAGGCCCAAGCCCCAAGGTTG    242

Query   6308    AATATGTCTGGAGAAACATCATCCTTATGTCTCTGCTACACTTGGGAGCCCTGTATGGGA    6367
                ||||||||||||||||||||||||||||||||||||||||||||||||||||||||||||
Sbjct   243     AATATGTCTGGAGAAACATCATCCTTATGTCTCTGCTACACTTGGGAGCCCTGTATGGGA    302

Query   6368    TCACTTTGATTCCTACCTGCAAGTTCTACACCTGGCTTTGGGGGGTATTCTACTATTTTG    6427
                ||||||||||||||||||||||||||||||||||||||||||||||||||||||||||||
Sbjct   303     TCACTTTGATTCCTACCTGCAAGTTCTACACCTGGCTTTGGGGGGTATTCTACTATTTTG    362

Query   6428    TCAGTGCCCTGGGCATAACAGCAGGAGCTCATCGTCTGTGGAGCCACCGCTCTTACAAAG    6487
                ||||||||||||||||||||||||||||||||||||||||||||||||||||||||||||
Sbjct   363     TCAGTGCCCTGGGCATAACAGCAGGAGCTCATCGTCTGTGGAGCCACCGCTCTTACAAAG    422

Query   6488    CTCGGCTGCCCCTACGGCTCTTTCTGATCATTGCCAACACAATGGCATTCCAGAATGATG    6547
                ||||||||||||||||||||||||||||||||||||||||||||||||||||||||||||
Sbjct   423     CTCGGCTGCCCCTACGGCTCTTTCTGATCATTGCCAACACAATGGCATTCCAGAATGATG    482
```

```
Query  6548   TCTATGAATGGGCTCGTGACCACCGTGCCCACCACAAGTTTTCAGAAACACATGCTGATC   6607
               ||||||||||||||||||||||||||||||||||||||||||||||||||||||||||||
Sbjct  483    TCTATGAATGGGCTCGTGACCACCGTGCCCACCACAAGTTTTCAGAAACACATGCTGATC   542

Query  6608   CTCATAATTCCCGACGTGGCTTTTTCTTCTCTCACGTGGGTTGGCTGCTTGTGCGCAAAC   6667
               ||||||||||||||||||||||||||||||||||||||||||||||||||||||||||||
Sbjct  543    CTCATAATTCCCGACGTGGCTTTTTCTTCTCTCACGTGGGTTGGCTGCTTGTGCGCAAAC   602

Query  6668   ACCCAGCTGTCAAAGAGAAGGGGAGTACGCTAGACTTGTCTGACCTAGAAGCTGAGAAAC   6727
               ||||||||||||||||||||||||||||||||||||||||||||||||||||||||||||
Sbjct  603    ACCCAGCTGTCAAAGAGAAGGGGAGTACGCTAGACTTGTCTGACCTAGAAGCTGAGAAAC   662

Query  6728   TGGTGATGTTCCAGAGGAGGTACTACAAACCTGGCTTGCTGCTGATGTGCTTCATCCTGC   6787
               ||||||||||||||||||||||||||||||||||||||||||||||||||||||||||||
Sbjct  663    TGGTGATGTTCCAGAGGAGGTACTACAAACCTGGCTTGCTGCTGATGTGCTTCATCCTGC   722

Query  6788   CCACGCTTGTGCCCTGGTATTTCTGGGGTGAAACTTTTCAAAACAGTGTGTTCGTTGCCA   6847
               ||||||||||||||||||||||||||||||||||||||||||||||||||||||||||||
Sbjct  723    CCACGCTTGTGCCCTGGTATTTCTGGGGTGAAACTTTTCAAAACAGTGTGTTCGTTGCCA   782

Query  6848   CTTTCTTGCGATATGCTGTGGTGCTTAATGCCACCTGGCTGGTGAACAGTGCTGCCCACC   6907
               ||||||||||||||||||||||||||||||||||||||||||||||||||||||||||||
Sbjct  783    CTTTCTTGCGATATGCTGTGGTGCTTAATGCCACCTGGCTGGTGAACAGTGCTGCCCACC   842

Query  6908   TCTTCGGATATCGTCCTTATGACAAGAACATTAGCCCCCGGGAGAATATCCTGGTTTCAC   6967
               ||||||||||||||||||||||||||||||||||||||||||||||||||||||||||||
Sbjct  843    TCTTCGGATATCGTCCTTATGACAAGAACATTAGCCCCCGGGAGAATATCCTGGTTTCAC   902

Query  6968   TTGGAGCTGTGGGTGAGGGCTTCCACAACTACCACCACTCCTTTCCCTATGACTACTCTG   7027
               ||||||||||||||||||||||||||||||||||||||||||||||||||||||||||||
Sbjct  903    TTGGAGCTGTGGGTGAGGGCTTCCACAACTACCACCACTCCTTTCCCTATGACTACTCTG   962

Query  7028   CCAGTGAGTACCGCTGGCACATCAACTTCACCACATTCTTCATTGATTGC   7077
               ||||||||||||||||||||||||||||||||||||||||||||||||||
Sbjct  963    CCAGTGAGTACCGCTGGCACATCAACTTCACCACATTCTTCATTGATTGC   1012
```

Sequencing data part 2: HindIII site and Stopcodon of SCD1
GGGNNANAGGGNTGCCACCCATC<mark>AAGCTT</mark>**TCA**GCCACTCTTGTAGTTTCCATCTCCGGTTCTTTTAATCCTGGCCAAGATGGC
GGCCTTGGAGACTTTCTTCCGGTCATAGGCCAGACCGAGGGCGGCCATGCAATCAATGAAGAATGTGGTGAAGTTGATGTGCC
AGCGGTACTCACTGGCAGAGTAGTCATAGGGAAAGGAGTGGTGGTAGTTGTGGAAGCCCTCACCCACAGCTCCAAGTGAAACC
AGGATATTCTCCCGGGGGCTAATGTTCTTGTCATAAGGACGATATCCGAAGAGGTGGGCAGCACTGTTCACCAGCCAGGTGGC
ATTAAGCACCACAGCATATCGCAAGAAAGTGGCAACGAACACACTGTTTTGAAAAGTTTCACCCCAGAAATACCAGGGCACAA
GCGTGGGCAGGATGAAGCACATCAGCAGCAAGCCAGGTTTGTAGTACCTCCTCTGGAACATCACCAGTTTCTCAGCTTCTAGG
TCAGACAAGTCTAGCGTACTCCCCTTCTCTTTGACAGCTGGGTGTTTGCGCACAAGCAGCCAACCCACGTGAGAGAAGAAAAA
GCCACGTCGGGAATTATGAGGATCAGCATGTGTTTCTGAAAACTTGTGGTGGGCACGGTGGTCACGAGCCCATTCATAGACAT
CATTCTGGAATGCCATTGTGTTGGCAATGATCAGAAAGAGCCGTAGGGGCAGCCGAGCTTTGTAAGAGCGGTGGCTCCACAGA
CGATGAGCTCCTGCTGTTATGCCCAGGGCACTGACAAAATAGTAGAATACCCCCCAAAGCCAGGTGTAGAACTTGCAGGTAGG
AATCAAAGTGATCCCATACAGGGCTCCCAAGTGTAGCAGANACATAAGGATGATGTTTCTCCAGACATATTCAACCTTGGGGC
TTGGGCCTTCCTTATCCTTGTAGGTGGGGTCATANANATCATCTTTTNNNTCAGGGCGAATGTCNNCTTCCAAGTANAGGGGC
ATCGNCNCCAACTTAT

TGA: Stopcodon of SCD1

HindIII: <mark>AAGCTT</mark>

```
Query  6257   ATATATATGACCCCACCTACAAGGATAAGGAAGGCCCAAGCCCCAAGGTTGAATATGTCT   6316
               ||  ||||||||||||||||||||||||||||||||||||||||||||||||||||||||
Sbjct  952    ATATATATGACCCCACCTACAAGGATAAGGAAGGCCCAAGCCCCAAGGTTGAATATGTCT   893

Query  6317   GGAGAAACATCATCCTTATGTCTCTGCTACACTTGGGAGCCCTGTATGGGATCACTTTGA   6376
               ||||||||||||||||||||||||||||||||||||||||||||||||||||||||||||
Sbjct  892    GGAGAAACATCATCCTTATGTATCTGCTACACTTGGGAGCCCTGTATGGGATCACTTTGA   833
```

```
Query  6377  TTCCTACCTGCAAGTTCTACACCTGGCTTTGGGGGGTATTCTACTATTTTGTCAGTGCCC  6436
             ||||||||||||||||||||||||||||||||||||||||||||||||||||||||||||
Sbjct  832   TTCCTACCTGCAAGTTCTACACCTGGCTTTGGGGGGTATTCTACTATTTTGTCAGTGCCC  773


Query  6437  TGGGCATAACAGCAGGAGCTCATCGTCTGTGGAGCCACCGCTCTTACAAAGCTCGGCTGC  6496
             ||||||||||||||||||||||||||||||||||||||||||||||||||||||||||||
Sbjct  772   TGGGCATAACAGCAGGAGCTCATCGTCTGTGGAGCCACCGCTCTTACAAAGCTCGGCTGC  713

Query  6497  CCCTACGGCTCTTTCTGATCATTGCCAACACAATGGCATTCCAGAATGATGTCTATGAAT  6556
             ||||||||||||||||||||||||||||||||||||||||||||||||||||||||||||
Sbjct  712   CCCTACGGCTCTTTCTGATCATTGCCAACACAATGGCATTCCAGAATGATGTCTATGAAT  653

Query  6557  GGGCTCGTGACCACCGTGCCCACCACAAGTTTTCAGAAACACATGCTGATCCTCATAATT  6616
             ||||||||||||||||||||||||||||||||||||||||||||||||||||||||||||
Sbjct  652   GGGCTCGTGACCACCGTGCCCACCACAAGTTTTCAGAAACACATGCTGATCCTCATAATT  593

Query  6617  CCCGACGTGGCTTTTTCTTCTCACGTGGGTTGGCTGCTTGTGCGCAAACACCCAGCTG  6676
             ||||||||||||||||||||||||||||||||||||||||||||||||||||||||||||
Sbjct  592   CCCGACGTGGCTTTTTCTTCTCACGTGGGTTGGCTGCTTGTGCGCAAACACCCAGCTG  533

Query  6677  TCAAAGAGAAGGGGAGTACGCTAGACTTGTCTGACCTAGAAGCTGAGAAACTGGTGATGT  6736
             ||||||||||||||||||||||||||||||||||||||||||||||||||||||||||||
Sbjct  532   TCAAAGAGAAGGGGAGTACGCTAGACTTGTCTGACCTAGAAGCTGAGAAACTGGTGATGT  473

Query  6737  TCCAGAGGAGGTACTACAAACCTGGCTTGCTGCTGATGTGCTTCATCCTGCCCACGCTTG  6796
             ||||||||||||||||||||||||||||||||||||||||||||||||||||||||||||
Sbjct  472   TCCAGAGGAGGTACTACAAACCTGGCTTGCTGCTGATGTGCTTCATCCTGCCCACGCTTG  413

Query  6797  TGCCCTGGTATTTCTGGGGTGAAACTTTTCAAAACAGTGTGTTCGTTGCCACTTTCTTGC  6856
             ||||||||||||||||||||||||||||||||||||||||||||||||||||||||||||
Sbjct  412   TGCCCTGGTATTTCTGGGGTGAAACTTTTCAAAACAGTGTGTTCGTTGCCACTTTCTTGC  353

Query  6857  GATATGCTGTGGTGCTTAATGCCACCTGGCTGGTGAACAGTGCTGCCCACCTCTTCGGAT  6916
             ||||||||||||||||||||||||||||||||||||||||||||||||||||||||||||
Sbjct  352   GATATGCTGTGGTGCTTAATGCCACCTGGCTGGTGAACAGTGCTGCCCACCTCTTCGGAT  293

Query  6917  ATCGTCCTTATGACAAGAACATTAGCCCCCGGGAGAATATCCTGGTTTCACTTGGAGCTG  6976
             ||||||||||||||||||||||||||||||||||||||||||||||||||||||||||||
Sbjct  292   ATCGTCCTTATGACAAGAACATTAGCCCCCGGGAGAATATCCTGGTTTCACTTGGAGCTG  233

Query  6977  TGGGTGAGGGCTTCCACAACTACCACCACTCCTTTCCCTATGACTACTCTGCCAGTGAGT  7036
             ||||||||||||||||||||||||||||||||||||||||||||||||||||||||||||
Sbjct  232   TGGGTGAGGGCTTCCACAACTACCACCACTCCTTTCCCTATGACTACTCTGCCAGTGAGT  173

Query  7037  ACCGCTGGCACATCAACTTCACCACATTCTTCATTGATTGCATGGCCGCCCTCGGTCTGG  7096
             ||||||||||||||||||||||||||||||||||||||||||||||||||||||||||||
Sbjct  172   ACCGCTGGCACATCAACTTCACCACATTCTTCATTGATTGCATGGCCGCCCTCGGTCTGG  113

Query  7097  CCTATGACCGGAAGAAAGTCTCCAAGGCCGCCATCTTGGCCAGGATTAAAAGAACCGGAG  7156
             ||||||||||||||||||||||||||||||||||||||||||||||||||||||||||||
Sbjct  112   CCTATGACCGGAAGAAAGTCTCCAAGGCCGCCATCTTGGCCAGGATTAAAAGAACCGGAG  53

Query  7157  ATGGAAACTACAAGAGTGGC**TGA**AAGCTTGATGGGTGGCATCCCT  7201
             ||||||||||||||||||||||||||||||||||||||||||| ||||
Sbjct  52    ATGGAAACTACAAGAGTGGC**TGA**AAGCTTGATGGGTGGCANCCCT  8
```

156

14.3. Supplemental Table

List of probe sets detecting up-regulated genes of the cardiac lipid metabolic process of different models of heart failure. Probe set intensities of up-regulated genes of the cardiac lipid metabolic process are shown of six-month-old, male Apoe-/- mice with heart failure triggered by two months of pressure overload imposed by abdominal aortic constriction (AAC-Apoe-/-1; AAC-Apoe-/-2). Age-matched (6-month-old), sham-operated Apoe-/- mice (Apoe-/-sham1; Apoe-/-sham2) served as controls, and 6-month-old B6 mice (B6-1; B6-2) are shown for comparison. In the second model, heart failure was induced by aortic coarctation induced by atherosclerosis of 18-month-old Apoe-/- mice (Apoe-/-18mo1; Apoe-18mo2). Age-matched, male B6 mice (B6-18mo1; B6-18mo2) were used as controls. In the third model, heart failure of Apoe-/- mice was induced by *Pparg* activation (2 months of rosiglitazone treatment: Rosiglit-1; Rosiglit-2). Age-matched (8-month-old), untreated male Apoe$^{-/-}$ mice (Apoe-/-8mo1; Apoe-/-8mo2) were used as controls, and age-matched, untreated, male B6 mice (B6-8mo1; B6-8mo2) are shown for comparison. In the fourth model, heart failure of 10-month-old, male B6 mice was induced by pressure overload imposed by 6 months of AAC (AAC-6mo1; AAC-6mo2). Age-matched (10-month-old) sham-operated B6 mice (Sham-6mo1; Sham-6mo2) served as controls. Two gene chips are shown for each group (four individuals/gene chip). Probe sets of the lipid metabolic process (GO analysis) are marked in red, which were significantly up-regulated (-fold change ≥2; $p ≤ 0.01$; just alpha; unpaired, two-tailed t-test) in hearts of the different heart failure models. As a control of *Apoe* deficiency of *Apoe-/-* mice, the probe set detecting *Apoe* is also shown. Two-fold difference was not reached of probe set intensities detecting *Scd2*, *Elovl3* and *Tmem195* (AAC-Apoe-/- vs. Sham Apoe-/-), *Scd2*, *Acaca*, and *Cidea* (Apoe-/-18mo vs. B6-18mo) and *Acly* (AAC-B6 vs. Sham B6).

Heart Failure induced by:

Affymetrix ID	Gene	Pressure overload (Apoe-/-)						Atherosclerosis (aged Apoe-/-)				Pparg activation (Apoe-/-)						Pressure overload (B6)			
		AAC Apoe-/-1	AAC Apoe-/-2	Apoe-/- sham1	Apoe-/- sham2	B6-1	B6-2	Apoe-/- 18mo1	Apoe-/- 18mo2	B6 18mo1	B6 18mo2	Rosiglit-1	Rosiglit-2	Apoe-/- 8mo1	Apoe-/- 8mo2	B6 8mo1	B6 8mo2	AAC 10mo1	AAC 10mo2	Sham 10mo1	Sham 10mo2
1423828_at	Fasn	3458.4	3555.6	554.4	570.2	540.8	639.6	4071.6	4039.9	725.1	759	2058.5	2008	576.4	583.6	747.3	771.3	4586.4	4420.4	708.3	824.1
1415964_at	Scd1	10213.2	9825.8	807.8	841.9	972	1069.8	8648	9007.8	1002.3	1083.6	4657.8	4933.8	642.3	618.7	955.6	1063.9	9983.6	9823.4	817.6	804.5
1415965_at	Scd1	782.6	776.4	49	55.9	73.3	80.8	437.5	427.8	26.8	48.2	272	319.7	82.4	49.7	56.1	86.4	627.1	533.8	59.7	38.7
1415823_at	Scd2	280.9	237.6	175.6	147	107.4	128.3	200.6	176	98.4	100.1	438.2	424.1	172.7	164.8	121.3	151	353.1	247.8	109.7	93.7
1420722_at	Elovl3	54.2	50.4	38.1	52.9	66.9	34.7	348	337.4	57.9	76.2	805.9	828.2	98.8	83.2	61.5	23.5	143	130.2	34.2	45.3
1417403_at	Elovl6	173.9	160.2	17.9	24.7	49.7	52.1	188.3	172.5	25.3	34.5	102.5	124.1	34.1	64	37.6	63.3	243.8	237.1	53.2	37.2
1417404_at	Elovl6	278.2	260.9	63.7	11.2	59	58.4	393.5	396.4	57.2	67.7	143.6	174.1	30	33.3	33.7	29.3	439.3	537.2	62.1	66.8
1416316_at	Slc27a2	140.7	142.6	36.1	4.9	34.1	5.9	214.1	218.5	15.5	30.4	515.7	471.8	47.9	34.9	11	12.3	236.8	217.5	11.9	13.8
1423439_at	Pck1	637.6	669.7	32.9	19.5	42.8	60.4	928	880.1	43.9	34.8	1510.3	1480.8	3.6	1.7	54.2	32.1	1260.7	1254.5	41.6	51.6
1439617_s_at	Pck1	229.2	199.4	55.2	27.4	45.4	35	222.9	198.6	20.3	18.2	585.3	578.1	54.2	49.5	63.3	40.3	360.7	434.8	42.5	27.4
1434185_at	Acaca	866.1	773.5	422.8	324.2	339.1	289.6	788.5	794.4	437.1	368.4	623.7	606.3	275.3	234.7	246.8	270.1	876.9	892.8	398.4	406.2
1434191_at	Tmem195	237.5	268.8	158.8	152.5	83	93.7	330.2	342.3	114.8	132.1	330.1	361.2	164.4	143.6	110.4	150.4	351.2	375.2	100	125.5
1428190_at	Ctp	781.2	736.3	249.3	239.6	254.1	274.4	1301.6	1326.9	268.5	274.5	579.8	615.1	227.5	253.5	273.2	353.5	793.9	767.8	368	308.8
1417561_at	Apoc1	373.5	317.3	48.5	51.2	65.4	42.2	8668.9	8732.1	44.1	33.9	422.3	478.6	78	60	65.3	74.7	621.3	670.6	42.1	22.8
1417956_at	Cidea	3022.8	2855.2	1390.5	1402.6	1448.1	1467.3	2107.6	2054.1	1281.7	1284.7	5925	6227.2	1573	1526.8	1477.3	1473.6	5317.7	5004.8	1214.8	1299.8
1452260_at	Cidec	694.9	684.4	51.6	56.9	65.1	29.4	261.4	268.1	46.5	26.4	1228.1	1179.3	24.4	24.8	58.9	64.4	825.7	754.4	64.5	26.5
1418190_at	Pon1	237.7	214.4	64.2	63.6	61.3	26.5	672.7	656.8	53.1	55.2	95.1	74.5	18.7	5.1	66.1	49.4	700.6	688	30	45
1418197_at	Ucp1	282.2	269.4	14.5	9	31.8	40.3	2406.7	2294	27.4	9.5	8104.9	8647.6	5.2	7.8	62	11.1	6319.5	6405.9	16.3	26.5
1424451_at	Acaa1b	46.6	65.5	9	16.5	37.7	8.8	10754	11163.6	28.2	3.3	1278.8	1181.4	12.3	31.1	36.3	21	242.3	198.9	17.4	1
1439459_x_at	Acly	1294.4	1319.7	591.9	570.5	650.6	662.8	1845.4	1664	781.5	825.6	979.5	892.5	439.4	419.2	690.3	637.7	1408.2	1353.5	846.4	768.2
1416468_at	Aldh1a1	2068.2	2037.3	785.3	797.3	768.4	734	7659.1	7861.8	571.1	705.7	1778.1	1807.1	816.7	798.7	780.7	740.8	2516.5	2394.5	699.3	688.5
1418601_at	Aldh1a7	191.2	187.4	48.6	53.7	37.4	54.9	2592.4	2578.4	51.9	23.7	270.2	252	19.4	43.7	33.7	39.4	387.9	435.9	45.2	63.8
1426225_at	Rbp4	327.1	272.7	65.9	53.7	42.8	63.3	3135.1	3412.6	127	63.4	134.1	145.1	67.5	23.9	43.5	89.8	744.6	828.3	48.9	70.4
1422651_at	Adipoq	4490.1	4373.5	232.7	240.2	215.3	261	1629	1665.6	215.3	236.4	4593.9	4939.5	120.7	124	265.6	229.8	6107.9	5880.6	269.5	198.1
1449182_at	Retn	538.9	617.9	108	61	10.1	78.6	80.5	76.7	71.4	57.4	227.6	184.5	74.9	88.3	13.7	57.5	314.2	303.3	44.3	55.6
1430640_a_at	Prkar2b	103.4	108.5	24.9	28.2	38.8	11.9	64.8	104.5	24.5	29.2	345.2	291.5	9.7	19.8	3.7	12.8	303.3	333.2	24.5	2
1438664_at	Prkar2b	342.4	328.2	32.6	52.1	45.3	45.3	382.1	313.4	29.4	42	1167.9	1082.3	5.2	39.5	42.5	57.3	981.5	1128.7	45.6	38.1
1456475_s_at	Prkar2b	243	229.3	51.1	44.6	60.2	44	220.7	230.8	43.4	54.9	777.4	712.7	60.4	36	34.4	42.4	709.5	741	53.7	42.4
1432466_a_at	Apoe	122.6	121.8	102.4	100.3	4718.2	4779.7	126.3	156	5037	5194.8	96.8	102.6	43	97.6	5933.5	5832	6100.5	6182.7	5539.9	6020.7